

Thread-Wire Surfaces

by

Benjamin K. Stephens

Bachelor of Arts, Harvard University, June 1999

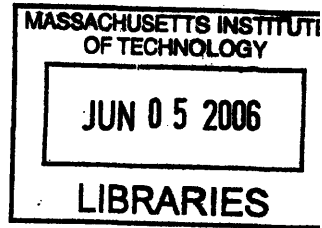
Submitted to the Department of Mathematics
in partial fulfillment of the requirements for the degree of
Doctor of Philosophy

at the

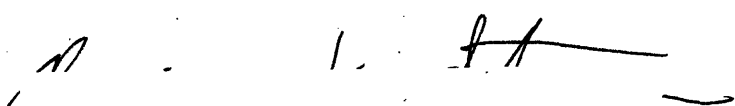
MASSACHUSETTS INSTITUTE OF TECHNOLOGY


June 2006


© Benjamin K. Stephens, MMVI. All rights reserved.



The author hereby grants to MIT permission to reproduce and
distribute publicly paper and electronic copies of this thesis document
in whole or in part.

Author 
Department of Mathematics
May 11, 2006

Certified by 
David S. Jerison
Professor of Mathematics
Thesis Supervisor

Accepted by 
Pavel Etingof
Chairman, Department Committee on Graduate Students

ARCHIVES

Thread-Wire Surfaces

by

Benjamin K. Stephens

Submitted to the Department of Mathematics
on May 11, 2006, in partial fulfillment of the
requirements for the degree of
Doctor of Philosophy

Abstract

This thesis studies surfaces which minimize area, subject to a fixed boundary and to a free boundary with length constraint. Based on physical experiments, I make two conjectures. First, I conjecture that minimizers supported on generic wires have finitely many surface components. I approach this conjecture by proving that surface components of near-wire minimizers are Lipschitz graphs in wire Frenet coordinates, and appear near maxima of wire curvature. Second, I conjecture and prove that surface components of near-wire minimizers are C^1 at corners where the thread touches the wire interior. Moreover, the limit of the surface normal field is the Frenet binormal of the wire at the corner point. This shows local wire geometry dominates global wire geometry in influencing the surface corner. Third, I show that these two conjectures are related: assuming additional regularity up to the corner, the finiteness conjecture follows.

Thesis Supervisor: David S. Jerison

Title: Professor of Mathematics

Acknowledgments

During the winter of 2002-3 I searched for a thesis topic. I finally found what I was looking for when I did a thought experiment involving wire, thread, and soap-water. This led to some physical experiments and a lot of time at the Someday Café in Davis square. In January I approached Professor David Jerison with my thesis proposal. Thankfully he offered to take me on. He is curious and enthusiastic and very sharp. I learned a lot from him about what it is to be a mathematician. I could not have asked for a better advisor. *Professor Jerison, thank you first and foremost.*

Ping: Tang Hall, Inman Street, and Porter Street were happy places because of you. Thank you for your calm and sweet support.

My family: You understood, as I took my thesis with me to San Diego or Houston or Philadelphia. Thanks to you, I always returned to Boston full of love and support. Also, special thanks to my mother for volunteering her copy-editing skills.

Larry Guth: I remember at the beginning of grad school you spent several months crumpling paper and studying its geometry. Your creativity and self-reliance inspired me as I looked for my own thesis topic. Thanks for the conversations, and the good times.

The Bishop Allen Drive Coop and my friends of Cambridge, Somerville, Boston, JP: You define community for me. I will miss you all very much. My home is your home.

Contents

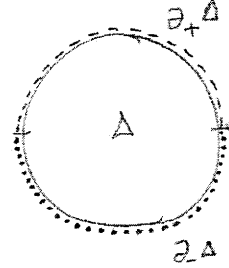
1	Introduction	11
1.1	Two related conjectures	12
1.2	Results	13
1.3	Outline of thesis	18
2	Background and preliminaries	19
2.1	Wires	20
2.2	Alt competitors	21
2.3	Generic wires	29
3	Alt minimizers	31
3.1	New first variation property	31
3.2	The Gauss image of a crescent	34
3.3	Convex hull results for thread-wire surfaces	38
3.4	How planes may intersect crescents	42
3.5	Level sets of harmonic functions on the disc	43
4	Near-wire Crescent Theorem	51
4.1	Slope bound in Γ' direction	57
4.2	Slope bound in ν_Γ direction	60
4.3	Lipschitz graph in varying Frenet frame	67
4.4	Near-wire crescents appear near maxima of wire curvature	72
4.5	Corner Γ' -slope improvement	77
4.6	Proof of Near-wire Crescent Theorem (Thm. 1.4)	80
5	C^1 Corner Theorem	83
5.1	A monotonicity property for the thread binormal	84

5.2	A crucial slope inequality	86
5.3	Coordinates	87
5.4	Gauss image constrained by wire-related curves	89
5.5	Gauss map is injective and is an embedding on the interior	93
5.6	Obtaining the crucial slope inequality	107
5.7	Laplacian on Gauss image with Dirichlet-Neumann boundary conditions	109
5.8	Lower bound on thread torsion near corner	111
5.9	Proof of C^1 Corner Regularity Theorem (Thm. 1.5)	112
6	Sufficient $C^{1,1}$ control implies crescent finiteness	113
6.1	Counting crescents using maxima of wire curvature	114
6.2	Proof of Lemma 1.3	114
7	Examples	123
7.1	Extensible thread-wire surfaces	123
7.2	Helicoidal thread-wire surfaces	128
7.3	Beeson's skewed chevron	130
8	Physical experiment	131
8.1	Experimental method	132
8.2	Heart curve	134
8.3	Bent paperclip curve	136
8.4	Tie-clip curve: Bifurcation	139
8.5	Möbius strip	142
A	Appendix	145
A.1	Properties of Frenet curves	145
A.2	Generalized Descartes's rule	148
A.3	Immersive lifts of a curve	149
A.4	A family of constant-curvature curves	152
A.5	Deferred proofs	157
A.6	Proof of Wire-Plane Intersection Number Lemma (Lem. 2.17)	157
A.7	Smoothing a kink in the thread	162

B Appendix: Series solutions	165
B.1 The Taylor expansion of a minimal surface	170
B.2 WOC Relations	171
B.2.1 Inductive plan	171
B.2.2 Wire lies in surface	172
B.2.3 Thread lies in surface	173
B.2.4 Thread curvature is tangential to surface	174
B.2.5 Solving the WOC problem: Proof of Theorem B.7	177
B.3 Solving the ThIP problem: Proof of Theorem B.6	178
Notation index	10
List of figures	179
References	183
Index	186

Notation index

We say a C^1 curve σ is a **regular curve** if its derivative never vanishes. The constant C may have different values in different equations. The expressions $C(\Gamma)$, $R(\Gamma)$ indicate positive constants depending only on the geometry of a wire curve Γ . Marks like hat ($\hat{}$), tilde ($\tilde{}$), star (\ast) do not have defined meanings. The prime symbol (\prime) does not have a defined meaning for sets.



$$\partial_+\Delta: y \geq 0 \text{ on } \partial\Delta$$

$$\partial_+^\circ\Delta: y > 0 \text{ on } \partial\Delta$$

$$\partial_-\Delta: y \leq 0 \text{ on } \partial\Delta$$

$$\partial_-^\circ\Delta: y < 0 \text{ on } \partial\Delta$$

Figure 0-1: Arcs of the unit circle.

Symbol	Usage
Δ	unit disc, lying in \mathbb{R}^2 or \mathbb{C}
$S^2(1)$	unit sphere, or Gauss sphere
U°	interior of a set U in a topological space
∂U	set of boundary points of a set U in a topological space
\bar{U}	closure of a set U in a topological space
$(\)_x$	differentiation of an expression $(\)$ by x
$B_X(c, r)$	metric ball in metric space X with radius r , center c
$\text{Tub}_r U$	r -tubular neighborhood of a set U in Euclidean space
\mapsto	“maps to” (used to define inline functions, such as $t \mapsto 2t$)
$f \circ g$	the composed function $x \mapsto f(g(x))$
$f _C$	function f restricted to subset C of its domain
$\text{Im } f$	image of a function f
$\text{dom } f$	domain of a function f
$f(U)$	image of a subset U of the domain of a function f
$f^{-1}(U)$	preimage of a subset U of the target of a function f
$d_p f$	differential $d_p f : T_p M \rightarrow T_{f(p)} N$ of a manifold map $f : M \rightarrow N$
$\#U$	cardinality of a set U
i	imaginary unit, unless obviously not in the complex context
\times	cross-product in \mathbb{R}^3
$\Gamma_{[x]}$	the x component function for the curve Γ ; similarly for y, z .

Chapter 1

Introduction

In the winter of 2002-2003, I was thinking about how to count and describe the stable minimal surfaces spanning a contour. Working with wire, thread, and soap-water, I demonstrated a *thread-pull method* of creating stable soap-water surfaces spanning a contour. (See **Figure 1-1**, also Section 8.) My method worked for many contours, and the robustness of the process inspired me. The thread-wire surfaces I observed usually had several surface components, each tapering to two *cusp-corners* where the thread re-joined the wire tangentially. I called these surface components *crescents* because of their typical shape. Through experiment I gained intuition about thread-wire surfaces and their crescents. I observed several phenomena which I thought should be theorems about a corresponding mathematical idealization.

I then looked in the literature and found that such an idealization had been studied. In 1973 H.W. Alt defined the *thread problem* $\mathcal{P}(\Gamma, L)$ to be (roughly¹) the problem of finding a least-area surface consisting of discs spanning a wire curve Γ and a thread curve of length L . Alt proved the existence of a minimizer to his thread problem [1]. Several other authors also studied the problem,²

¹See Assumption 2.15, p. 29, for the full definition.

²See Section 2.

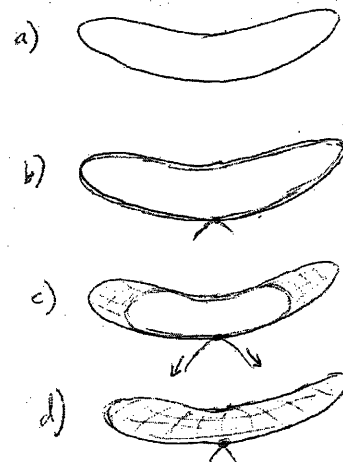


Figure 1-1: Thought experiment.

but I found that many of my observations had not been proved as theorems.

1.1 Two related conjectures

First, I conjectured that minimizers supported on generic wires have finitely many surface components. I approached this conjecture by proving that small surface components are Lipschitz graphs in wire Frenet coordinates, and appear near maxima of wire curvature. Second, I conjectured and proved that near-wire surface components are C^1 at corners where the thread touches the wire interior. Moreover, the limit of the surface normal field is the Frenet binormal of the wire at the corner point. This shows local wire geometry dominates global wire geometry in influencing the surface corner. Third, I showed that these two conjectures are related: given additional regularity at the corner, the finiteness conjecture follows. We discuss each of these three points below.

Here is the first conjecture:

Conjecture 1.1. [Crescent Finiteness] For each generic wire curve Γ , there is a constant $C(\Gamma)$ depending on the geometry of Γ , so that any minimizer to Alt's thread problem $\mathcal{P}(\Gamma, L)$ has at most $C(\Gamma)$ surface components.

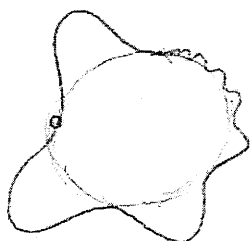


Figure 1-2: Non-generic wire with infinite-component Alt minimizer.

A wire is generic if it is C^4 , has curvature which is a nonvanishing Morse function, and has torsion which crosses zero transversely and only where the curvature is not critical. (See Assumption 2.15.) The idea of the finiteness conjecture is that experimentally I always see small surface components straddled on local maxima of wire curvature. I thus propose that the number of maxima of wire curvature of Γ should control the number of surface components that may appear in Alt minimizers. This is a strong statement relative to Alt's existence result, which only guarantees a minimizer with a countable number of surface components. Conjecture 1.1 also uses genericness in

a meaningful way. Indeed, it is easy to demonstrate a non-generic wire supporting an Alt minimizer with infinitely many surface components. See **Figure 1-2**.

The second conjecture concerns how the normal vector field of an Alt minimizer behaves at the cusp-corners which typically appear in Alt minimizers:

Conjecture 1.2. [C^1 Corner Regularity] Let Γ be a generic embedded wire curve. There is a small R so any Alt minimizer μ lying in the R -tubular neighborhood has the following property at any cusp-corner P in the interior of the wire. The surface is a C^1 graph in the Frenet coordinates of the wire at P , and the Frenet binormal of the wire is attained as the limit of the normal vector field of μ .

The idea behind this conjecture is that at the corner, local and global effects compete. On the one hand, the local curvedness of the wire encourages the surface and the free thread to come in to meet the wire in a way which osculates the Γ', Γ'' plane. On the other hand, the global shape of the wire may work against this effect. Depending on the path one takes to approach the corner, one could imagine the surface normal behaving in different ways—having one limit, having another limit, not having a limit. Conjecture 1.2 makes the bold claim that the local effect completely wins at the level of the first derivative of surface position. Regardless of the path one takes to approach the corner, the normal field approaches a limit. Moreover, no matter the path taken, it approaches the same limit. Even better, it approaches a limit which is dictated by the geometry of the fixed wire exactly at the place where the thread joins the wire. Even better, the limit is simply described: the Frenet binormal of the wire at that point.

We would like to remove the tubular neighborhood assumption in Conjecture 1.2. However, a result limited by this assumption is just enough to prove the Crescent Finiteness Conjecture (Conj. 1.1). This is our third point:

Lemma 1.3. Assume Conjecture 1.2 holds with the stronger conclusion that the surface has $C^{1,1}$ norm bounded by $C(\Gamma)$ for a certain constant $C(\Gamma)$. Then Conjecture 1.1 follows.

Having listed the three points (two conjectures and a lemma) at the center of the thesis, we now state our results.

1.2 Results

Our first theorem is aimed at proving the Crescent Finiteness Conjecture (Conj. 1.1). It shows that near-wire crescents are Lipschitz graphs, supported by small wire segments near maxima of wire curvature. This does not prove the Crescent Finiteness

Conjecture (Conj. 1.1) because infinitely many crescents could appear near a single maximum of wire curvature. However, our theorem still makes significant progress; indeed, Alt minimizers are a priori immersed and could be quite complicated. For example, according to the existing regularity theory, they could come into a wire at a cusp-corner by spinning repeatedly around the wire. My theorem prohibits this.

Theorem 1.4. [Near-wire Crescent] Let Γ be an embedded generic wire in \mathbb{R}^3 . For R less than a constant $R(\Gamma)$ depending on the geometry of Γ , the following will hold. If A is any Alt minimizer lying in an R tubular neighborhood of the wire, then the thread of A is C^1 and touches the interior of Γ only tangentially. Each crescent μ of A satisfies the following.

- (i) The wire supporting the crescent μ is short (arclength bounded by $C(\Gamma)R^{1/12}$).
- (ii) Let $\Gamma(s_0)$ be a corner of μ on the interior of Γ . Then s_0 is within $C(\Gamma)R^{1/12}$ of a maximum of wire curvature.
- (iii) Let x, y, z be the Frenet coordinates of Γ at $\Gamma(s_0)$. Then the crescent μ may be expressed as a graph

$$z = f(x, y)$$

over a domain with $y \geq 0$. See **Figure 1-3**. Here f is a Lipschitz function

$$|(\nabla f)(x, y)| < C(\Gamma)R^{1/12}$$

with additional slope control

$$|f_x(x, y)| < C(\Gamma)x.$$

- (iv) Where the wire supports the crescent μ , κ_Γ is within $C(\Gamma)R^{1/12}$ of the free thread curvature κ .
- (v) The Frenet frame of the thread is within $C(\Gamma)R^{1/12}$ of the Frenet coordinates x, y, z .

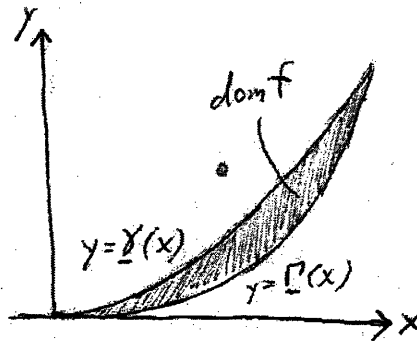


Figure 1-3: Crescent as a graph in Frenet coordinates. The crescent μ vertically projects to a domain $\text{dom } f$ lying in either the first or second quadrant of the x - y plane. The boundary of the domain is defined by the **wire shadow curve** $y = \underline{\Gamma}(x)$ and **thread shadow curve** $y = \underline{\gamma}(x)$. The domain tapers to a cusp at the origin: $0 \leq \underline{\Gamma}(x) \leq \underline{\gamma}(x) \leq \kappa x^2 + o(x^2)$.

Our second theorem proves Conjecture 1.2 and also shows many other properties of the Gauss image of near-wire Alt minimizers.

Theorem 1.5. [C^1 Corner Regularity] Let Γ be a generic embedded wire. There is a small R so any Alt minimizer μ lying in the R -tubular neighborhood has the following property. Let Σ be any crescent supported in the interior of Γ . Let N be a unit normal vector field to Σ .

- (i) The normal vector field is continuous up to each corner of Σ . The limit of N as one approaches a corner $\Gamma(s)$ is the Frenet binormal $\eta_\Gamma(s)$.
- (ii) The Gauss map for Σ is injective and is an embedding on its interior.
- (iii) The Gauss image of the thread and wire curves bounding Σ have the properties described in **Figure 1-4**.
- (iv) Consider the first eigenvalue λ_1 of the Laplacian on the Gauss image of Σ with Dirichlet boundary condition on the Gauss image of the wire and Neumann condition on the Gauss image. This eigenvalue is large:

$$\lambda_1 > C(\Gamma)R^{-1/3}. \tag{1.1}$$

Showing property (iv) fulfills a prerequisite for future work imitating the beautiful result of do Carmo and Barbosa [2]. They considered a minimal disc D spanning a wire loop. They showed that D is stable, provided that the Laplacian on the Gauss image of D with Dirichlet conditions on the boundary is at least that of the upper hemisphere of the Gauss sphere. Formal calculations by the author show that a similar argument for stationary thread-wire surfaces would depend on the eigenvalue bounded in (1.1).

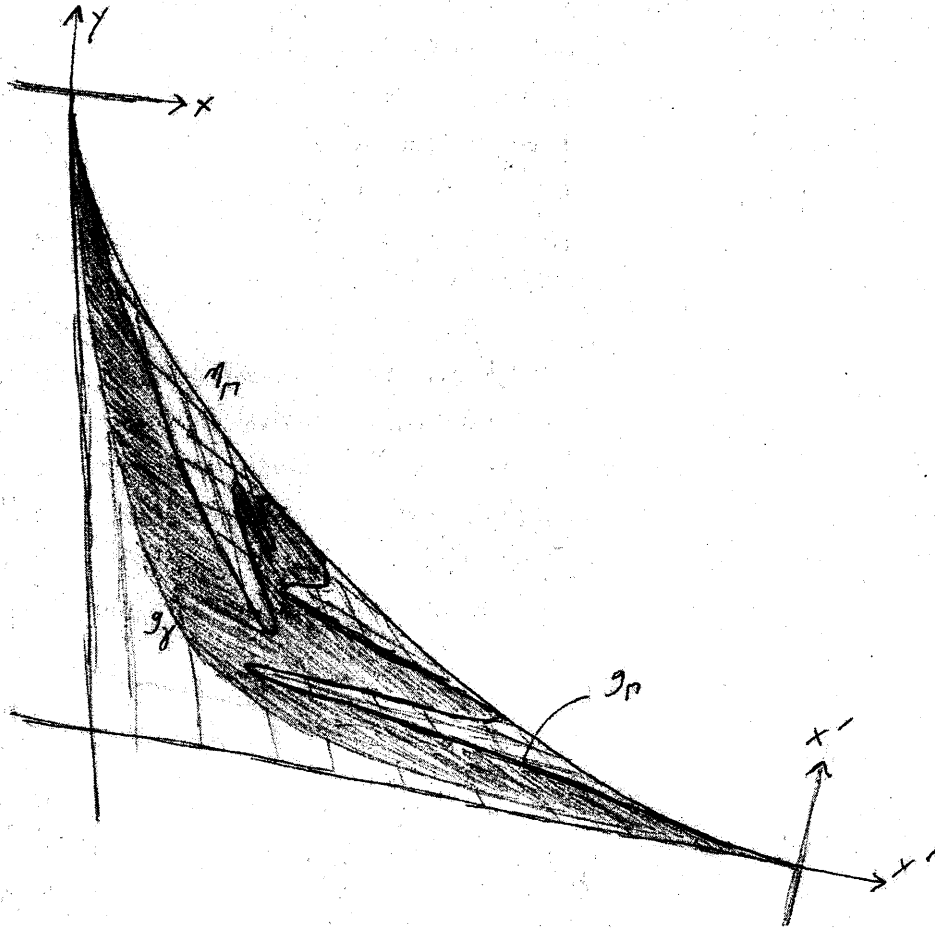


Figure 1-4: Gauss image control. The above diagram takes place in a small neighborhood of $\eta_{\Gamma}(P)$ (the Frenet binormal of the wire at the corner point). In this neighborhood, we may project the sphere to the tangent plane at η_{Γ} to get x and y coordinates on the sphere. We may do the same at the other corner of the crescent to get x' and y' coordinates. The Gauss image of the thread is a graph over the x axis in x - y coordinates and also a graph over the x' axis in x' - y' coordinates. Its geodesic curvature has a definite sign. The Gauss image of the thread satisfies something close to a graph condition: it may be parametrized as $\exp_{\eta_{\Gamma}(s)}(v(s)\nu_{\Gamma}(s))$ for some continuous function $v(s)$. For more information see Section 5.

1.3 Outline of thesis

In Section 2 we review the existing work on Alt's thread problem and make the necessary definitions for this thesis. We define generic wires and discuss their properties. In Section 3 we study Alt minimizers in general. Here we present a new first variation property that came out of my experimental observation and which will be important later. We also study how Alt minimizers interact with planes. In Section 4 we apply our tools to near-wire Alt minimizers in order to prove Theorem 1.4. Section 5 describes the Gauss image of near-wire crescents and proves Theorem 1.5. In Section 6 we prove Lemma 1.3; this shows that sufficient $C^{1,1}$ corner regularity implies the Crescent Finiteness Conjecture (Conj. 1.1). Section 7 examines mathematical examples of thread-wire surfaces. Section 8 surveys experimental examples and provides commentary on videos of my experiments (see www.bkstephens.net). Some of the more technical or mundane proofs have been relegated to Appendices A and B.

The author has tried to choose notation that is clear and concise. As an aid to the reader, a general **notation index** is provided on page 10. To look up more specific notation or definitions, the reader may consult the **index** at the end of the thesis.

Chapter 2

Background and preliminaries

PHYSICAL QUESTION. *Given a piece of rigid wire fixed in place and a flexible thread tied to the ends of the wire, what stable soap-water surfaces span the wire and thread?*

In the physical world, a length of wire or thread has thickness. The thread resists curving or twisting on a small scale. Gravity and air currents affect threads and soap surfaces. However, in this thesis we will assume that these objects have no thickness, no weight, and are not under any net pressure.

Having made these general physical assumptions, we must define a mathematical model suitable to our purposes. We adopt Alt's original model [1] of competitors for the minimization problem called the "thread problem." This is a good model for showing the existence of a solution which has disc-type components. It exploits the same idea that J. Douglas and T. Radó exploited to solve the Plateau problem minimal discs—namely, minimizing the Dirichlet energy furnishes a minimum of area.¹

Alt's set of competitors admits calculus of variations for variations of each extant component. However, emerging or disappearing components are problematic. In experiment we see components appear or disappear smoothly. (See for example the heart thread-pull in Section 8.2.) When a component disappears, it becomes very thin, and its Dirichlet-energy-minimizing parametrization by the unit disc might vary wildly. This is unfortunate, for we would like such a continuous variation in our physical experiment to correspond to a continuous variation in our mathematical model. For now

¹See [5, p. 276–302] for a detailed discussion of historical progress on the Plateau problem. We mention here a paper of Douglas [8] and a summary by Radó of the work of Haar, Douglas and Radó [24].

we may get around this problem, but in the future, once the regularity at zero-angle corners of thread-wire surfaces is better understood, we would like to define a new



Figure 2-1: This physical thread-wire surface is not orientable. It cannot be modelled by an integral current.

space suitable for doing calculus with all variations, even crescent-creating and crescent-destroying ones. The author has created examples of such spaces, but is waiting until the corner regularity is resolved before proceeding.

We should note that K. Ecker [13] has treated the thread problem from the point of view of geometric measure theory. This has the advantage of allowing surface components with more complicated topologies than the disc. The GMT point of view has limitations, of course. For example one could not represent the non-orientable physical thread-wire surface shown in **Figure 2-1** because it does not correspond to an orientable surface.

2.1 Wires

Definition 2.1. A **wire** Γ is a C^1 map of a compact interval into \mathbb{R}^3 , parametrized by arclength. A **Frenet wire** is a wire which is C^2 and has curvature that never vanishes. Such a wire has a continuously-varying (right-handed) **Frenet frame**

$$\hat{\Gamma}, \quad \nu_{\Gamma} = \ddot{\Gamma}/|\ddot{\Gamma}|, \quad \eta_{\Gamma} = \hat{\Gamma} \times \nu_{\Gamma}$$

consisting of the **tangent vector** σ' , the **Frenet normal vector** ν_{σ} , and the **Frenet binormal vector** η_{σ} . The torsion of the curve is

$$T_{\Gamma}(s) = \langle \eta'_{\Gamma}(s), \nu_{\Gamma}(s) \rangle.$$

See **Figure 2-2**.

In this thesis we will typically treat embedded wires, to streamline the presentation. However the phenomena that we discuss naturally applies to immersed wires. As a technical point, we allow the following to count as an embedded wire:

Definition 2.2. An **embedded wire loop** is a C^1 wire curve $\Gamma : [0, b] \rightarrow \mathbb{R}^3$ which intersects itself only at $\Gamma(0) = \Gamma(b)$. Moreover, we require $\Gamma'(0) = \Gamma'(b)$.

Usually we will work with wires that have additional regularity and generic properties. This is because we are interested in phenomena observed in experiments which relate to high order geometric quantities like curvature and torsion. We will not work with wires less regular than C^1 (such as rectifiable Jordan curves), even though Alt worked in that setting.

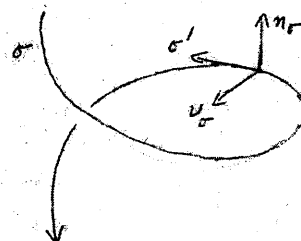


Figure 2-2: Frenet frame.

2.2 Alt competitors

In Alt's original work related to our Physical Question, Alt considered surfaces in \mathbb{R}^3 parametrized by countably many discs overlaid on the real interval $[-1, 1]$. See Figure 2-3.

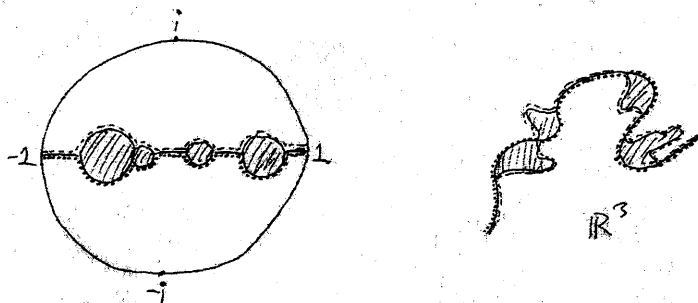


Figure 2-3: Alt competitor (B, M) . The shaded region on the left is an admissible domain B . Its image under X is the shaded surface shown in \mathbb{R}^3 . The dashed upper boundary of B maps to the dashed "thread" curve in \mathbb{R}^3 . The dotted lower boundary of B maps to the dotted wire curve in \mathbb{R}^3 . The latter must be monotonic relative to the fixed parametrization of the wire. Note that the competitor pictured is not a minimizer. For example its Dirichlet energy could be improved by pushing in parts of the free thread, or straightening out the free thread where it meets the wire.

He considered only the case where the wire Γ and thread length L satisfy

$$|\Gamma(0) - \Gamma(\ell(\Gamma))| < L < \ell(\Gamma). \quad (2.1)$$

Obviously the thread cannot be shorter than the distance between its endpoints. On the other hand, if the thread length meets or exceeds the length of the wire, then in the physical system one may achieve zero area by letting the thread trace the wire (possibly backtracking on itself to use up excess length).

We will call these objects *Alt competitors*.²

Definition 2.3. Let Γ be a wire³ and let L satisfy (2.1). The set of **Alt competitors** $\mathcal{C}_{\text{Alt}}(\Gamma, L)$ consists of pairs (B, M) , where

- (i) The set B consists of $[-1, 1]$ unioned with unit discs lying in Δ centered on the real line such that the discs' interiors are pairwise disjoint. Let $p_+^B : [-1, 1] \rightarrow \Delta$ parametrize the points on the upper boundary of B as by their x -coordinate. Similarly let p_-^B parametrize the lower boundary of B .
- (ii) The map M is $H^1(B^\circ, \mathbb{R}^3) \cap C^0(B, \mathbb{R}^3)$.
- (iii) The curve $M \circ p_+$ has length at most L .
- (iv) There is a Lipschitz non-decreasing map $\phi : [-1, 1] \rightarrow [-1, 1]$ so ϕ is the identity where p_+^B lies on the x -axis and

$$M \circ p_-^B \circ \phi = \Gamma \circ \xi. \quad (2.2)$$

Here ξ is the fixed identification $\xi : [-1, 1] \rightarrow \text{dom } \Gamma; s \mapsto \ell(\Gamma) \cdot (s + 1)/2$.

See **Figure 2-3** for an example of an Alt competitor.

Definition 2.4. In an Alt competitor (B, M) , the portion of thread not adhering to the wire is called the **free thread**. It is parametrized by M restricted to the upper boundary of B , minus the real line. The portion of the thread which adheres to the wire is **wire-adhering thread**. It is parametrized by M restricted to $\partial B \cap [-1, 1]$.

²He called them "admissible maps."

³Alt treated the case of a rectifiable Jordan arc.

The Alt competitors compete to have minimal Dirichlet energy:

Definition 2.5. We define the **Dirichlet energy** of an Alt competitor (B, M) to be

$$D(B, M) = \frac{1}{2} \int_{B^\circ} (|M_x|^2 + |M_y|^2) dx dy.$$

Requiring M to be $H^1(B^\circ)$ means that we require $D(B, M)$ to be finite.

Figure 2-4 shows an example of an Alt competitor which minimizes Dirichlet energy. See Section 8.2 for a physical experiment corresponding to this picture.

Here is a version of Alt's result in our setting:

Theorem 2.6. Assuming (2.1), there exists an **Alt minimizer** $(B, M) \in \mathcal{C}_{\text{Alt}}(\Gamma, L)$ which minimizes the Dirichlet energy on $\mathcal{C}_{\text{Alt}}(\Gamma, L)$ and has the properties

$$\begin{aligned} \Delta M &= 0 \\ |M_x|^2 &= |M_y|^2 & \langle M_x, M_y \rangle &= 0 \end{aligned}$$

in B° . Moreover, the free boundary attains the maximum allowed length:

$$\ell(M \circ p_+^B) = L.$$

We say that (B, M) solves the **thread problem** $\mathcal{P}(\Gamma, L)$.

We will need to do analysis on individual surface components of Alt minimizers, which we call *crescents*. **Figure 2-5** shows how to parametrize the middle crescent of the Alt minimizer (B, M) in **Figure 2-4** by pulling back M on the middle disc of B to the unit disc. To describe this middle crescent we need this new map $X : \Delta \rightarrow \mathbb{R}^3$ and the gluing information which tells us how the lower boundary of the disc, $\partial_- \Delta$, attaches to the wire. This information is contained in the *gluing map*, a homeomorphism $\phi_- : \partial_- \Delta$. Together the pair (X, ϕ_-) encodes the middle crescent of (B, M) .

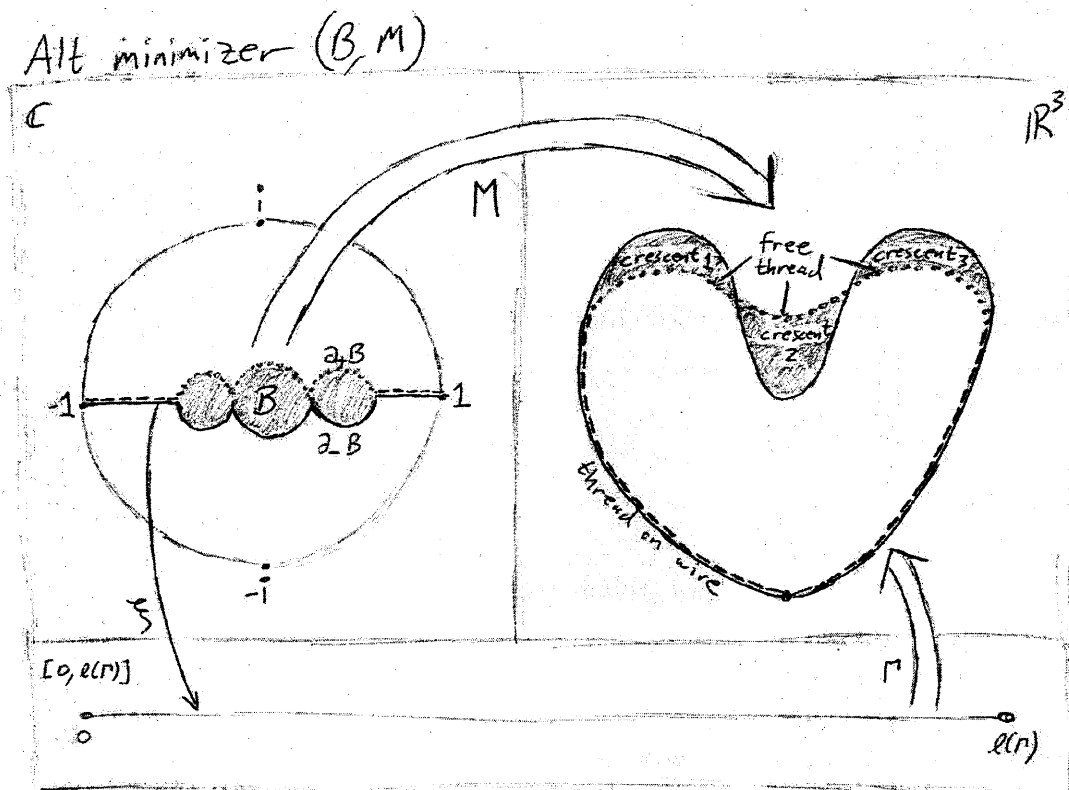


Figure 2-4: Alt minimizer (B, M) . On the left we see the admissible domain B sitting in the unit disc in \mathbb{C} . It consists of three osculating closed discs, union the interval $[-1, 1]$. The map M sends this closed set to the thread-wire surface shown at right. It lies in \mathbb{R}^3 , although this example is planar for simplicity. We see that the dashed region on the left maps to (dashed) thread lying on wire. The dotted region on the left maps to (dotted) pieces of free thread. The solid bottom boundary ∂_B maps to the wire. The conditions of Definition 2.3 mandate that M map the horizontal pieces of ∂_B to Γ in a manner prescribed by ξ . The map M may send the rest of ∂_B arbitrarily, so long as it does so weakly monotonically.

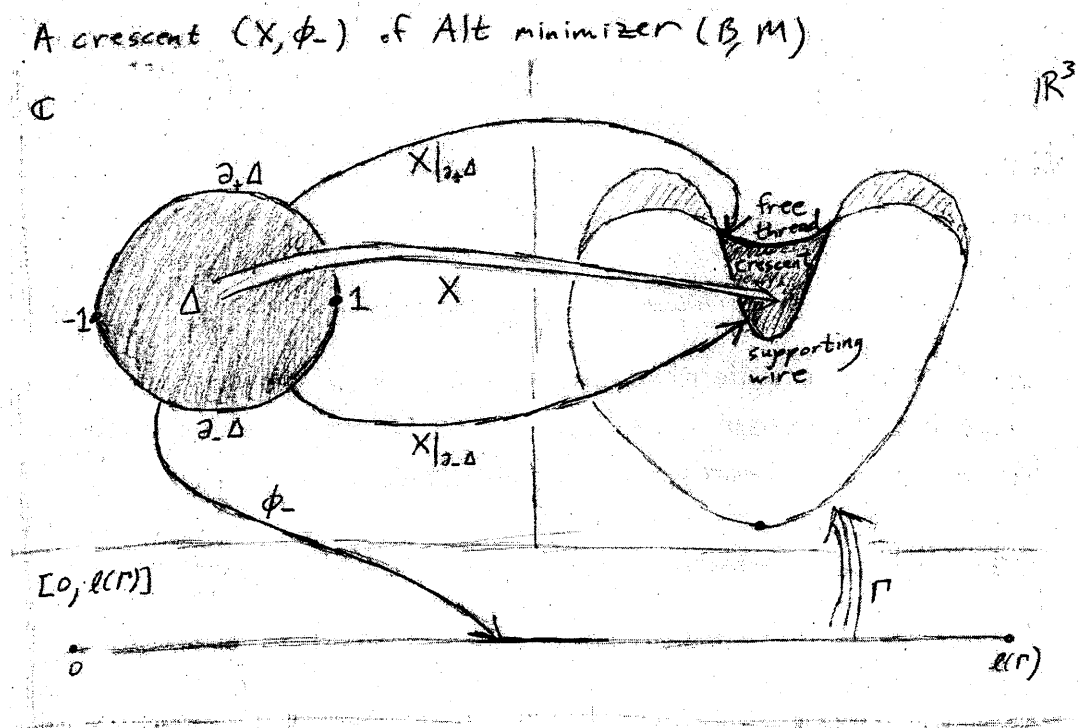
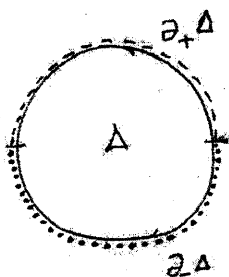


Figure 2-5: An Alt crescent (X, ϕ_-) of Alt minimizer (B, M) shown in Figure 2-4.



$$\partial_+\Delta: y \geq 0 \text{ on } \partial\Delta$$

$$\partial_+\Delta: y > 0 \text{ on } \partial\Delta$$

$$\partial_-\Delta: y \leq 0 \text{ on } \partial\Delta$$

$$\partial_-\Delta: y < 0 \text{ on } \partial\Delta$$

Figure 2-6: Arcs of the unit circle.

Below is the general definition of Alt crescent. (Also, see notation in **Figure 2-6**.)

Definition 2.7. Let Γ be a wire. Let (B, M) be an Alt minimizer for some thread problem $\mathcal{P}(\Gamma, L)$. For each disc B^i of B^o we may obtain an **Alt crescent** as follows:

- Let $X : \Delta \rightarrow \mathbb{R}^3$ be M pulled back by the affine map from Δ to B^i which sends $[-1, 1]$ to $B^i \cap [-1, 1]$ in an increasing manner.
- Let ϕ_- be the homeomorphism from $\partial_-\Delta \rightarrow [0, \ell(\Gamma)]$ which satisfies

$$\Gamma \circ \phi_- = X \quad (2.3)$$

on $\partial_-\Delta$.

The map ϕ_- is the **gluing map**.

Definition 2.8. The part of the wire bounding the crescent is called the crescent's **supporting wire**; it is parametrized on the domain $\text{Im } \phi_-$. The (possibly empty) portion Γ which does not support any crescent is called **thread-bearing wire**.

Lemma 2.9. In the above definition, the gluing map ϕ_- is in fact an isomorphism.

Proof. The idea is that if X mapped an interval of $\partial_-\Delta$ to a point on the wire, we could show that X maps all of Δ to that point. See [5, p. 248, Thm. 3]. ■

Theorem 2.10. Let $X : \Delta \rightarrow \mathbb{R}^3$ be an Alt crescent of an Alt minimizer (B, M) for a thread problem $\mathcal{P}(\Gamma, L)$. Let $\gamma(s)$ reparametrize the free boundary $X|_{\partial_+\Delta}$ by arclength. Then on the interior of the free thread, $(0, \ell(\gamma))$,

$$|\ddot{\gamma}(s)| = \kappa,$$

where κ is a constant associated to (B, M) . If this crescent is isolated (there are positive length pieces of wire-clinging thread on either side of it) and the wire Γ is smooth, then Alt also shows that the free thread meets the wire tangentially.⁴

⁴See [1] and [6, p. 273]. For the last sentence, see [6, p. 292].

Note that because only the *magnitude* of the curvature vector is controlled, we cannot conclude that the thread is C^2 on $[0, \ell(\gamma)]$. So all we can say is that $\gamma(s)$ is $C^{1,1}$. In this thesis we will show that near-wire crescents meet the wire tangentially whether they are isolated or not. We will also show the existence of limits of $\ddot{\gamma}$ at the endpoints of the free thread in the case of near-wire crescents. This will establish the full C^2 property for the free thread bounding these crescents. Note that if one looks past the corner of an isolated crescent, the thread curvature might very well change, because there the thread coincides with the wire. For example, **Figure 2-4** shows such a change in thread curvature at the left boundary of the first crescent.

What about the regularity of the free thread in its interior? Here we have a very strong result of Dierkes-Hildebrandt-Lewy:⁵

Theorem 2.11. Let $X : \Delta \rightarrow \mathbb{R}^3$ be an Alt crescent. Then X may be continued analytically across the free boundary $\partial_+^o \Delta$ and on this boundary it has no branch points of odd order nor any true branch points of even order. Moreover, if X is assumed to be an embedding, then $X(w)$ has no false branch points of even order on $\partial_+^o \Delta$. In this case the free trace $\Sigma = X|_{\partial_+^o \Delta}$ is a regular, real analytic curve of constant curvature κ .

In any case, we have on the interior of the free thread (except at branch points),

$$\ddot{\gamma}(s) = \kappa \nu(s) \tag{2.4}$$

where $\nu(s)$ is the **outer side-normal** to the surface. That is, $\nu(s)$ is perpendicular to the thread and tangent to the surface.

Note that a false branch point is one where the surface may be locally reparametrized to make it an immersion. We will show using other methods than those of Dierkes-Hildebrandt-Lewy that near-wire components of thread-wire surfaces have no branch points and are in fact Lipschitz graphs. The main reason we need Theorem 2.11 is that it allows us to extend Alt minimizers across the thread in a real-analytic way.

One consequence of this regularity theory is that each crescent (X, ϕ_-) of an Alt minimizer has a Gauss map g defined on $\Delta \setminus \{(-1, 0), (1, 0)\}$ except at countably many points on $\partial_- \Delta$ where $\nabla X = 0$. If the crescent is locally a graph near one of these points, and the wire is smooth enough, we will be able to continue the Gauss map across the point. We will see this in Section 4.3.

⁵This statement is adapted from [6, p. 273]. Also see [7], [16], and [17].

From the Plateau problem, we also have a regularity result for Alt minimizers at the wire boundary: We adapt the following result from [6, p. 33, Thm 1].

Theorem 2.12. Consider a minimal surface defined by a map $X : \Delta \rightarrow \mathbb{R}^3$ which is continuous on $\Delta^\circ \cup \sigma$ where σ is an open subarc of $\partial\Delta$, and which maps σ onto a Jordan arc Γ of \mathbb{R}^3 which is a regular curve of class $C^{m,\mu}$ for some integer $m \geq 1$ and some $\mu \in (0, 1)$. Then X is of class $C^{m,\mu}(\Delta^\circ \cup \sigma)$. Moreover, if Γ is a regular real analytic Jordan arc, then X can be extended as a minimal surface across σ .

Finally, the following lemma relates the Dirichlet-minimizing property of Alt minimizers to area.

Lemma 2.13. Let $(B, M) \in \mathcal{C}_{\text{Alt}}(\Gamma, L)$ be the minimizer found in Theorem 2.6. Then (B, M) also minimizers area relative to the competitors in $\mathcal{C}_{\text{Alt}}(\Gamma, L)$.

We prove this lemma using *Morrey's ϵ -Conformal Lemma*. We reprint a version of it here.⁶

Lemma 2.14. Let X be of class $C^0(\Delta, \mathbb{R}^3) \cap H^1(\Delta^\circ, \mathbb{R}^3)$. Then, for every $\epsilon > 0$, there exists a homeomorphism τ_ϵ of Δ onto itself which is of class H^1 on Δ which reparametrizes X as $Z_\epsilon = X \circ \tau_\epsilon$ so that

$$Z_\epsilon \in C^0(\Delta, \mathbb{R}^3) \cap H^1(\Delta^\circ, \mathbb{R}^3)$$

and

$$D(Z_\epsilon) \leq A(X) + \epsilon.$$

Here $A(X)$ is the area

$$A(X) = \int_{B^p} \sqrt{|\det dX|} dx dy.$$

We may now prove our lemma.

Proof–Lemma 2.13. If to the contrary there were an Alt competitor (B', M') with $A(M') < A(M)$ then we employ Morrey's ϵ -conformal lemma to reparametrize each disc of (B', M') to get a map $M_\epsilon : B' \rightarrow \mathbb{R}^3$ with

$$D(M_\epsilon) \leq A(M') + \epsilon.$$

⁶See [5, p. 252] and original sources [19, pp. 141–143] and [20, pp. 814–815].

For small enough ϵ we have a competitor with $D(M_\epsilon) < A(M')$. But since M' is conformally parametrized, we have $A(M') = D(M')$ so we've shown $D(M_\epsilon) < D(M')$.

■

2.3 Generic wires

In this section we make precise what we mean by generic wires. We then interpret our definition in terms of how planes intersect the tubular neighborhoods of wires.

Assumption 2.15. [Generic Wire] We say a wire is **generic** if the following hold.

- (i) The wire Γ is C^4 .
- (ii) The curvature κ_Γ does not vanish. Hence Γ is a Frenet curve (Definition 2.1).
- (iii) The curvature κ_Γ is a Morse function. In other words, wherever its first derivative vanishes, its second derivative does not.
- (iv) The torsion T_Γ crosses zero transversely. In other words, wherever it vanishes, its first derivative does not.
- (v) The torsion T_Γ does not vanish at any critical point of curvature κ_Γ .

In this definition we don't allow the curvature to vanish. We should not ask the same of the torsion, however, because then C^3 wire loops would be required to have their binormals wind at least once around the wire as one traverses the wire loop. In order to avoid encoding this topological requirement, we find it natural to let the torsion vanish.

Definition 2.16. Let Γ be a wire curve. We define the **wire-plane intersection number** in the tubular neighborhood $\text{Tub}_R\Gamma$ to be

$$n_{\text{Wire-Plane}}(\Gamma, R) = \max_C \#(C \cap \text{Im } \Gamma) \quad (2.5)$$

where the maximum is taken over connected components C of $V \cap \text{Tub}_R(\Gamma)$ for every plane V in \mathbb{R}^3 .

We interpret our generic wire assumptions in terms of the wire-plane intersection number.

Lemma 2.17. [Wire-Plane Intersection Number] Let Γ be a generic wire. Then:

- (i) For any $R > 0$, we have $n_{\text{Wire-Plane}}(\Gamma, R) \geq 3$.
- (ii) For sufficiently small R , we have $n_{\text{Wire-Plane}}(\Gamma, R) \leq 4$ (modulo an assumption⁷).
- (iii) For any critical point m of κ_Γ there is a subarc $\hat{\Gamma}$ of Γ containing m so for sufficiently small R , we have $n_{\text{Wire-Plane}}(\hat{\Gamma}, R) = 3$.

We prove this in Section A.5 of Appendix A.

⁷For claim (ii)—and claim (iii) only—we must make the additional assumption that Γ is C^5 . Claim (ii) is not used in this thesis, since we work with C^4 generic wires. However, the author feels it illustrates a useful property of the wire-plane intersection number.

Chapter 3

Alt minimizers

In this section we describe some global properties of Alt minimizers. Unlike later in this thesis, we do not assume that the Alt minimizers lie near a wire.

3.1 New first variation property

The properties of stationary solutions to Alt's thread problem given in the literature (as represented in [6]) do not capture all the properties of stationary thread-wire surfaces that I observed in experiment. In this section we show additional properties of Alt's minimizer related to it being stationary under first variation. The author thinks that these variation results are still weaker than what is suggested by experiment. To progress farther, we will need to better understand of the regularity of Alt minimizers at cusp-corners.

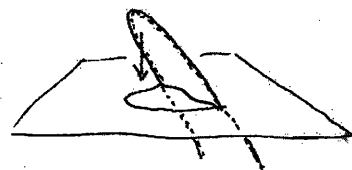


Figure 3-1: An Alt competitor with $\kappa < 0$ may be improved.

Lemma 3.1. If (B, M) is an Alt minimizer, then it has free thread curvature $\kappa \geq 0$.

Proof. This is straightforward. If the thread has negative curvature, we can find a point $p \in \partial_+^o \Delta$ which is not a branch point. We may then pick a plane perpendicular to the side normal to the surface at $X(p)$ and translate the plane towards the surface a small amount. Then we have a situation like the one shown in **Figure 3-1**. Projecting

the thread and surface onto that plane reduces the Dirichlet energy of the map X , and it also reduces the length of the free thread. In this way we show that there is another Alt competitor in $\mathcal{C}(\Gamma, L)$ with strictly less Dirichlet energy. This contradicts the minimizing property of (B, M) . ■

Theorem 3.2. [Thread-Bearing Wire Curvature Bound] If (B, M) is an Alt minimizer with positive free thread curvature κ , then anywhere the thread adheres to a positive length of wire, the wire curvature $\kappa_\Gamma(s)$ is dominated by the free thread curvature:

$$\kappa_\Gamma(s) \leq \kappa.$$

Proof. We remember first that Alt's assumption (equation (2.1), p. 22)—that the thread length is less than the wire length—guarantees us that (B, M) has at least one component. Let $q \in B$ parametrize a thread point $X(q)$. Let γ reparametrize X restricted to the upper boundary of B near q so that γ parametrizes the thread boundary by arclength, with $\gamma(0) = X(q)$. By Theorem 2.11 we may assume that X does not have any branch points at q or within arclength λ of q .

Assume to the contrary of Thread-Bearing Wire Curvature Bound Theorem that there is a small positive length arc of wire Γ parameterized by $[s_1, s_2]$ where the thread adheres and

$$\kappa_\Gamma(s) \geq (1 + c)\kappa \tag{3.1}$$

for $c > 0, s \in [s_1, s_2]$. Here we consider c and s_1 to be fixed. However, we set

$$w = s_2 - s_1 \tag{3.2}$$

and below we will impose smallness restrictions on w . This means moving s_2 toward s_1 . For one, we require

$$w < \lambda/2. \tag{3.3}$$

We illustrate our situation in **Figure 3-2a**. The idea is that we can then create a new surface component on the arc $\Gamma|_{[s_1, s_2]}$ which increases Dirichlet energy but decreases length. Meanwhile, we may modify an existing surface component to reduce Dirichlet energy and increase thread length. (See **Figure 3-2b**.) Because of (3.1) we will end up making a net profit, and finding a new element with strictly less Dirichlet energy and strictly less length. This will then contradict the assumption that (B, X) was an

Alt minimizer.

Let $\rho(s) : [0, w] \rightarrow \mathbb{R}$ be a smooth function which equals 1 on $[w/4, 3w/4]$ and then decays monotonically to zero at 0 and w . Define the surface

$$\Xi(s, t) = \Gamma(s) + t\rho(s - s_1)\nu_\Gamma(s)$$

where $\nu_\Gamma(s)$ is from the Frenet frame of Γ . Then we have

$$\begin{aligned} \Xi_s(s, t) &= \begin{pmatrix} 1 - \kappa_\Gamma(s)\rho(s - s_1)t \\ t\rho'(s - s_1) \\ -T_\Gamma(s)\rho(s - s_1)t \end{pmatrix} \\ \Xi_t(s, t) &= \begin{pmatrix} 0 \\ \rho(s - s_1) \\ 0 \end{pmatrix} \end{aligned}$$

with respect to the Frenet frame $\dot{\Gamma}(s), \nu_\Gamma(s), \eta_\Gamma(s)$ of Γ . (See Section A.1, p. 145, for Frenet differentiation formulas.) The area form is $|\Xi_s \times \Xi_t| = \rho(s - s_1) + O(t)$. For small positive t_I we may thus consider the surface parameterized by Ξ on $[s_1, s_2] \times [0, t_I]$. Our first modification (“modification I”) to (B, M) is to add a surface component attached to the wire on $[s_1, s_2] \subset \text{dom } \Gamma$, parameterized by Ξ . (Formally, we pull back Ξ to the appropriate disc in the unit circle, so that our modification obeys the rules of Definition 2.3.) This modification affects the area and thread length of (B, M) as follows:

$$\begin{aligned} (\Delta \text{ Area})_I &= \int_{s=s_1}^{s_2} t_I \rho(s - s_1) ds + O(\max(w, t_I)^2) \\ (\Delta \text{ Thread Length})_I &= - \int_{s=s_1}^{s_2} t_I \kappa_\Gamma(s) \rho(s - s_1) ds + O(\max(w, t_I)^2). \end{aligned} \tag{3.4}$$

We perform a second modification (“modification II”) of (B, M) near our pre-selected point $M(q)$. The surface is real-analytic near $M(q)$ and is locally a graph over its tangent plane V . (Here we use (3.3) to rule out branch points.) Let w be small enough so $\gamma(s), |s| \leq w$ lies in this local picture. Let $\nu_\gamma(0)$ be the outer side-normal to the surface at $\gamma(0)$. We may modify M near q by retracting it inward along itself. This gives sends each point $\gamma(s)$ on the thread curve to a new point $\tilde{\gamma}(s)$. Specifically, we modify M so

$$\langle \tilde{\gamma}(s) - \gamma(s), \nu_\gamma(0) \rangle = -t_{II}\rho(s).$$

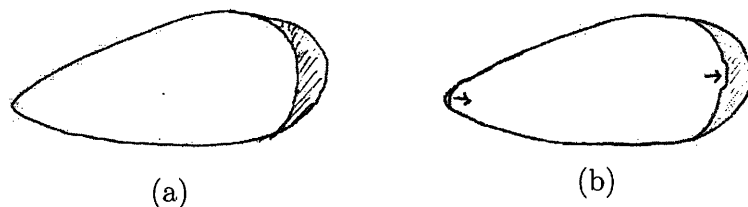


Figure 3-2: Thread-Bearing-Wire Curvature Bound variation.. If an element in Alt's set has a region of wire which is more curved than the free thread curvature (as in the left part of (a)), then we may create a new surface component in this region and diminish an existing surface component to reduce the overall area.

where t_{II} is a small positive constant to be determined later. We may then calculate the effects of this second modification on total area and total thread length:

$$\begin{aligned} (\Delta \text{Area})_{II} &= - \int_{s=0}^w t_{II} \rho(s) ds + O(\max(w, t_{II})^2) \\ (\Delta \text{Thread Length})_{II} &= \int_{s=0}^w t_{II} \kappa \rho(s) ds + O(\max(w, t_{II})^2) \end{aligned} \quad (3.5)$$

Combining (3.4) and (3.5) we see that the total effect of our modifications is:

$$\begin{aligned} \Delta \text{Area} &= (t_I - t_{II}) \int_{s=0}^w \rho(s) ds + O(\max(w, t_I, t_{II})^2) \\ \Delta \text{Thread Length} &= \int_{s=0}^w (t_I \kappa_{\Gamma}(s_1 + s) - t_{II} \kappa) \rho(s) ds + O(\max(w, t_I, t_{II})^2). \end{aligned} \quad (3.6)$$

By choosing $t_{II} = (1+c/2)t_I$ and then making t_I and w sufficiently small, we may ensure that the net affect is a decrease in total area and an increase in total thread length. Using Morrey's ϵ -conformal lemma we may reparameterize to translate our decrease of area into a decrease of Dirichlet energy. (See Lemma 2.13.) This contradicts the assumption that (B, M) is a minimizer of Dirichlet energy in Alt's set $\mathcal{C}(\Gamma, L)$. We conclude that there does not exist any positive length arc of Γ on which κ_{Γ} exceeds κ .

■

3.2 The Gauss image of a crescent

Stability of classical minimal surfaces was profitably studied by pulling back normal variations to the Gauss sphere via the Gauss map (see [2]). In this section we describe

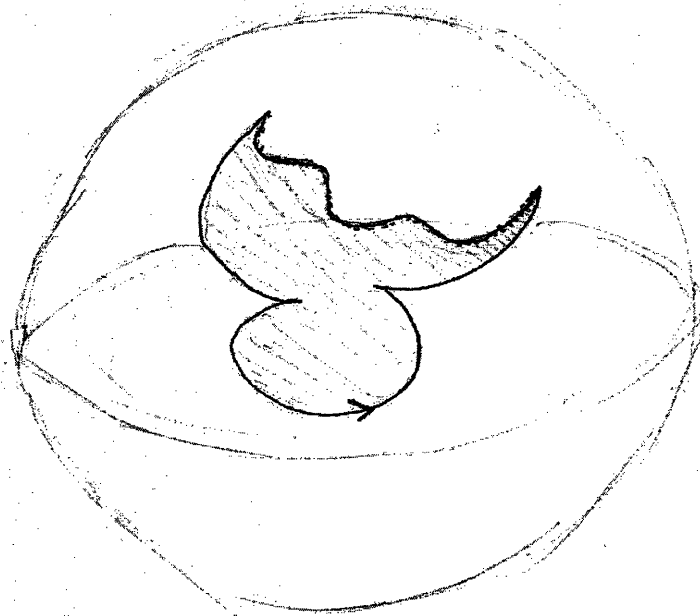


Figure 3-3: Gauss image of thread. In this diagram, the slightly dotted curve is the Gauss image of the wire, and the cusped curve with the arrow is the Gauss image of the thread. We see that the Gauss image of the thread always turns left and towards the Gauss image of the interior of the surface. Cusps occur in the thread's Gauss image when the torsion of the thread changes signs. In the diagram we do not show any branch points in the Gauss map, although these may occur on the interior or at the boundary. They may occur when the Gauss curvature of the surface vanishes.

the Gauss image of an Alt crescent. We show that the Gauss image of the thread always turns convexly—towards the Gauss image of interior crescent points near the thread boundary. The only exception to this is when the thread torsion is zero; then the Gauss image of the thread curve may have non-convex cusps. See **Figure 3-3**.

Let (X, ϕ_-) be an Alt crescent. For this section we assume that X does not have any branch points. This assumption is valid for near-wire crescents. (See Slicewise Parametrization Lemma (Lem. 4.4).) Let Σ refer to the immersed surface parametrized by X . We may then define a manifold (Δ, h) with metric h being the pull-back along X of the standard metric on \mathbb{R}^3 .

In this section we adopt the notation g for the Gauss map: that is, for each $x \in \Delta$, we get a unit vector $g(x) \in S^2(1)$ normal to Σ at $X(x)$. We refer to the unit sphere $S^2(1)$ as the Gauss sphere. We use the standard outward normal vectorfield to make

$S^2(1)$ an oriented manifold. Let $\phi_+ : \partial_+\Delta \rightarrow \mathbb{R}$ be a bijection reparametrizing the free thread:

$$\gamma(\phi_+(x)) = X(x)$$

for $x \in \partial_+\Delta$ so that $\gamma(s)$ is parametrized by arclength. Then $N(s) = g((\phi_+)^{-1}(s))$ is the corresponding field of normal vectors. Because of the Lagrange multiplier condition on the free thread, the Frenet frame of the thread curve aligns with the surface Σ . We have that the Frenet normal to the curve $\nu(s)$ is the sidenormal of the surface at $\gamma(s)$. Finally, we orient the surface Σ by picking a normal vectorfield which at the thread boundary equals the binormal of γ .

Standard differential geometry tells us for $s \in (0, \ell(\gamma))$:

$$\begin{aligned} \langle N'(s), \eta(s) \rangle &= \frac{1}{2}(\langle N(s), N(s) \rangle)_s = 0 \\ \langle N'(s), \nu(s) \rangle &= T_\gamma(s) \\ \langle N'(s), \gamma'(s) \rangle &= \frac{1}{2}(\langle N(s), \gamma'(s) \rangle)_s - \langle N(s), \gamma''(s) \rangle = 0 \\ N'(s) &= T_\gamma(s)\nu(s), \end{aligned}$$

and along $\partial_+\Delta$:

$$\begin{aligned} \langle \nabla_\nu N, \eta \rangle &= \frac{1}{2} \nabla_\nu \langle N, N \rangle = 0 \\ \langle \nabla_\nu N, \nu \rangle &= -\text{II}(\nu, \nu) = 0 \\ \langle N_\nu, \gamma' \rangle &= -\text{II}(\nu, \gamma') = T \\ \nabla_\nu N &= T\gamma'. \end{aligned}$$

Here ∇ is the Levi-Civita connection of the metric h . It is defined on $\partial_+\Delta$ because the Alt crescent may be continued across the thread boundary as a minimal surface.

So the thread maps to the Gauss sphere with velocity $T_\gamma(s)\nu(s)$. We care how the points on Σ near the thread boundary map near the Gauss image of the thread boundary. The basic idea is that the Gauss map is orientation-reversing (the determinant of its Jacobian is the Gauss curvature of Σ which is almost everywhere negative). Thus we expect the interior of Σ , which lay to the *right* of the thread $\gamma(s)$ as it moved in the direction of increasing s , to lie on the *left* of the Gauss image of the thread curve as it moves in the direction of increasing s .

We may see this directly in our coordinate system, using the orientations chosen

above. Our coordinate system on Σ has the the thread oriented so the interior of the surface is to its right—in the $-\nu$ direction—as it moves in the direction of positive s . We see that points near the thread on the surface map to the Gauss sphere so they lie in the $dg(-\nu) = -T_\gamma\gamma'$ direction from the thread. (Here dg is the differential of the Gauss map g .) Now for $x \in \partial_+^o\Delta$ and $s = \phi_+(x)$,

$$dg_x(\gamma'(s)) \times dg_x(-\nu(s)) = -T_\gamma(s)^2\nu(s) \times \gamma'(s) = T_\gamma(s)^2g(x).$$

The normal vector $g(x)$ points outward from the Gauss sphere at the base point $g(x)$. So for $T_\gamma(s) \neq 0$, the above equation shows that $dg_x(-\nu(s))$ points to the right of $dg_x(\gamma'(s))$. In other words, points nearby the thread boundary get mapped to lie on the right of the oriented curve $g(\partial_+\Delta)$. We can also detect the effect g has on orientation: the ordered basis $(\gamma'(s), -\nu(s))$ is negatively oriented on the immersed Alt crescent because

$$\gamma'(s) \times (-\nu(s)) = -g(x).$$

The image of this basis under dg_x gives a pair which is positive oriented, because its cross product $T_\gamma(s)^2g(x)$ points outward (for $T_\gamma(s) \neq 0$).

What is the curvature of the Gauss image of the thread, defined by the curve $\xi : s \mapsto N(s)$? For $s \in [0, \ell(\gamma)]$ and $x = \partial_+^{-1}(s)$ we calculate

$$\begin{aligned} \kappa_\xi(s) &= \left\langle \frac{1}{|T_\gamma(s)|} \left(\frac{N'(s)}{|T_\gamma(s)|} \right)', \frac{-N_\nu(x)}{|N_\nu(x)|} \right\rangle \\ &= \left\langle \frac{N''(s)}{T_\gamma(s)^2}, \frac{-N_\nu(x)}{|N_\nu(x)|} \right\rangle \\ &= -\frac{1}{T_\gamma(s)|T_\gamma(s)|} \langle N''(s), \gamma'(s) \rangle \\ &= \frac{1}{T_\gamma(s)|T_\gamma(s)|} \langle N'(s), \gamma''(s) \rangle = \frac{\kappa}{|T_\gamma(s)|}. \end{aligned}$$

Here $N_\nu(x)$ is short for $\nabla_\nu N$ at x . This gives us the curvature measured relative to the inward side normal of the Gauss image of $\partial_+^o\Delta$. So the image of the thread always turns left—towards the Gauss image of the interior of the thread surface. See **Figure 3-3**.

3.3 Convex hull results for thread-wire surfaces

The following follows by applying the Maximum Principle:¹

Lemma 3.3. If $Y \in C^0(\Delta) \cap C^2(\Delta^\circ)$ is a minimal surface, then it lies within the convex hull of its boundary:

$$Y(\Delta) \subset \text{Convex Hull}(Y(\partial\Delta)).$$

In this section we show that a stronger enclosure results holds for an Alt minimizer—the minimizer lies in the convex hull of *just the wire part* of its boundary.

Theorem 3.4. [TWS Convex Hull] Let $\mu = (X, \phi_-)$ be an Alt crescent with non-negative free thread curvature. Then the surface $X(\Delta)$ lies in the convex hull of supporting wire $\Gamma(\text{Im } \phi_-)$.

Proof. It will suffice to show that the thread curve lies in the convex hull of the wire curve. Indeed, we have

$$X(\partial_+\Delta) \subset \text{Convex Hull}(\partial_-\Delta) \quad \text{implies} \quad X(\Delta) \subset \text{Convex Hull}(\partial\Delta) = \text{Convex Hull}(\partial_-\Delta) \quad (3.7)$$

by Lemma 3.3.

When the free thread curvature κ of (X, ϕ_-) is zero, the free thread is a straight segment. We thus fulfill the condition of (3.7) and our lemma follows. Otherwise, we have by Lemma 3.1 that $\kappa > 0$. Consider a point $p \in \partial_+\Delta$ parametrizing a thread point $X(p)$. Let F be an arbitrary linear function on \mathbb{R}^3 . By (3.7), proving our lemma reduces to showing

$$F(X(p)) < \max_{\partial_-\Delta} F \circ X. \quad (3.8)$$

We do this by showing that the harmonic function $h = F \circ X$ does not attain a local maximum at p . To see this, extend h across the boundary $\partial_+\Delta$ near p . It has an expansion whose lead term in a homogeneous harmonic polynomial $P(x, y)$. If this polynomial is degree 2 or higher, it is easy to find larger values of h by moving into the interior of Δ from p . If $P(x, y)$ is linear, then consider $(\nabla h)(p)$. If this vector does not point normally out of Δ , then we may move along a path in Δ from p and find h increasing to first order. If this vector points normally out of Δ , then we may use the fact that $\kappa > 0$ to show that as we move along $\partial\Delta$ away from p , we have h increasing to second order. ■

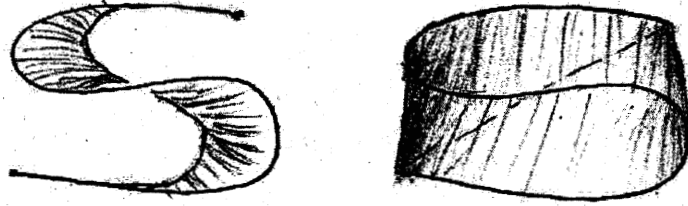


Figure 3-4: Alt crescent lies in convex hull of supporting wire. On the left we show an example of an Alt crescent. On the right we show the convex hull of its supporting wire.

See **Figure 3-4**. As an aside, we show a slightly more complicated property for the adjoint surfaces to Alt crescents. An adjoint surface to (X, ϕ_-) is a map $X^* : \Delta \rightarrow \mathbb{R}^3$ where the respective components of X^* are harmonic conjugates of the components of X . We do not use adjoint surfaces elsewhere in this thesis. See **Figure 3-5** and **Figure 3-6**.

Theorem 3.5. [TWS Adjoint Convex Hull] Let $\mu = (X, \phi_-)$ be an Alt crescent with positive free thread curvature κ . Let X^* be a minimal surface adjoint to X . Then by previous work,² the adjoint thread $X^*|_{\partial_+\Delta}$ is a curve lying in a sphere S of radius κ^{-1} and centered at some point p . We show the surface $X^*(\Delta)$ lies in the convex hull of the adjoint wire $X^*(\partial_-\Delta)$ union $\{p\}$.

Proof. Following the reasoning at the beginning of the previous proof, we reduce to having to show for arbitrary linear function F and $p \in \partial_+^o$:

$$F(X^*(q)) \leq \max(F(p), \max_{\partial_-\Delta} F \circ X^*). \quad (3.9)$$

To see this, extend h across the boundary $\partial_+\Delta$ near q . It has an expansion whose lead term in a homogeneous harmonic polynomial $P(x, y)$. If this polynomial is degree 2 or higher, it is easy to find larger values of h by moving into the interior of Δ from q . If $P(x, y)$ is linear, then consider $(\nabla h)(q)$. If this vector does not point normally out of Δ , then we may move along a path in Δ from q and find h increasing to first order. If this vector points normally out of Δ , then we may conclude that the outer normal ν

¹See, for example, [5, p. 369, Cor. 1].

²See [6, p. 275, Thm. 2] and [6, p. 281, Lem. 4].

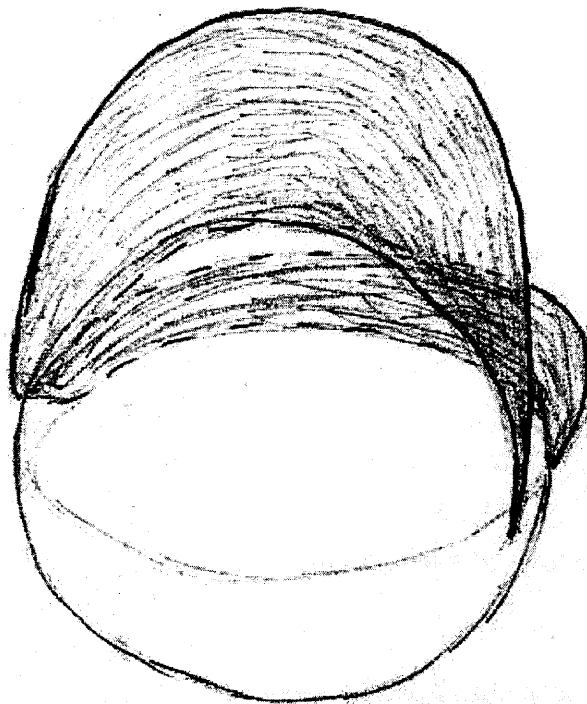


Figure 3-5: The adjoint of an Alt crescent, satisfying the adjoint convex hull property. Here we see a adjoint surface of the one shown in **Figure 3-4**. It is a stationary point of the free boundary problem for surfaces bounded by the adjoint wire and a curve lying in the surface of the sphere. Experimentally this can be realized with wire, a glass sphere, and soap-water. In the diagram, we see that the surface lies in the convex hull of its wire and the center of the sphere.

at $X^*(q)$ satisfies

$$(D_\nu F) > 0.$$

Then the Lagrange multiplier condition for the adjoint surface [6, p. 275] dictates that ν points from $X^*(q)$ towards the center p of the sphere. We have

$$F(p) = F(X^*(q)) + \kappa^{-1} D_\nu F > F(X^*(q)).$$

We have thus shown (3.9), and our result follows. ■

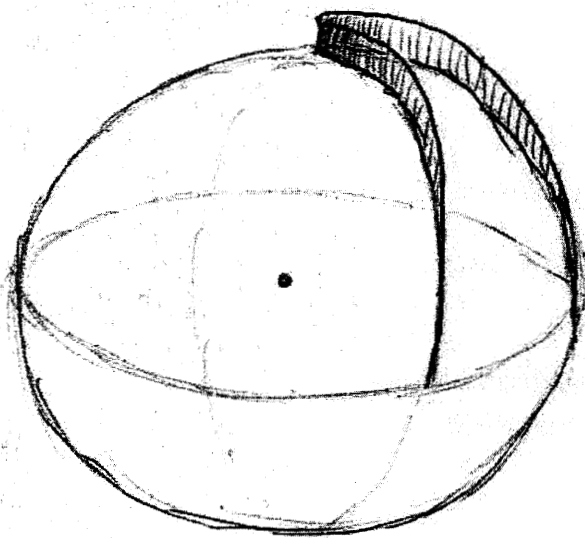


Figure 3-6: An adjoint surface of an Alt crescent, which does not lie in the convex hull of its supporting wire. This is a surface which satisfies the adjoint free boundary problem. If Y is a harmonic, conformal parametrization of this surface, then the adjoint surface $X = -Y^*$ is a stationary thread-wire surface. We see that Y lies in the convex hull of its supporting wire and the center of the sphere. However, it does *not* lie in the convex hull of just its supporting wire. This suggests the necessity of including the sphere's center in TWS Adjoint Convex Hull Theorem (Thm. 3.5).

3.4 How planes may intersect crescents

In this section we investigate what the intersection between a plane and an Alt minimizer can look like. Essentially, we show that if a connected component of the intersection contains finitely many wire points, then that component has the structure of a finite graph. Moreover, this graph can only touch the thread curve in one point. We state the full lemma below. The full statement is more technical. It only requires knowledge about how a compact piece of the plane intersects the wire. Moreover, there is a technical issue which arises in the case that the free thread curvature is zero.

Lemma 3.6. [Intersection Graph] Let Γ be an embedded nonplanar C^1 wire curve. Let V be a plane in \mathbb{R}^3 .

- (a) Let W be a compact subset of V which Γ intersects at most a finite number m times.
- (b) Let (X, ϕ_-) be an Alt crescent with $\text{Im } X$ disjoint from $\partial_V W$ (the boundary of W in the topology of V).

(See **Figure 3-7.**) Then the pre-image $X^{-1}(W)$ has at most m connected components. Each connected component is either

- (i) a single point of $\partial_- \Delta$, or
- (ii) a finite tree graph
 - (a) with all interior nodes having even valence of at least 4,
 - (b) with at least one node on $\partial_- \Delta$,
 - (c) with at most one node on $\partial_+ \Delta$.
- (iii) a set containing all of $\partial_+ \Delta$. Moreover, in this case, the free thread curvature of (X, ϕ_-) is zero.

In particular, if $\kappa > 0$ and $m = 0$, then the Alt minimizer does not touch the set W . If $\kappa > 0$ and $m \leq 2$, then the pre-image $X^n(W)$ has no interior nodes; this implies that the interior of the Alt crescent $(X|_{\Delta^\circ})$ never osculates the set W .

In this lemma, case (ii) is by far the most important. Case (iii) is only relevant in the special case where the free thread curvature is zero and the free thread consists of straight segments.

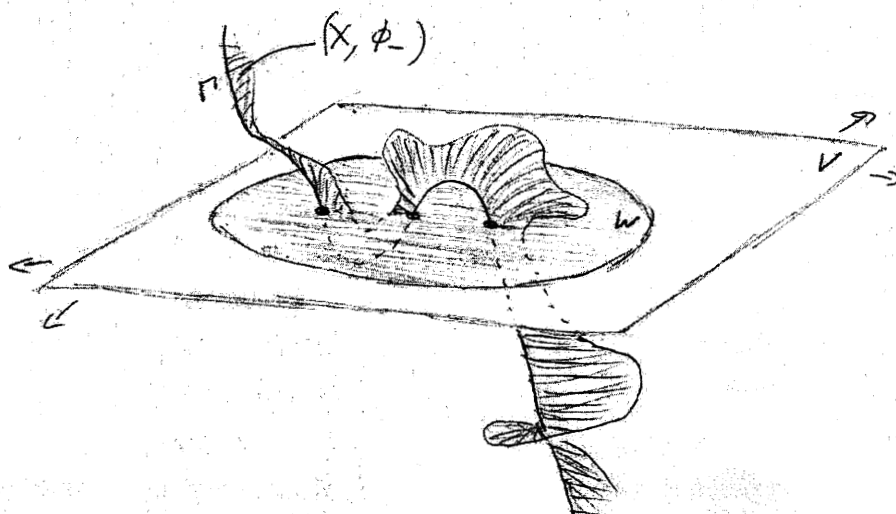


Figure 3-7: Conditions for Intersection Graph Lemma (Lem. 3.6).

We may reduce the proof of this lemma to a statement about the level sets of harmonic functions on the unit disc. Below we prove the relevant lemma. Then we prove the Intersection Graph Lemma.

3.5 Level sets of harmonic functions on the disc

Consider a minimal surface $Y : \Delta \rightarrow \mathbb{R}^3$ spanning a contour. Let us cut this surface with a plane, expressed as $F = a$ for F a linear function on \mathbb{R}^3 . Assume that Y is parametrized conformally and harmonically on Δ° , so as to minimize Dirichlet energy. Then we may pull back a linear function F by Y to obtain a function $F \circ Y$ on Δ which is harmonic on Δ° . The intersection of the minimal surface with the plane is parametrized by Y on the subdomain $F \circ Y = a$.

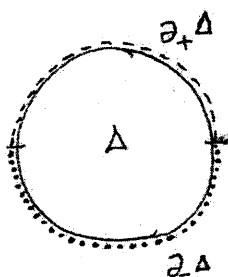
In this context, Radó's lemma helps us understand intersections between planes and minimal surfaces.

Lemma 3.7. [Radó's lemma]³ If $h : \Delta \rightarrow \mathbb{R}$ is harmonic in Δ° and if its derivatives vanish to orders $0, 1, \dots, m$ at some point $p \in \Delta^\circ$, then h changes sign on $\partial\Delta$ at least $2(m+1)$ times.

³See [5, p. 272]. For more about Radó's work, see [24].

Roughly speaking, the idea of Radó's lemma is that the level set $h = 0$ looks like a graph. The graph cannot have cycles (closed loops) because then by the Maximum Principle an entire open set would have $h = 0$, whence by analytic continuation h vanishes on all of Δ . Since the graph does not have cycles, we expect that an interior zero of order $m + 1$ —which gives a node with valence $2(m + 1)$ —propagates outward to force at least $2(m + 1)$ sign changes on the boundary. The type of result we need is similar, but it has a special condition on the top boundary $\partial_+\Delta$ of the unit disc. There we assume that h does not achieve any strict local extrema. Under that assumption, we are able to guarantee a certain number of sign changes on the lower boundary $\partial_-\Delta$.

The following lemma characterizes a level set $h = a$ of a harmonic function h on the unit disc Δ . It is written in a form that allows it to be applied when we know properties of h only for a part U of the level set. To understand the essence of the lemma, the reader may find it helpful to read it in the case that U is the entire level set. Our final preparation is to clarify some notation in **Figure 3-8** and the following definition.



$$\partial_+\Delta: y \geq 0 \text{ on } \partial\Delta$$

$$\partial^o_+\Delta: y > 0 \text{ on } \partial\Delta$$

$$\partial_-\Delta: y \leq 0 \text{ on } \partial\Delta$$

$$\partial^o_-\Delta: y < 0 \text{ on } \partial\Delta$$

Figure 3-8: Arcs of the unit circle.

Definition 3.8. A **(planar) graph** is a set of points V (**nodes**) in \mathbb{R}^2 and a set of continuous curves (**edges**) from V to V . We allow multiple edges to connect the same pair of nodes and to connect a node to itself. The **valence** of a node is the number of edges emanating from it. We assume that every node has valence at least 1. A graph is a **tree graph** if it is connected and simply connected.

Lemma 3.9. [Harmonic Level Set] Let $h \in C^0(\Delta, \mathbb{R})$ be harmonic and real-analytic on $\Delta \setminus \partial_-\Delta$. Let U be a nonempty union of connected components of a level set $h = a$ on Δ . Assume that:

- (a) The function h is nonconstant on $\partial_+\Delta$ and does not attain any local extrema on the domain Δ at points of the set $\partial^o_+\Delta$. In other words, for each point p in $\partial^o_+\Delta$ and each neighborhood \mathcal{N} of p in Δ ,

$$\min_{\mathcal{N}} h < h(p) < \max_{\mathcal{N}} h.$$

(b) We have $h = a$ at only m points of $U \cap \partial_- \Delta$.

Then U consists of at most m connected components. Each component P is either a single point on $\partial_- \Delta$ or is a planar graph

- (i) which is a finite tree graph,
- (ii) with all interior nodes having even valence of at least 4,
- (iii) with at least one node on $\partial_- \Delta$,
- (iv) with at most one node on $\partial_+ \Delta$.

In this section we prove the Harmonic Level Set Lemma by proving several supporting lemmas.

Lemma 3.10. Let $h \in C^0(\Delta, \mathbb{R})$ be a nonconstant function which is harmonic and real-analytic on $\Delta \setminus \partial_- \Delta$. Then

- (i) the level set $h = a$ cannot contain a Jordan curve.

Moreover, if assumption (a) of Harmonic Level Set Lemma (Lem. 3.9) holds then:

- (ii) the level set $h = a$ cannot contain a curve $\gamma : [0, b] \rightarrow \Delta$ mapping $(0, b)$ to Δ° and $0, b$ to $\partial \Delta$.

Proof. If the level set did contain a Jordan curve, then the interior of the Jordan curve would be an open set V for which $h = a$ on ∂V . Then by the Maximum Principle, we would have $h \equiv a$ on V . By analytic continuation we get $h \equiv a$ on Δ , contrary to assumption. So the level set did not contain a Jordan curve in the first place.

As for (ii), we again have an open set V formed by the curve and the top boundary $\partial_+ \Delta$. We again apply the Maximum Principle. To avoid the contradiction that threatened to occur in the previous paragraph, an extremal value other than a must be attained by h on ∂V . This means that ∂V attains an extremal value for V on $\partial V \cap \partial_+^o \Delta$. But then assumption (a) of the Harmonic Level Set Lemma has been violated. ■

Lemma 3.11. Let $h \in C^0(\Delta, \mathbb{R})$ be harmonic and real-analytic on $\Delta \setminus \partial_- \Delta$. Let P be a connected component of the level set $h = a$ on Δ which intersects $\partial_- \Delta$ at only finitely many points. Then P is a planar graph in the following sense. Let N be the set of critical points of h in $\Delta \setminus \partial_- \Delta$. Let B_- be the (finite) set of places where $h = a$ on $\partial_- \Delta$. Let B_+

be the places where $h = a$ on $\partial_+^o \Delta$ and $\nabla h \neq 0$. Let E be the remainder of P . Then E is a disjoint union of continuous curves with ends in $N \cup B_- \cup B_+$. The curves are real-analytic on their interiors, and they remain real-analytic up to any end points lying in $N \cup B_+$. The valence of any node of P in Δ^o is at least 4.

Proof. Let E be the subset of $P \setminus \partial_- \Delta$ where ∇h is non-zero. Let N be the remainder of P , where ∇h vanishes. For each $n \in N$ not lying in $\partial_- \Delta$, we examine the convergent expansion for h near n . The lead term must be a homogeneous harmonic polynomial⁴ $\text{Real}(az^k)$, for a a nonzero complex number and $k \geq 2$.⁵ It is easy to show that in some “nodal” neighborhood U_n of n , P has the structure of a graph which consists of $2k \geq 4$ edges, each connecting n to a point in ∂U_n . Now consider a point $e \in E$. For ϵ a small positive value, let W^ϵ be the set of points x of Δ not lying in any nodal neighborhood U_n and having $(\nabla h)(x)$ exceeding ϵ . For sufficiently small ϵ , there is a connected component C_ϵ^ϵ of $E \cap W^\epsilon$ containing e . Applying the Implicit Function Theorem to h at each point of $\overline{C_\epsilon^\epsilon}$ and taking a finite subcover, we conclude that C_ϵ^ϵ is a continuous curve from ∂W^ϵ to itself. As we let ϵ decrease, we obtain extensions of this curve. For each end of the curve, one of two things happens.

- (i) Either at some value of ϵ the curve touches a boundary of a nodal neighborhood U_n for some n . In this case we can use our analysis of h in U_n to demonstrate that the curve in this direction connects the point e to the node n .
- (ii) Case (i) never occurs as ϵ goes to zero. In case (ii), we have that the curve terminates closer and closer to $\partial_- \Delta$. By the compactness of $\partial \Delta$, it must have limit point(s) on $\partial \Delta$. Can it have more than one? Say it did, at q_1, q_2 . Then by assumption (b) of Harmonic Level Set Lemma (Lem. 3.9), we can draw a segment on Δ from $\partial_+^o \Delta$ to a point q^* in $\partial_-^o \Delta$ between q_1 and q_2 with $h(q^*) \neq a$. By construction, the curve C_ϵ^ϵ crosses this segment at an infinite sequence of distinct places as ϵ goes to zero. These intersections must accumulate somewhere on the segment. But they cannot: not at q^* because $h(q^*) \neq a$ and h is continuous; not elsewhere on the segment by real analyticity of h . So the curve C_ϵ^ϵ approaches a unique limit point as ϵ goes to zero.

⁴The $\text{Real}()$ function extracts the real part of a complex number.

⁵We cannot have $k = 0$ because then by analytic continuation, h would be constant on all of Δ ; this would violate both assumptions (a) and (b) of the Harmonic Level Set Lemma (Lem. 3.9).

We have shown that P consists of interior nodes N , boundary nodes B_-, B_+ , and a set E which decomposes into continuous curves connecting these nodes. Curves which connect $N \cup B_+$ to $N \cup B_+$ stay a positive distance from $\partial_- \Delta$ and so are real-analytic.

■

Lemma 3.12. Let $h \in C^0(\Delta, \mathbb{R})$ be harmonic and real-analytic on $\Delta \setminus \partial_- \Delta$. Let U be a union of some connected components of the level set $h = a$ which intersects $\partial_- \Delta$ in at most finitely many places. Consider the set Z defined by either $h \geq a$ in U or $h \leq a$ in Δ . Let p be any point on ∂Z in Δ° . Then there is a continuous simple curve $\gamma : [-1, 1] \rightarrow \partial Z$ which passes through p at $\gamma(0)$ and intersects $\partial \Delta$ at two places, $\gamma(1)$ and $\gamma(-1)$.

Proof. We define the curve γ iteratively. For $k = 1, 2, \dots$, consider Z restricted to the closed disc $L_k = B(0, 1 - 1/(2k))$ centered on the origin. Say that L_{k_0} contains p . Then for $k \geq k_0$, the set $L_k \cap \partial Z$ has a graph structure inherited from that of P . We may trace ∂Z from p in either direction, following an edge to a new node in each step. Operating in this way we can never encounter a node we've already been to, for that would imply a closed loop in the $h = a$ level set and would violate Lemma 3.10.(i). Moreover, our operation must end after finitely many steps because there are only finitely many nodes in L_k . (Indeed, nodes are zeroes of ∇h , which is real analytic up to the boundary of L_k .) In this way we can define a curve $\gamma_k : [-(1 - 1/(2k)), 1 - 1/(2k)] \rightarrow \partial Z \cap L_k$ which is continuous and non-self-intersecting and has $\gamma_k(0) = p$. Moreover, we can define such a curve so γ_{k+1} extends γ_k . Taking γ to be the limit of such curves, we obtain a curve defined on $(-1, 1)$. Now consider the sequence $\gamma(1 - 1/(2k))$. It must approach a point b^* of B arbitrarily closely. Moreover, it cannot have two points of B as limit points. Indeed, construct a circle C^* about b^* cutting it off from the other points of B . Then γ cannot intersect C^* infinitely many times, because these intersection points would have to accumulate and they can't (not in the interior of Δ by real analyticity of h , and not at $C^* \cap \partial \Delta$ because $h \neq a$ there). We conclude that $\gamma(s)$ stays inside C^* after sufficiently large s , and converges to b^* . Similarly we can show that $\gamma(s)$ converges as s goes to -1 .

■

Lemma 3.13. Let γ, p, Z be as in Lemma 3.12. Additionally assume that Lemma 3.10.(ii) holds. Then the curve γ may be extended to a curve γ_2 which exhausts the component of ∂Z containing p and has at most one endpoint in $\partial_+ \Delta$.

Proof. Let C_Z be the component of ∂Z containing C . Applying Lemma 3.12 to each point of $C_Z \cap \Delta^\circ$, we get many curves lying in ∂Z . Observing Lemma 3.10, we see that they must join together to form a curve which does not self-intersect, touches $\partial_- \Delta$ at most once in each of the finitely many points of B , and touches $\partial_+ \Delta$ at most once. ■

We may now marshal our supporting lemmas to prove the main analytic result of this section: Harmonic Level Set Lemma (Lem. 3.9).

Proof–Lemma 3.9. We consider the component P defined in the lemma. There are several cases.

- (i) The component P does not venture into the interior of the unit disc. Then it is a closed arc of $\partial \Delta$, possibly degenerate. If its intersection with $\partial_+^o \Delta$ is an arc of positive length, then by analytic continuation we can show that h is constant on $\partial_+ \Delta$; this contradicts assumption (a). Combining this observation with assumption (b) of the Harmonic Level Set Lemma, we see that P must be a point in $\partial \Delta$. It cannot be a point in $\partial_+^o \Delta$, because then if we study the expansion for h at P , we see that the only way to achieve a single point level set is for h to have ∇h non-zero and be perpendicular to $\partial \Delta$. But that would then violate assumption (a) of the Harmonic Level Set Lemma. So we conclude that if the component P does not contain points of Δ° ; it must consist of a single point of $\partial_- \Delta$.
- (ii) The alternative is that P contains a point in Δ° . By Lemma 3.11, the set P has a graph structure. We demonstrate that it in fact is a finite tree graph. First pick an edge point $e \in P \cap \Delta^\circ$ and apply Lemma 3.13. For $\epsilon > 0$, we can consider the connected component P_ϵ of e in P restricted to the shrunken unit disc $B(0, 1 - \epsilon)$. Because of the real analyticity of h , edges and nodes of P_ϵ cannot accumulate; therefore, it has the structure of a finite graph. Applying Lemma 3.10 we see that P_ϵ does not have cycles, and so is a tree graph. Moreover, by applying Lemma 3.12 we are able to take P_ϵ and augment it by extending each node on $\partial B(0, 1 - \epsilon)$ and each edge exiting through $B(0, 1 - \epsilon)$ by a path which reaches a point on $\partial \Delta$. These paths do not intersect each other or P_ϵ , at peril of violating the first part of Lemma 3.10. Also, the augmented P_ϵ touches $\partial_+ \Delta$ at most once, at peril of violating the second part of Lemma 3.10. In this way we see that P_ϵ has been augmented by adding at most $m + 1$ paths where m is the finite number of times that h attains a on $\partial_- \Delta$. Since P_ϵ is a tree graph with interior node

valence of at least 4 (see Lemma 3.11), this means that P_ϵ has n_N nodes and n_E edges bounded like

$$1 + 3n_N \leq m + 1 \quad 1 + 4n_N \geq 2n_E.$$

For $\epsilon' < \epsilon$, the graph $P_{\epsilon'}$ extends the graph P_ϵ . But the number of nodes and edges of P_ϵ is uniformly bounded. So for sufficiently small ϵ , the augmented graph of P_ϵ has no nodes of P on the augmenting paths. We thus show that P is a finite tree graph. Moreover, it must touch $\partial_+\Delta$ at most once. This then forces P to touch $\partial_-\Delta$ at least once.

This completes our proof of Harmonic Level Set Lemma (Lem. 3.9). ■

With the Harmonic Level Set Lemma (Lem. 3.9) in hand, we may prove the main geometric result of this section.

Proof–Lemma 3.6. Consider an Alt crescent (X, ϕ_-) . Define the function $h = F \circ X$. It is harmonic (and therefore real-analytic) on Δ° because F has constant derivative and X is harmonic. We get that it is harmonic and real-analytic on $\partial_+\Delta$ because the Alt minimizer is real-analytic on the interior of the free thread and can be extended real-analytically across the boundary as a minimal surface (Theorem 2.11). If h is constant on $\partial_+\Delta$ then the free thread lies in a plane. This means it has torsion $T_\gamma \equiv 0$. If the free thread curvature κ is nonzero, then we may look at the expansion of the surface at a non-branch point on the interior of the thread and show that the surface is locally planar. (See the proof of Series Solutions to ThIP problem Theorem (Thm. B.6, p. 168).) By analytic continuation the whole Alt crescent is planar, contrary to assumption. We conclude that if h is constant on $\partial_+\Delta$ then the free thread curvature is not positive; by Lemma 3.1 we must have $\kappa = 0$. This establishes conclusion (iii) of the lemma we are proving. Otherwise, we may assume that h is nonconstant on $\partial_-\Delta$.

Next we show that conclusion (ii) of Lemma 3.10 holds. If there were any path γ in the level set $h = a$ beginning and ending in $\partial_+\Delta$, with its interior lying in Δ° , then its image $X \circ \gamma$ is a curve lying in the plane $F = a$. Let U be the region of with nonempty interior defined by γ and $\partial_+\Delta$. By TWS Convex Hull Theorem (Thm. 3.4), the piece of surface $X|_U$ is planar. By analytic continuation, the whole crescent is planar, contrary to assumption. So we see that conclusion (ii) of Lemma 3.10 holds. It suffices to show that this condition holds, instead of showing that condition (a) of Harmonic Level Set

Lemma (Lem. 3.9) holds. The reason this suffices is that the proof of Harmonic Level Set Lemma only depends on the conclusion Lemma 3.10.(ii).

Condition (b) of the Harmonic Level Set Lemma is already met by assumption (a) of Intersection Graph Lemma (Lem. 3.6). We have thus confirmed that the function f satisfies the conditions of Harmonic Level Set Lemma. Now we define U to be the preimage $X^{-1}(W)$. We would like to show that U is a union of connected components of the level set $f^{-1}(a) = X^{-1}(V)$. It suffices to show for each $q \in U$ that the connected component C'_q of q in U is the same as the connected component C_q of q in the entire level set.

We have that

$$C_q = \bigcap_S S$$

where S are sets in $X^{-1}(V)$ which contain q and are simultaneously open and closed (*open-and-closed*) in the $X^{-1}(V)$ topology. Now consider the operations on subsets $S \subset X^{-1}(V)$,

$$\begin{aligned}\pi_1(S) &= S \cap X^{-1}(W) \\ \pi_2(S) &= S \cap X^{-1}(W \setminus \partial_V W).\end{aligned}$$

The first sends closed subsets to closed subsets as W is compact; the second sends open subsets to open subsets (it can be rewritten as the pre-image of set which is open in \mathbb{R}^3). But because we assume that $X^{-1}(\partial U)$ is empty, these are actually the same operation, which we can call π . The map π sends sets open-and-closed subsets of $X^{-1}(V)$ to possibly smaller open-and-closed subsets of $X^{-1}(V)$. Moreover, if S contains q then $\pi(S)$ will contain q . We obtain

$$C_q = \bigcap_{S'} S' = C'_q$$

where S' are open-and-closed subsets of $X^{-1}(W)$ which contain q . This confirms that $C_q = C'_q$. And so we know that the set U defined above is indeed a union of connected components of the level set $f^{-1}(a)$.

Having verified that the conditions of the Harmonic Level Set Lemma are all met, we may now employ its conclusions about U , which is a union of connected components of $X^{-1}(V)$. They are exactly sufficient for our purposes. ■

Chapter 4

Near-wire Crescent Theorem

In this section we use the plane-crescent intersection analysis of the last section to control the geometry of Alt minimizers which are near the wire. By the end of the section we prove Near-wire Crescent Theorem (Thm. 1.4). This theorem was stated in the Introduction; we reprint it here.

Theorem 4.1. [Near-wire Crescent] Let Γ be an embedded generic wire in \mathbb{R}^3 . For R less than a constant $R(\Gamma)$ depending on the geometry of Γ , the following will hold. If A is any Alt minimizer lying in an R tubular neighborhood of the wire, then the thread of A is C^1 and touches the interior of Γ only tangentially. Each crescent μ of A satisfies the following.

- (i) The wire supporting the crescent μ is short (arclength bounded by $C(\Gamma)R^{1/12}$).
- (ii) Let $\Gamma(s_0)$ be a corner of μ on the interior of Γ . Then s_0 is within $C(\Gamma)R^{1/12}$ of a maximum of wire curvature.
- (iii) Let x, y, z be the Frenet coordinates of Γ at $\Gamma(s_0)$. Then the crescent μ may be expressed as a graph

$$z = f(x, y)$$

over a domain with $y \geq 0$. See **Figure 4-1**. Here f is a Lipschitz function

$$|(\nabla f)(x, y)| < C(\Gamma)R^{1/12}$$

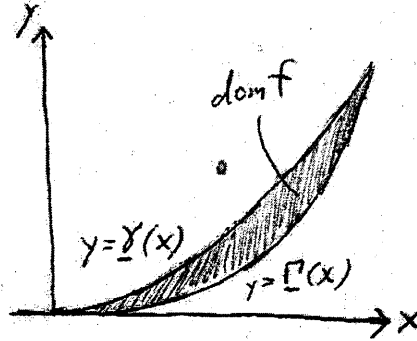


Figure 4-1: Crescent as a graph in Frenet coordinates. The crescent μ vertically projects to a domain $\text{dom } f$ lying in either the first or second quadrant of the x - y plane. The boundary of the domain is defined by the **wire shadow curve** $y = \Gamma(x)$ and **thread shadow curve** $y = \gamma(x)$. The domain tapers to a cusp at the origin: $0 \leq \Gamma(x) \leq \gamma(x) \leq \kappa x^2 + o(x^2)$.

with additional slope control

$$|f_x(x, y)| < C(\Gamma)x.$$

- (iv) Where the wire supports the crescent μ , κ_Γ is within $C(\Gamma)R^{1/12}$ of the free thread curvature κ .
- (v) The Frenet frame of the thread is within $C(\Gamma)R^{1/12}$ of the Frenet coordinates x, y, z .

Definition 4.2. If Γ is an embedded wire loop, we say its tubular neighborhood does not **self-intersect** if it decomposes into slices: disjoint discs $D(s)$, each passing through Γ perpendicularly at $\Gamma(s)$. If Γ is an embedded wire which is not an embedded wire loop, then we say its tubular neighborhood does not self-intersect if it decomposes into normal discs $D(s)$ and a half-ball at each endpoint of Γ .

Definition 4.3. Consider an Alt minimizer (B, M) which lies strictly within a tubular R -neighborhood of an embedded wire Γ . Let R be sufficiently small that the tubular neighborhood does not **self-intersect**. We may extend the arclength coordinate s on Γ perpendicularly along the slices to obtain a function $\hat{s} : \bigcup_{s \in \text{dom } \Gamma} D(s) \rightarrow \mathbb{R}$ with

$$\hat{s} = s \text{ on } D(s).$$

REMARK. If we pick an orthonormal frame $E_1(s), E_2(s)$ of vectors along Γ which span the orthogonal complement to $\Gamma'(s)$ at $\Gamma(s)$, then we may write the exponential map $\exp : \mathbb{R}^2 \times \text{dom } \Gamma \rightarrow \mathbb{R}^3$ as

$$\exp(x, y, s) = xE_1(s) + yE_2(s) + \Gamma(s).$$

We are working with cases where \exp is an embedding on $B_{\mathbb{R}^2}(0, R) \times \text{dom } \Gamma$ and where the Alt minimizer lies in the image of this embedding. Actually it would be natural to work in the case where R is just small enough that \exp is an *immersion* and the Alt minimizer map $X : B \rightarrow \mathbb{R}^3$ can be factored through the exponential map. This is advantageous because it allows us to prove results about self-intersecting curves. It is even useful for embedded curves, because the relevant geometric quantity to our estimates is the more forgiving “immersive” injectivity radius, not the “embedding” injectivity radius. In a previous version of this thesis, all results were proved in the immersive case. However, the author decided to present the embedded point of view because the proofs are much easier to read.

A priori, a near-wire Alt crescent could be a very complicated beast, intersecting itself in a swirling surface which could range far up and down the tubular enclosure, far from its supporting wire. It could also have branch points. See **Figure 4-2**. The next lemma tames such potential behavior. It shows that the domain of X can be split into continuous curves which correspond bijectively with the slices of the tubular neighborhood corresponding to the supporting wire. See **Figure 4-3**.

Lemma 4.4. Let Γ be an embedded wire curve. Let R be small enough so that the R -tubular neighborhood of Γ does not self-intersect. Let (X, ϕ_-) be an Alt crescent lying in this tubular neighborhood, supported on the interval of wire parametrized by $\text{Im } \phi_- = [s_0, s_1]$.

Proof. When the wire curve is planar, the Alt crescent is planar by TWS Convex Hull Theorem (Thm. 3.4). This case is easy; in the remainder of the proof we assume that Γ is nonplanar.

As we saw in Definition 4.2, when the wire Γ is an embedded loop, its tubular neighborhood decomposes into normal discs. If Γ is an embedded wire which is not

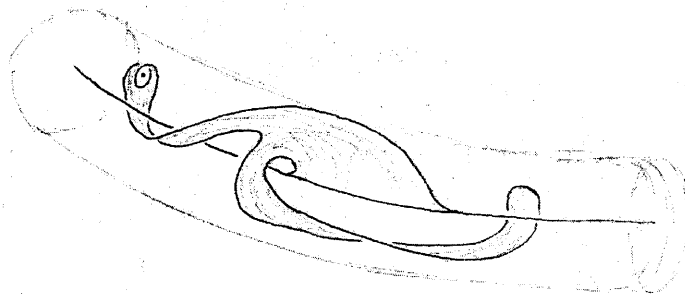


Figure 4-2: Near-wire Alt minimizers could be quite wild, a priori. A near-wire Alt minimizer could intersect itself, range far up and down the wire's tubular enclosure, and have branch points.

an embedded loop, then its tubular neighborhood decomposes into normal discs and two half-balls. In this case, however, the Alt crescent still lies in the union of normal discs, $\text{dom } \hat{s}$ (Definition 4.3), for if it protruded into either half-ball, we could project it back to the bounding disc of the half-ball and reduce both area and thread-length. This would yield a contradiction (Lemma 2.13). So whether the embedded wire is a loop or not, we have

$$\text{Im } X \subset \text{dom } \hat{s}.$$

Pulling back the extended arclength parameter function \hat{s} by X decomposes the domain Δ of X into connected level sets. Only values $\hat{s} \in [s_0, s_1]$ occur. The level sets for $\hat{s} \in (s_0, s_1)$ are continuous curves of positive length. The level sets $\hat{s} = s_0, s_1$ are points $(1, 0)$ or $(-1, 0)$. We prove this lemma by applying Intersection Graph Lemma (Lem. 3.6). For each $s \in \text{dom } \Gamma$, we consider the normal disc $D(s)$. This is a compact subset of a plane, and it intersects the plane in exactly one point, $\Gamma(s)$. The Alt crescent (X, ϕ_-) is disjoint from the circle bounding $D(s)$ because it lies strictly within the tubular neighborhood $\text{Tub}_R \Gamma$. By Intersection Graph Lemma (Lem. 3.6), the set $X^{-1}(D(s))$ is either

- (i) a single point $q \in \partial_- \Delta$, or
- (ii) a connected set whose only component is a finite tree graph. This graph can only touch $\partial_- \Delta$ at one point: $\phi_-^{-1}(s)$. The properties (a)-(c) listed under item (ii) in Intersection Graph Lemma (Lem. 3.6) force the graph to be a segment connecting $\phi_-^{-1}(s)$ in $\partial_- \Delta$ to a point in $\partial_+ \Delta$.

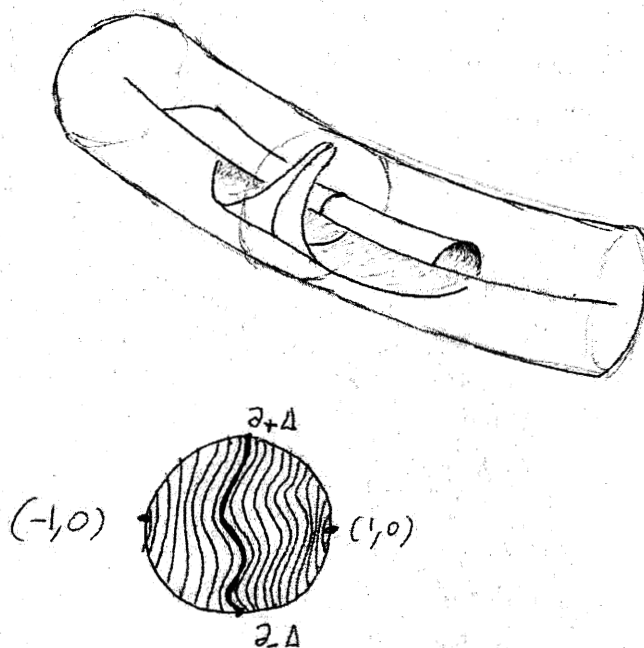


Figure 4-3: Slicewise Parametrization Lemma (Lem. 4.4) tames the potential behavior of an Alt minimizer. Here we see that the Alt minimizer only lies in slices of the tubular neighborhood which pass through its supporting wire. We may pull back the arclength function s of Γ , extended along these slices as \hat{s} , back to the domain of X and we get continuous curves.

- (iii) a set which contains $\partial_+\Delta$; moreover in this case we also have that the free thread curvature vanishes. But that means that the entire free thread for this crescent lies in the normal disc $D(s_0)$. This normal disc only intersects the wire at $\Gamma(s_0)$. So we have $\Gamma(\phi_-((-1,0))) = \Gamma(\phi_-((1,0)))$ which violates the embeddedness of Γ . We conclude that case (iii) cannot occur.

Thus we see that each level set contains a point of $\partial_-\Delta$. The map ϕ_- gives a bijection between $\partial_-\Delta$ and $[s_0, s_1]$; thus we see that Δ decomposes into level sets of $X^{-1}(\hat{s})$ for $s \in [s_0, s_1]$. We claim that item (i) cannot occur for $q \in \partial_-\Delta$; indeed in that case we could decompose $\Delta \setminus \{q\}$ into two non-empty open sets $(X \circ \hat{s})^{-1}([s_0, s])$ and $(X \circ \hat{s})^{-1}((s, s_1])$. But a disc minus a boundary point is connected! So case (i) can only occur for $q = (1,0), (-1,0)$. Moreover, it must occur for each of these points; if the level set $(X \circ \hat{s})^{-1}(s_0)$ were a curve from $(-1,0)$ to $\partial_+\Delta$ then we would violate Lemma 3.10. ■

We have thus decomposed the domain of X into two points and a family of curves that map to slices $D(s)$ corresponding to the supporting wire. This controls the behavior of the Alt crescent better (indeed, compare **Figure 4-2** with **Figure 4-3**) but we will go much farther. Subsequent lemmas in this section will show that these slice-wise curves join together to form a Lipschitz graph with nice properties.

Our main tool for controlling first-order properties of the Alt crescent is the following.

Lemma 4.5. [Normal Avoidance] Let Γ be a nonplanar embedded wire curve. Let R be small enough so that the tubular neighborhood of Γ does not self-intersect. Consider a single point $\Gamma(s_0)$ on the curve. Let Ω be an open subset of the unit sphere with the following property:

- For every plane V passing through $D(s_0)$ with normal vector in Ω , the component of $V \cap \text{Tub}_R \Gamma$ containing $\Gamma(s_0)$ intersects Γ at most twice.

Then if (B, M) is an Alt minimizer on Γ lying in $\text{Tub}_R(\Gamma)$ with positive free thread curvature, then any points of (B, M) lying in $D(s_0)$ must have normal vectors *not in* Ω .

Proof. Say a plane V with normal in Ω were the tangent plane to an Alt minimizer (B, M) at a point $X(p)$ for $p \in B^\circ$. Then by definition of Ω , the plane V intersects the wire at most twice. We may then apply the Intersection Graph Lemma (Lem. 3.6) to conclude that it is not a tangent plane of (B, M) . This shows that Gauss map g_M maps the interior of B to the complement of Ω . But then because g_M is continuous and Ω is open, we know that the image of g_X on its full domain¹ lies outside Ω . ■

Before embarking on our quest to control the Gauss image of the near-wire crescents, we must handle a technicality. In Lemma 3.1 we showed that Alt minimizers have free thread curvature $\kappa \geq 0$. For near-wire Alt minimizers we may improve this:

Lemma 4.6. Let Γ be a nonplanar embedded C^1 wire curve. There is an $R(\Gamma) > 0$ so if (B, M) is an Alt minimizer in $\text{Tub}_R(\Gamma)$, then the free thread curvature κ of (B, M) is positive.

Proof. See Lemma A.11 (p. 164) and Lemma 2.13. ■

¹Remember: the domain of the Gauss map excludes crescent corners.

4.1 Slope bound in Γ' direction

Lemma 4.7. [Bound on Γ' -Slope] Let Γ be an embedded C^2 Frenet wire curve. There is a constant $R(\Gamma)$ depending only on the geometry of Γ so for $R < R(\Gamma)$ if an Alt crescent (X, ϕ_-) lying in the R tubular neighborhood of Γ , it has a slope bound. Specifically, for any point $X(p)$ on the thread-wire surface, the unit normal vector $g_X(p)$ lies in a strip in the Gauss sphere:

$$| \langle g_X(p), \Gamma'(\hat{s}(X(p))) \rangle | < C(\Gamma)R^{1/2}. \quad (4.1)$$

The slicewise extended arclength function \hat{s} is explained in Definition 4.2.

Proof. The case where Γ is planar is easy. (See TWS Convex Hull Theorem (Thm. 3.4).) For the remainder of the proof we assume that Γ is nonplanar. Choose $C(\Gamma) = 3 + |\kappa_\Gamma|_{C^0(\text{dom } \Gamma)}$. Pick $R(\Gamma)$ small enough so the $R(\Gamma)$ -tubular neighborhood of Γ does not intersect itself and so the free thread curvature κ is positive. (See Lemma 4.6.) Also pick R small enough so that at any point $\Gamma(s)$ on the curve, the conditions of **Figure 4-4** hold:

- The curve Γ is a graph over the x axis for $|x| < R^{1/2}$, (Or, if it fails to be a graph, it does so because the curve has ended within this domain.)
- The curve Γ lies in a quadratic trumpet Q defined by

$$\sqrt{y^2 + z^2} < |\kappa_\Gamma|_{C^0(\text{dom } \Gamma)} x^2$$

out to $|x| = R^{1/2}$. (This is generous; the asymptotic relation holds with a multiplier of $1/2$.)

Then $\text{Tub}_R \Gamma$ lies in $\text{Tub}_R Q$. A plane V with normal lying in the spherical strip (4.1) has entirely left $\text{Tub}_R Q$ at $x = \pm R^{1/2}$ and is guaranteed to be strictly more than $(3 + |\kappa_\Gamma|_{C^0(\text{dom } \Gamma)})R$ distance from the x -axis, whereas $\text{Tub}_R Q$ lies strictly within this distance on $|x| = R^{1/2}$. (Or it might not reach all the way to $x = R^{1/2}$ or $x = -R^{1/2}$; this makes our life even easier.²) Also, for small enough $R(\Gamma)$ we may ensure that V intersects the piece of wire in $|x| < R^{1/2}$ in at most one place. We have thus satisfied the conditions of the Normal Avoidance Lemma (Lem. 4.5). See **Figure 4-5**. This completes our proof the Bound on Γ' -Slope Lemma (Lem. 4.7). ■

²The reason this case is easier is that then we do not have to worry about how the Alt crescent intersects the cut off tubular neighborhood in that direction.

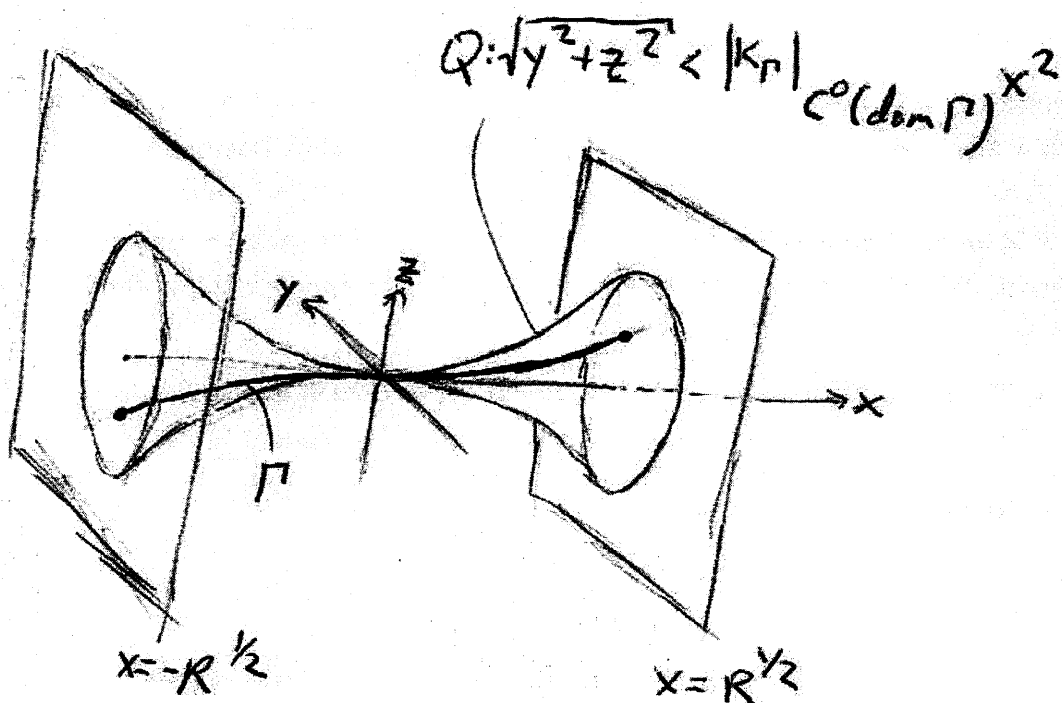


Figure 4-4: Slope bound in Γ' direction. Illustration for the Bound on Γ' -Slope Lemma (Lem. 4.7). Note that the wire curve might not always reach all the way to the two planes. If so, that just makes the estimate easier.

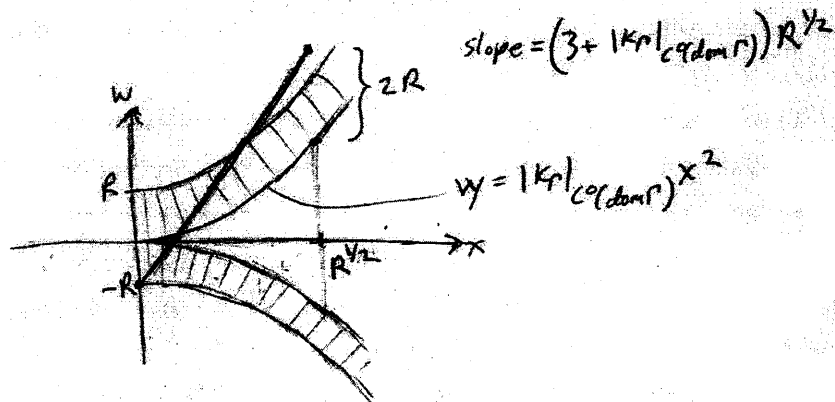


Figure 4-5: Slope bound in Γ' direction, part II.. Here the x axis is the same as in **Figure 4-4** and w measures in the direction of the normal to V . We show the worst case, where the plane V is based least advantageously in the normal disc of the tubular neighborhood. Even in this case we show that the plane V avoids the end of $\text{Tub}_R Q$, for R sufficiently small relative to the geometry of Γ .

4.2 Slope bound in ν_Γ direction

Lemma 4.8. [Bound on ν_Γ -Slope] Let Γ be an embedded C^3 Frenet wire curve or loop. There is a constant $R(\Gamma)$ depending only on the geometry of Γ so for $R < R(\Gamma)$, if an Alt crescent (X, ϕ_-) with positive free thread curvature lies in the R tubular neighborhood of Γ , it has a slope bound. Specifically the Gauss image of points of the Alt crescent lying in normal disc $D(s)$ lies outside the open diamond region $\diamond_{\psi_1, \psi_2}$ shown in **Figure 4-6**, and lies outside its antipodes $-\diamond_{\psi_1, \psi_2}$. Here

$$\psi_1 = C(\Gamma)R^{1/3}, \quad \psi_2 = \frac{\pi}{2} - C(\Gamma)R^{1/3}. \quad (4.2)$$

Proof. The case where Γ is planar is easy. (See TWS Convex Hull Theorem (Thm. 3.4).) For the remainder of the proof we assume that Γ is nonplanar. Take any $s_0 \in \text{Im } \phi_-$. Then $\Gamma(s_0)$ is on part of the wire which supports the crescent X . The idea of this proof is to construct planes passing through the normal disc $D(s_0)$ of the tubular neighborhood which, restricted to $\text{Tub}_R(\Gamma)$, intersect the wire at most twice and satisfy the conditions of the Normal Avoidance Lemma (Lem. 4.5).

As usual, we require that R be small enough so that the R -tubular neighborhood of Γ does not self-intersect and so the free thread curvature of (X, ϕ_-) is positive. (See Lemma 4.6.) We begin with the central geometric picture of the proof, shown in **Figure 4-7**. Here we have adopted Frenet coordinates at $\Gamma(s)$. Pick $R(\Gamma)$ small enough so that Γ is a graph over the x -axis for $|x| < R^{1/3}$. (As before, it may be that the curve does not reach all the way to $|x| = R^{1/3}$ because s is close to the boundary of $\text{dom } \Gamma$. This will only make our job easier. In this proof we treat the case that the wire reaches all the way to $|x| = R^{1/3}$.)

Define the parabola

$$P(x) = \left(x, \frac{1}{2}\kappa_\Gamma(s_0)x^2, 0\right).$$

Define cubes C_\pm centered at $P(\pm R^{1/3})$ which are oriented rectilinearly with respect to coordinate basis and have side length equal to twice

$$\rho_C = \left(\frac{|\Gamma'''|_{C^0(\mathcal{S}_\Gamma)}}{3} + 2\right) R.$$

Let Q be the solid square $\{(x, y, z) \mid x = 0, |y| \leq R, |z| \leq R\}$.

Subclaim 4.9. If V is a plane passing through Q with normal in $\diamond_{\psi_1, \psi_2}$, then:

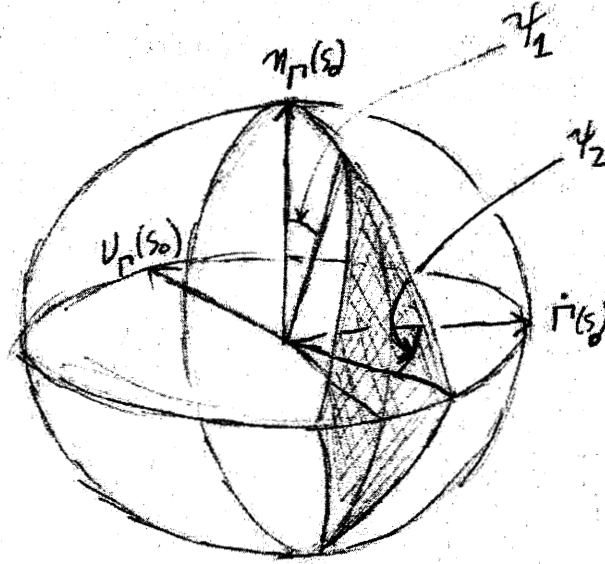


Figure 4-6: Diamond region for ν_Γ slope limitation. Normal vectors of the part of X associated to each normal disc $D(s_0)$ are prohibited from lying inside this geodesic diamond region $\diamond_{\psi_1, \psi_2}$.

- (i) The plane V does not intersect the interior of the cubes C_\pm .
- (ii) The plane V intersects the local piece of wire (parameterized on $|x| < R^{1/3}$) at most twice.
- (iii) The normal discs $D(s_\pm)$ corresponding to $x = \pm R^{1/3}$ lie within the respective cubes C_\pm .

Before proving the claim, we need to do some further visualization to understand the relationship between **Figure 4-7** and **Figure 4-6**.

Consider the points

$$\begin{aligned}
 a &= (0, -R, R) \\
 b &= (-R^{1/3} - \rho_C, \frac{1}{2}\kappa_\Gamma(s)R^{2/3} - \rho_C, \rho_C) \\
 c &= (R^{1/3} + \rho_C, \frac{1}{2}\kappa_\Gamma(s_0)R^{2/3} - \rho_C, \rho_C) \\
 d &= (R^{1/3} + \rho_C, \frac{1}{2}\kappa_\Gamma(s_0)R^{2/3} - \rho_C, -\rho_C)
 \end{aligned}$$

See **Figure 4-8**. Let V_1 be the plane defined by the points a, b, c and V_2 be the plane defined by points a, c, d . **Figure 4-9** and **Figure 4-10** show the top- and side-views of **Figure 4-8**. Direct calculation verifies that the angles ψ_1, ψ_2 defined in (??) measure the slopes of V_1 and V_2 as shown. This means that the normal vectors of V_1 and V_2 appear as points of the diamond $\diamond_{\psi_1, \psi_2}$. Reflecting the planes gives the other two corner points.

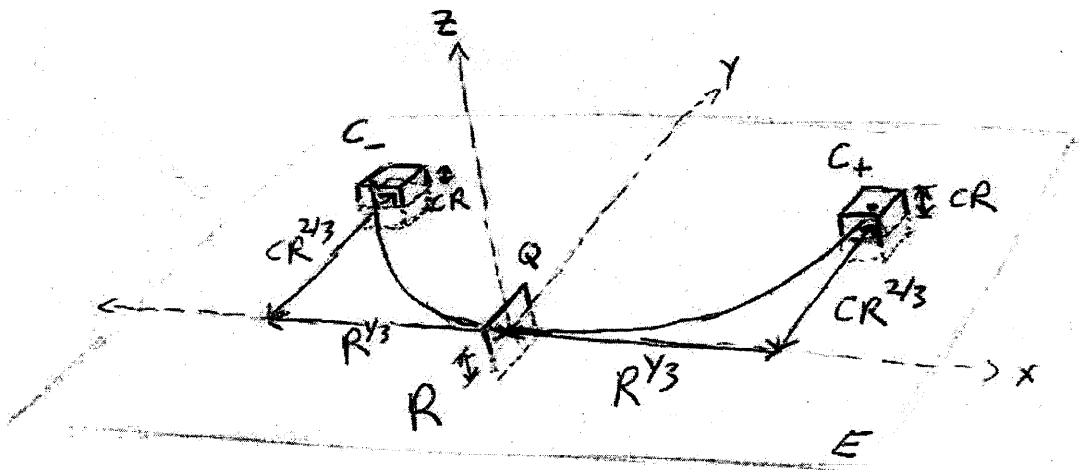


Figure 4-7: The setup for the Bound on ν_T -Slope Lemma (Lem. 4.8).

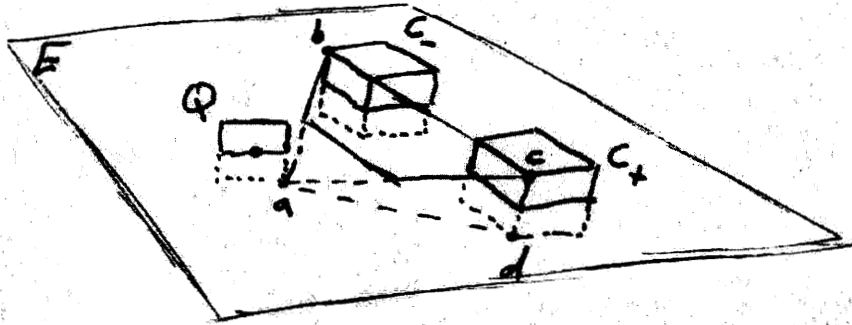


Figure 4-8: Consider the plane V_1 containing the triangle abc and the plane V_2 containing the triangle acd .

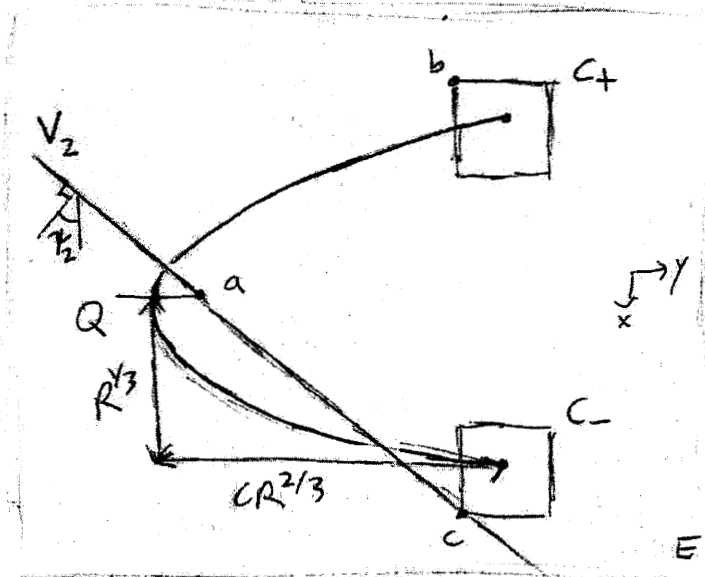


Figure 4-9: Top view.

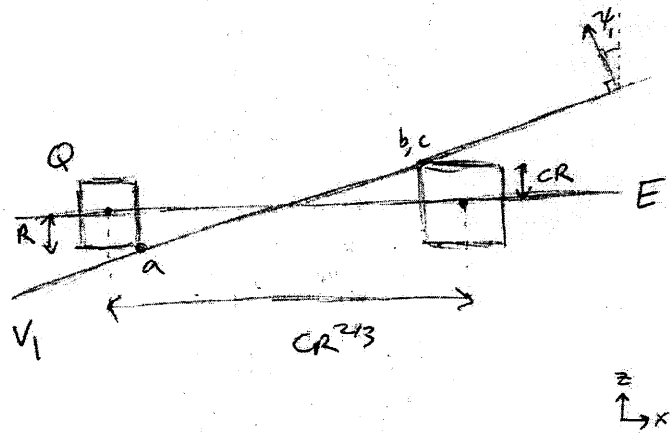


Figure 4-10: Side view.

Now let's prove Subclaim 4.9.(i). As we mentioned, the planes V_1 and V_2 have normal vectors corresponding to two corners of the diamond. Continuously transforming V_1 to V_2 by rotating it around the line \overleftrightarrow{ac} traces out a family of planes which also avoid the interior of the two cubes. Their normal vectors trace out the geodesic on the Gauss sphere from the normal of V_1 to the normal of V_2 . Translating this family of planes in the negative y direction only makes it farther from the cubes. So we see that if any point in Q has a plane passing through it with normal in this geodesic boundary of the diamond, the plane misses the interior of the cubes. By similar arguments we can show that if any plane passes through a point of Q and has normal in the boundary of the diamond, then it misses the interior of the cubes. The final step is to take any point $q \in Q$ and consider two planes W_1, W_2 with normals n_1, n_2 in the boundary of the diamond, which pass through q . They intersect in a common line ℓ_3 , which contains q . By continuously rotating W_1 into W_2 around line ℓ_3 , we trace out a path of normal vectors which is a geodesic on the Gauss sphere. If we do this along the shortest geodesic, then the associated planes also miss the interiors of the cubes. In this way we can fill in the geodesic diamond. In other words we show that given any plane passing through q with normal in the solid diamond, that plane misses the interiors of the cubes. See **Figure 4-11**. We have shown Subclaim 4.9(i).

As for Subclaim 4.9.(ii), for small R relative to the geometry of Γ , the quadratic y component of the wire dominates and these planes cannot intersect the wire at more than two places.

Finally, Subclaim 4.9.(iii) follows from the Taylor expansion of the wire, where R is sufficiently small relative to the geometry of Γ . We may now apply the Normal Avoidance Lemma (Lem. 4.5).

The estimates of (4.2) follow from evaluating the slope of reference plane V_1 in the $x - z$ direction and the plane V_2 in the $x - y$ direction. See **Figure 4-9** and **Figure 4-10**. This completes our proof of the Bound on ν_Γ -Slope Lemma (Lem. 4.8).
■

This lemma prohibits the Gauss image from being in a diamond which gets arbitrarily close to the poles of the Frenet unit sphere, but at the same time narrows in the Γ' direction. The reader may not think that this is very useful! In the next section we see the spherical band of the Γ' slope narrows faster than the diamond does. Combining the two lemmas yields a meaningful control on the Gauss image.

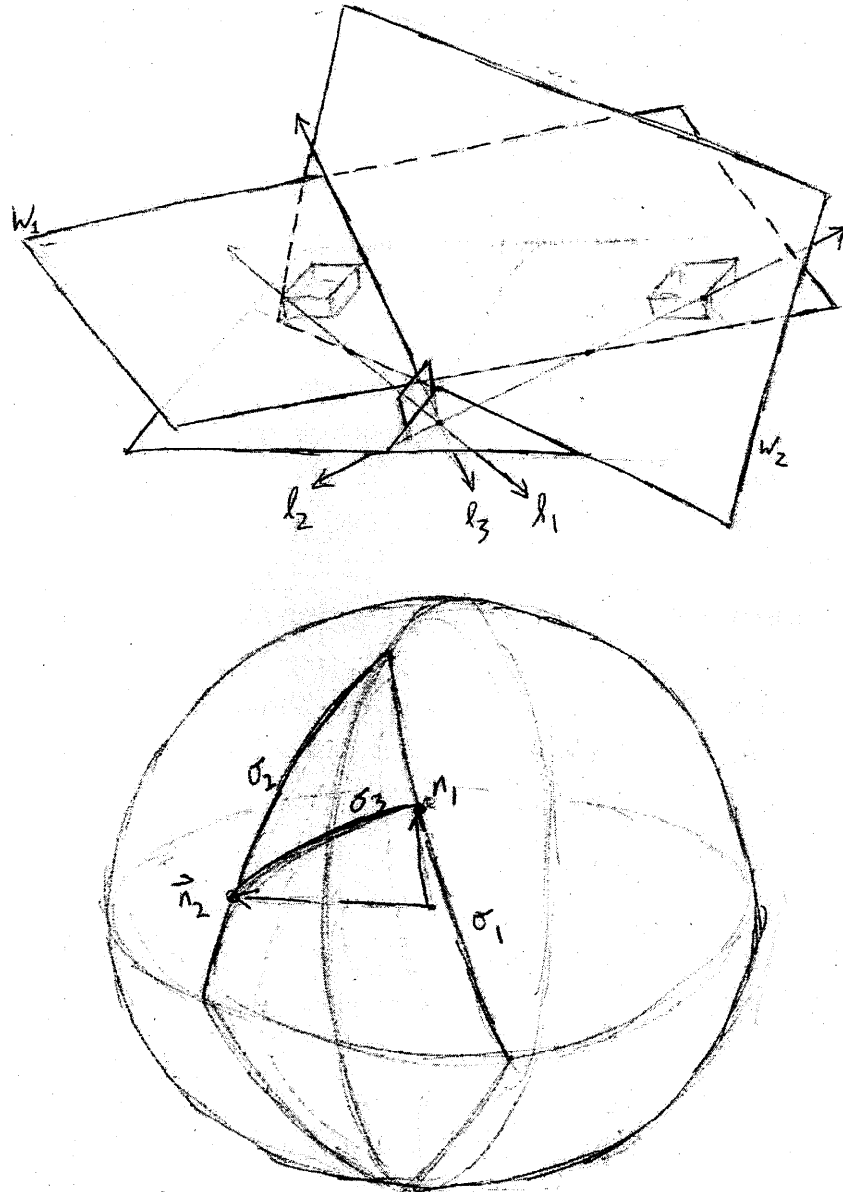


Figure 4-11: Filling in the diamond. We show an example where q lies on the positive y edge of the square Q . The two planes W_1, W_2 have normals n_1, n_2 and touch the cubes in the lines l_1, l_2 . Rotating these planes on l_1, l_2 defines the geodesic boundaries of the diamond σ_1, σ_2 . We may rotate W_1 into W_2 along their common line l_3 ; this causes the normal to move along the geodesic σ_3 on the Gauss sphere. In this way we may “fill in” the diamond of prohibited normal vectors of tangent planes.

4.3 Lipschitz graph in varying Frenet frame

We use the preceding results to control the slopes of the surface and the Frenet frame of the thread relative to the Frenet frame of a nearby wire point.

Definition 4.10. Let $(\sigma_s(s), \nu_\sigma(s), \eta_\sigma(s))$ and $(\tau_t(t), \nu_\tau(t), \eta_\tau(t))$ be the Frenet frames of two Frenet curves at s and t . We define the **distance between** these two frames by comparing corresponding vectors:

$$\text{distance} = |\sigma_s(s) - \tau_t(t)| + |\nu_\sigma(s) - \nu_\tau(t)| + |\eta_\sigma(s) - \eta_\tau(t)|.$$

Lemma 4.11. [Varying Frenet Frame Graph] Let Γ be an embedded C^3 Frenet wire curve or loop. For R sufficiently small relative to the geometry of Γ , if $\text{Tub}_R\Gamma$ encloses an Alt crescent $\mu = (X, \phi_-)$, the following holds.

The set $\text{Im } \phi_-$ parameterizes the arc of Γ supporting μ . There are functions $\rho : (\text{Im } \phi_-) \rightarrow \mathbb{R}_{\geq 0}$ and $u : (\text{Im } \phi_-) \times [0, 1] \rightarrow \mathbb{R}$ so that the crescent may be reparametrized as

$$\Xi(s, t) = \Gamma(s) + t\rho(s)\nu_\Gamma(s) + u(s, t)\eta_\Gamma(s) \quad (4.3)$$

for $s \in \text{Im } \phi_-$. Furthermore, the slopes u_s and $u_t/\rho(s)$ are bounded by $C(\Gamma)R^{1/6}$. And the Frenet frame of the thread at $\Xi(s, 1)$ is within distance $C(\Gamma)R^{1/6}$ of the Frenet frame of the wire at $\Gamma(s)$. Furthermore, the Gauss map may be defined continuously for all points on (X, ϕ_-) except the corners. Finally, if the thread returns to the wire at an interior point of the wire ($\rho(s) = 0$ for s in the interior of $\text{Im } \phi_-$), then it does so tangentially.

Proof. The case where Γ is planar is easy. (See TWS Convex Hull Theorem (Thm. 3.4).) For the remainder of the proof we assume that Γ is nonplanar. Let R be sufficiently small relative to the geometry of Γ so the Bound on Γ' -Slope Lemma (Lem. 4.7), the Bound on ν_Γ -Slope Lemma (Lem. 4.8), and Lemma 4.6 apply.

We adopt the coordinates for \mathbb{R}^3 given by the Frenet frame of Γ at s . Consider **Figure 4-12**. The points

$$A = (0, \sin \psi_1, \cos \psi_1) \quad B = (\cos \psi_2, \sin \psi_2, 0)$$

are vertices of the diamond $\diamond_{\psi_1, \psi_2}$. The point $C = (c_1, c_2, c_3)$ is where the spherical geodesic from A to B intersects the right boundary of the strip from the Bound on

Γ' -Slope Lemma (Lem. 4.7). We need to solve for c_3 . The three vectors \vec{OA} , \vec{OB} , \vec{OC} are coplanar so

$$\begin{vmatrix} c_1 & c_2 & c_3 \\ 0 & \sin \psi_1 & \cos \psi_1 \\ \cos \psi_2 & \sin \psi_2 & 0 \end{vmatrix} = 0.$$

We also have from **Figure 4-12** that $c_1 = \sin \varphi$. And of course $|\vec{OC}| = 1$. This gives

$$\begin{vmatrix} \sin \varphi & c_2 & \sqrt{\cos^2 \varphi - c_2^2} \\ 0 & \sin \psi_1 & \cos \psi_1 \\ \cos \psi_2 & \sin \psi_2 & 0 \end{vmatrix} = 0$$

or

$$\sin \varphi \cos \psi_1 \sin \psi_2 + \cos \psi_1 \cos \psi_2 c_2 - \cos \psi_2 \sin \psi_1 \sqrt{\cos^2 \varphi - c_2^2} = 0$$

which gives

$$(\cos^2 \psi_2) c_2^2 - (\sin \varphi \cos^2 \psi_1 \sin 2\psi_2) c_2 + \sin^2 \varphi \cos^2 \psi_1 \sin^2 \psi_2 - \cos^2 \varphi \sin^2 \psi_1 \cos^2 \psi_2 = 0.$$

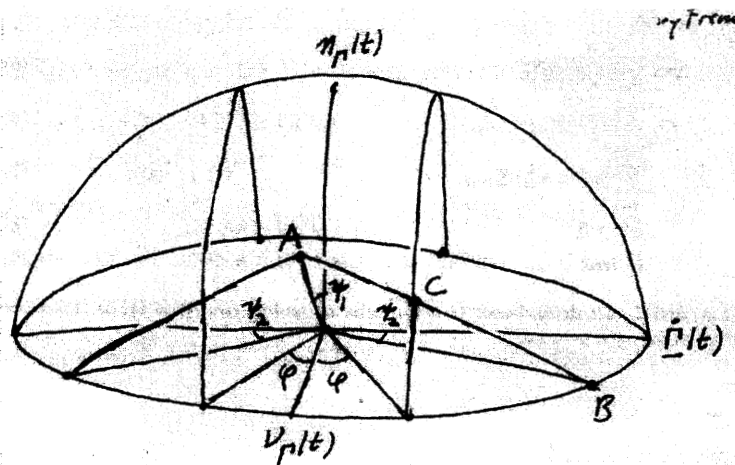


Figure 4-12: Diamond and annulus on sphere. We solve for the location of C , on the spherical geodesic between diamond vertices A and B and on the right boundary of the annular strip.

So the quadratic formula yields

$$2 \cos^2 \psi_2 c_3 = \sin \varphi \cos^2 \psi_1 \sin 2\psi_2 + \left(\sin^2 \varphi \cos^4 \psi_1 \sin^2 2\psi_2 - 4 \cos^2 \psi_2 (\sin^2 \varphi \cos^2 \psi_1 \sin^2 \psi_2 - \cos^2 \varphi \sin^2 \psi_1 \cos^2 \psi_2) \right)^{1/2}$$

Applying the Bound on Γ' -Slope Lemma (Lem. 4.7) and Bound on ν_Γ -Slope Lemma (Lem. 4.8) gives

$$c_2 = O(R^{1/6}).$$

We see that we have a slope bound

$$\tan \alpha(R) = \min \left(\tan \varphi, \frac{c_2}{c_3} \right) = O(R^{1/6}).$$

This means that the slope of any tangent plane to a point on the Alt crescent in the normal disc $D(s)$ has z - y and z - x slopes bounded by $C(\Gamma)R^{1/6}$ where x, y, z are the Frenet coordinates of the wire at $\Gamma(s)$.

The Gauss map is defined on Δ except at $(1, 0)$, $(-1, 0)$ and countably many points of $\partial_- \Delta$. (See p. 27.) At any interior point s of the supporting wire domain $\text{Im } \phi_-$, let $\sigma^s(t)$ parametrize the curve $(X \circ \hat{s})^{-1}(s)$ described in Slicewise Parametrization Lemma (Lem. 4.4). Let $\sigma^s(0)$ be the end lying on $\partial_- \Delta$. Then the analysis of above shows that for $t > 0$, the curve $\sigma^s(t)$ may be parametrized over the $\nu_\Gamma(s)$ axis of $D(s)$ as a C^1 graph with slope bounded by $C(\Gamma)R^{1/6}$.

We claim that the curve σ^s can only lie to the $\nu_\Gamma(s)$ side of $\Gamma(s)$ in the disc $D(s)$. Proving this is easy: in **Figure 4-7** we can clearly bring planes in to touch the wire from the $-\nu_\Gamma(s)$ direction without touching the ends of the enclosures caged in the cubes C_\pm . So by the standard argument (TWS Convex Hull Theorem (Thm. 3.4)) we know that the surface cannot extend in this direction.

We have thus shown that the curve $\sigma^s(0)$ may be reparametrized as a graph over the $\nu_\Gamma(s)$ axis of $D(s)$ for an interval from 0 to some value $\rho(s) > 0$. This justifies the parametrization (4.3). We would now like to show that the function $u(s, t)$ is C^1 up to the $t = 0$ boundary, for $s \in (s_0, s_1)$. For $\Gamma(s)$ where $(\nabla X)(\phi_-^{-1}(s)) \neq 0$, this is easy; the Taylor expansion of X shows that the surface has a tangent plane at $\Gamma(s)$ and is a C^3 graph over it. On the other hand, when $(\nabla X)(\phi_-^{-1}(s)) = 0$, things are less clear. Fortunately, if we look at X near such a point, the above work shows that the surface is

a Lipschitz graph in the Frenet coordinates of Γ at $\Gamma(s)$. We may find a neighborhood \mathcal{N} of q in Δ so $X|_{\mathcal{N}}$ parametrizes a minimal surface bounding a C^4 contour which is a graph over the x - y plane. Then we may solve this non-parametric minimal surface problem (see [15, p. 283, Theorem 11.5]) to obtain a reparametrization of $X|_{\mathcal{N}}$ as a graph over the x - y plane which is $C^{2,\alpha}$. In any case it is C^1 which is all we need to show that u is C^1 up to this point.

Now we show the ρ' bound. We may parameterize the thread as

$$\gamma(\tau) = \Gamma(\tau) + \rho(\tau)\nu_{\Gamma}(\tau) + u(\tau, 1)\eta_{\Gamma}(\tau)$$

with derivative

$$\gamma_{\tau}(\tau) = \Gamma'(\tau) + \rho'(\tau)\nu_{\Gamma}(\tau) + \rho(\tau)\nu'_{\Gamma}(\tau) + u_s(\tau, 1)\eta_{\Gamma}(\tau) + u(\tau, 1)\eta'_{\Gamma}(\tau).$$

Consider a plane V passing through thread at a point $\gamma(s)$ lying in leaf s of the tubular enclosure of Γ . Let $p \in \partial_+^{\circ}\Delta$ be the corresponding point in $\text{dom } X$. Orient V to be perpendicular to the surface's side normal $\nu_{th}(s)$ at q . We know that ν_{th} may not lie in the double disk region of the Bound on Γ' -Slope Lemma (Lem. 4.7), for then pulling V back by X would produce a connected component C_p containing p and only intersecting $\partial_-\Delta$ once. But by construction, the set $X^{-1}(V)$ near p is a line segment which osculates p and otherwise stays in Δ° . By Intersection Graph Lemma (Lem. 3.6), we may trace C_p in either direction from p and hit a distinct point of $\partial_-\Delta$ in each direction. This contradicts the fact that $X^{-1}(V)$ only contains one point of $\partial_-\Delta$ when ν_{th} lies in the double disk region of Bound on Γ' -Slope Lemma (Lem. 4.7).

See **Figure 4-13**. This establishes that $\langle \nu_{th}(s), \Gamma'(s) \rangle$ is bounded by $CR^{1/2}$. Moreover, the slope control shown earlier in the proof establishes that the surface normal $\eta_{th}(s)$ at p is within $CR^{1/6}$ of $\nu_{\Gamma}(s)$.

We may parametrize the thread according to the arclength parameter of Γ in the following way:

$$\begin{aligned} \gamma(s) &= \Gamma(s) + \rho(s)\nu_{\Gamma}(s) + u(s, 1)\eta_{\Gamma}(s) \\ \gamma_s(s) &= \Gamma'(s) + \rho_s(s)\nu_{\Gamma}(s) + \rho(s)(\nu_{\Gamma})_s(s) + u_s(s, 1)\eta_{\Gamma}(s) + u(s, 1)(\eta_{\Gamma}(s))_s \\ \langle \nu_{\Gamma}(s), \gamma_s(s) \rangle &= \rho_s(s) - T_{\Gamma}(s)u(s, 1). \end{aligned} \tag{4.4}$$

Then $|u(s, 1)| < R$ because the Alt crescent is enclosed. Now we limited $\nu_{th}(s)$ to a

strip in the above argument. Furthermore, because of the Lagrange multiplier condition (2.4) on the free thread, the thread binormal $\eta_{th}(s)$ equals the surface normal on the thread. So we can control the thread binormal using our $CR^{1/6}$ slope control. Putting this together (see **Figure 4-14**), gives $|\langle \nu_T(s), \gamma_s(s) \rangle| < CR^{1/6}$. We conclude from (4.4) that

$$|\rho_s(s)| < CR^{1/6}.$$

Finally, we must show that if $\rho(s_*) = 0$ for s_* in the interior of the supporting wire domain \mathcal{S} , then the thread meets the wire tangentially. If this does not hold, then the $\rho \geq 0$ property which we have shown would cause some kink of angle $\alpha > 0$ in the thread. Now we may use our parametrization Ξ to demonstrate an Alt competitor which has the same area as (B, M) and has bounded derivatives. But this is prohibited by Lemma A.10 (p. 162) and Lemma 2.13. We conclude that the thread meets the wire tangentially whenever $\rho(s^*) = 0$ in the interior of the supporting wire. ■

REMARK. Note that Varying Frenet Frame Graph Lemma (Lem. 4.11) shows that the thread meets the wire tangentially at corner points of near-wire crescents. This was

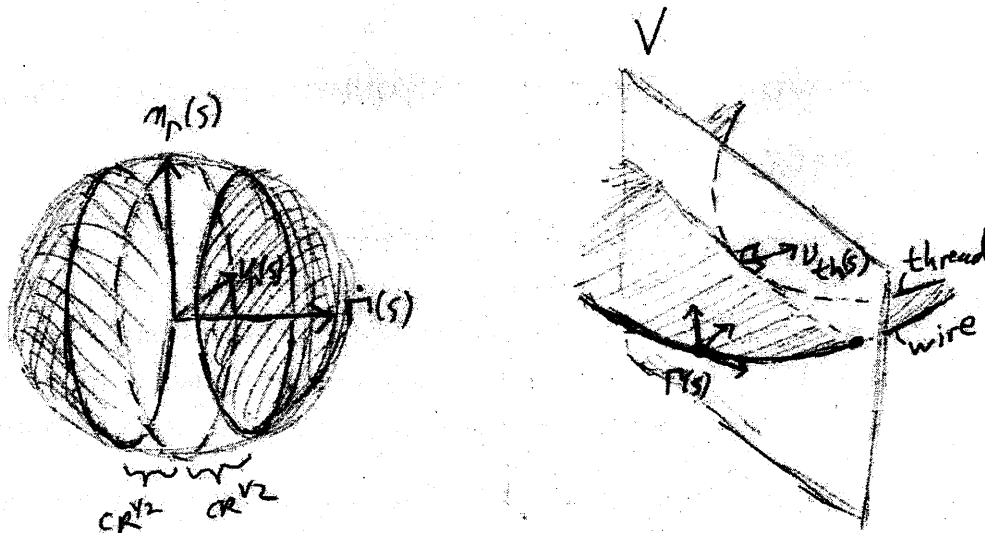


Figure 4-13: Control on ρ' . Let V be the plane passing through $\gamma(s)$ normal to the side normal $\nu_{th}(s)$. If V has normal in the double discs of the Bound on Γ' -Slope Lemma (Lem. 4.7), then V can only intersect the wire at one place, which yields a contradiction.

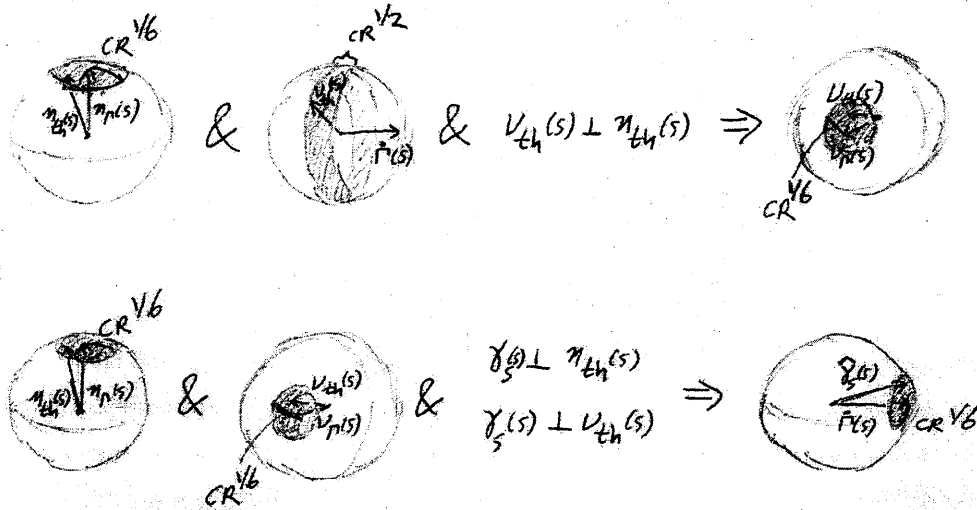


Figure 4-14: Closeness of Frenet frames of thread and wire. We combine the estimates of this section to show that the Frenet frames of the thread on a normal disc $D(s)$ is close to the Frenet frame of the wire at $\Gamma(s)$.

previously shown by Alt only for corners of crescents which adjoin a positive length piece of wire-adhering thread.

4.4 Near-wire crescents appear near maxima of wire curvature

The work of the preceding section shows that surface normal vectors and the thread Frenet frame of a near-wire crescent are closely aligned with Frenet information at corresponding wire points. We now use this information to demonstrate a closeness between the (globally constant) curvature of the free thread and the nearby wire curvature. This will enable us to localize near-wire crescents near maxima of wire curvature.

Lemma 4.12. [Crescents Near Maxima] Let Γ be an embedded generic wire curve. There are constants $R(\Gamma), C(\Gamma)$ so for $R < R(\Gamma)$, if an Alt minimizer (B, M) lies in the R -tubular neighborhood of Γ then every crescent of (B, M) satisfies

- (i) The crescent's supporting wire is shorter than $C(\Gamma)R^{1/12}$.
- (ii) The supporting wire's curvature stays within $C(\Gamma)R^{1/12}$ of κ .

(iii) The crescent lies within arclength $C(\Gamma)R^{1/2}$ of a maximum of wire curvature.

Proof. Let x, y, z to be Frenet coordinates at $\Gamma(0)$. Let $\Pi(x, y, z) = (x, y, 0)$. We always use s to denote arclength along the wire Γ . We parametrize all other curves using this parameter. For sufficiently small R we will examine the tubular neighborhood of Γ from $s = 0$ to $s = R^{1/2}$. In our proof we will assume that the wire extends this far. If it does not, the whole proof will succeed, and in fact all of the estimates will be easier.

Define the projected wire curve as $A(s) = \Pi(\Gamma(s))$. Let $B(s)$ be the unit normal to A at $A(s)$, pointing in the direction of curvature. We may then parametrize the x - y plane:

$$\Xi(s, t) = A(s) + tB(s).$$

The thread curve

$$\gamma(s) = \Gamma(s) + \rho(s)\nu_\Gamma(s) + u(s, 1)\eta_\Gamma(s) \quad (4.5)$$

projects to

$$\Xi(s, f(s)) = \Pi(\gamma(s)). \quad (4.6)$$

Lemma 4.13. There is a constant C so for $0 \leq s \leq R^{1/2}$,

$$|f_s(s)| < CR^{1/6}.$$

Proof. Differentiating (4.5) gives

$$\gamma_s = \Gamma_s + F_\Gamma(s)D_{F_\Gamma(s)} \begin{pmatrix} 0 \\ \rho(s) \\ u(s, 1) \end{pmatrix}.$$

Here $F_\Gamma(s)$ converts Frenet coordinates at $\Gamma(s)$ to our x, y, z coordinates, and $D_{F_\Gamma(s)}$

performs differentiation by arclength in Frenet coordinates at $\Gamma(s)$. Evaluating gives

$$\gamma_s = F_\Gamma(s) \begin{pmatrix} 1 \\ 0 \\ 0 \end{pmatrix} + F_\Gamma(s) \begin{pmatrix} \partial_s & -\kappa_\Gamma(s) & 0 \\ \kappa_\Gamma(s) & \partial_s & T_\Gamma(s) \\ 0 & -T_\Gamma(s) & \partial_s \end{pmatrix} \begin{pmatrix} 0 \\ \rho(s) \\ u(s,1) \end{pmatrix}. \quad (4.7)$$

$$= F_\Gamma(s) \begin{pmatrix} 1 \\ \rho_s(s) + T_\Gamma(s)u(s,1) \\ u_s(s,1) - T_\Gamma(s)\rho(s) \end{pmatrix}. \quad (4.8)$$

Now $F_\Gamma(s)$ is the matrix defined columnwise as

$$(\Gamma_s(s) \mid \nu_\Gamma(s) \mid \eta_\Gamma(s))$$

Because Γ has at least three derivatives (genericness guarantees C^4), we may write the Taylor expansion at zero:

$$\begin{aligned} F_\Gamma(s) &= F_\Gamma(0) + (F_\Gamma)_s(0)s + O(s^2) \\ &= \begin{pmatrix} 1 & 0 & 0 \\ 0 & 1 & 0 \\ 0 & 0 & 1 \end{pmatrix} + \begin{pmatrix} 0 & -\kappa_\Gamma(0) & 0 \\ \kappa_\Gamma(0) & 0 & T_\Gamma(0) \\ 0 & -T_\Gamma(0) & 0 \end{pmatrix} s + O(s^2). \end{aligned}$$

Now using that $0 \leq s \leq R^{1/12}$ and using the slope estimates of Varying Frenet Frame Graph Lemma (Lem. 4.11), we get

$$\gamma_s = \begin{pmatrix} 1 + O(R^{1/6}) \\ \kappa_\Gamma(0)s + O(R^{1/6}) \\ O(R^{1/6}). \end{pmatrix}$$

So then we see from (4.6) that

$$(\Xi(s, f(s)))_s = (1 + O(R^{1/6}), \kappa_\Gamma(0)s + O(R^{1/6})) \quad (4.9)$$

and

$$\langle A_s(s) + f_s(s)B(s) + f(s)B_s(s), \hat{y} \rangle = O(R^{1/6}). \quad (4.10)$$

Now using the Taylor expansion of Γ ,

$$\Gamma(s) = \left(s, \frac{1}{2}\kappa_\Gamma(0)s^2, 0 \right) + O(s^3),$$

we see that

$$\begin{aligned} A(s) &= \left(s, \frac{1}{2}\kappa_\Gamma(0)s^2 \right) + O(s^3) \\ A_s(s) &= (1, \kappa_\Gamma(0)s) + O(s^2) \\ B(s) &= (-\kappa_\Gamma(0)s, 1) + O(s^2) \\ B_s(s) &= (-\kappa_\Gamma(0), 0) + O(s); \end{aligned}$$

we may then use $f(s) = O(R)$ from the tubular enclosure to reduce (4.10) to

$$f_s + \kappa_\Gamma(0)s = \kappa_\Gamma(0)s + O(R^{1/6}).$$

We cancel and the desired result follows. ■

Lemma 4.14. For $0 \leq s \leq R^{1/12}$ we get

$$f_{ss}(s) = \kappa_\psi(s) - \kappa_\Gamma(0) + O(R^{1/6}).$$

Proof. Let $\psi(s) = \Pi(\gamma(s))$. Then

$$A_s + f_s B + f B_s = \psi_s.$$

Differentiating again gives

$$A_{ss}(s) + f_{ss}(s)B(s) + 2f_s(s)B_s(s) + f(s)B_{ss}(s) = \psi_{ss}(s).$$

Direct calculation shows

$$\kappa_\psi(s) = \frac{1}{|\psi_s(s)|} \left(\frac{\psi_s \cdot}{|\psi_s|} \right)_s = \langle B(s), \psi_{ss}(s) / |\psi_s(s)|^2 \rangle$$

Using (4.9) we obtain

$$|\psi_s| = 1 + O(R^{1/3});$$

using the other estimates above we get

$$\kappa_\psi(s) = \kappa_\Gamma(0) + f_{ss}(1 + O(s)) + O(s) + O(R).$$

■

We may now string our results together. On the interval $0 \leq s \leq R^{1/12}$, the thread tangent vector satisfies

$$|\gamma_s/|\gamma_s| - (1, 0, 0)| < \kappa s^2 < \kappa R^{1/6},$$

and we have

$$|\eta_\gamma(s) - (0, 0, 1)| < |\eta_\gamma(s) - \eta_\Gamma(s)| + |\eta_\Gamma(s) - (0, 0, 1)| < C(\Gamma)R^{1/6} + C(\Gamma)R^{1/12} < C(\Gamma)R^{1/12}.$$

At this point we employ a general lemma about space curves: that if the binormal is constrained, then a planar projection has curvature close to the original curve. See Lemma A.1 (p. 145). Applying this lemma with $\epsilon = C(\Gamma)R^{1/12}$ gives

$$|\kappa - \kappa_\psi(s)| < C(\Gamma, \kappa)R^{1/12}.$$

Then,

$$\begin{aligned} f_s(R^{1/12}) - f_s(0) &= \int_0^{R^{1/12}} f_{ss}(\underline{s}) d\underline{s} \\ O(R^{1/6}) &= \int_0^{R^{1/12}} (\kappa_\psi(\underline{s}) - \kappa_\Gamma(0)) d\underline{s} \\ O(R^{1/6}) &= \int_0^{R^{1/12}} (\kappa - \kappa_\Gamma(0)) d\underline{s} = (\kappa - \kappa_\Gamma(0))R^{1/12}. \end{aligned}$$

In this way we show $|\kappa - \kappa_\Gamma(0)| < CR^{1/12}$. Our estimates were made using geometric properties of Γ at $s = 0$. But using the fact that Γ is generic and compact, we may obtain a global constant so

$$|\kappa - \kappa_\Gamma(s)| < C(\Gamma)R^{1/12}.$$

This proves (ii) in Crescents Near Maxima Lemma (Lem. 4.12). We may then use the

fact that κ_Γ is a Lipschitz (in fact it is C^2) on a compact domain to show (i). Finally, imagine that κ were far from the global maximum of κ_Γ . Then there are regions of wire where the thread lies on the wire and $\kappa_\Gamma(s) > \kappa$. This is prohibited from happening in Alt minimizers by our first variation analysis (Lemma ??). See Figure 4-15. So in fact we must have

$$|\kappa - \max_{s \in \text{dom } \Gamma} \kappa_\Gamma(s)| < C(\Gamma)R^{1/12}.$$

But then by the Lipschitz property of the curvature of Γ (in fact it is C^2), we have shown claim (iii) in Crescents Near Maxima Lemma (Lem. 4.12). ■

4.5 Corner Γ' -slope improvement

Let $\mu = (X, \phi_-)$ be an Alt crescent satisfying the conditions for Varying Frenet Frame Graph Lemma (Lem. 4.11).

Let $\gamma(t), 0 \leq t \leq a$ parameterize part of the free thread by arclength as usual.

Lemma 4.15. [Quadratic Trumpet for Thread] Let $r > 0$ be any value less than κ^{-1} . Let $B = B_r(P)$ be a sphere tangent to Γ at $\Gamma(s_1)$. Then, independent of P , there is an $\ell_0 > 0$ so $\gamma(s)$ lies outside B for $0 < s < \ell_0$. This shows that the thread $\gamma|_{[0, \ell_0]}$ lies in a quadratic trumpet $\sqrt{y^2 + z^2} < Cx^2$.

Proof. For $s > 0$, consider the function

$$f(s) = |\gamma(s) - P|.$$

Then

$$\begin{aligned} f'(s) &= \left\langle \gamma'(s), \frac{\gamma(s) - P}{|\gamma(s) - P|} \right\rangle \\ f''(s) &= \left\langle \gamma''(s), \frac{\gamma(s) - P}{|\gamma(s) - P|} \right\rangle + \frac{\langle \gamma'(s), \gamma'(s) \rangle}{|\gamma(s) - P|} - \frac{1}{|\gamma(s) - P|} \left\langle \gamma'(s), \frac{\gamma(s) - P}{|\gamma(s) - P|} \right\rangle^2 \\ &= \left\langle \gamma''(s), \frac{\gamma(s) - P}{|\gamma(s) - P|} \right\rangle + \frac{1}{|\gamma(s) - P|} \left(1 - \left\langle \gamma'(s), \frac{\gamma(s) - P}{|\gamma(s) - P|} \right\rangle^2 \right). \end{aligned}$$

The quantity

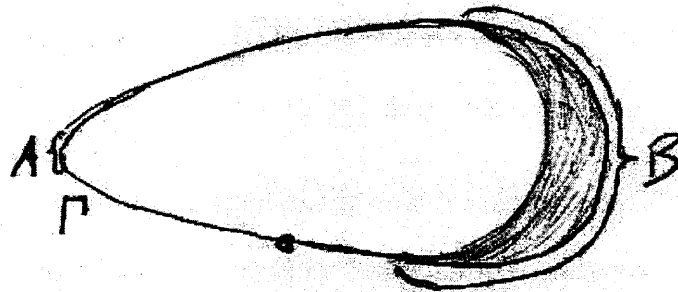
$$\Theta(\sigma, \epsilon) = \frac{1}{r + \sigma} \left(1 - \left(\frac{\sigma}{r - \sigma} + \epsilon \right)^2 \right)$$

approaches 1 from below as one chooses smaller and smaller positive values for σ, ϵ .
Let's choose σ and ϵ so

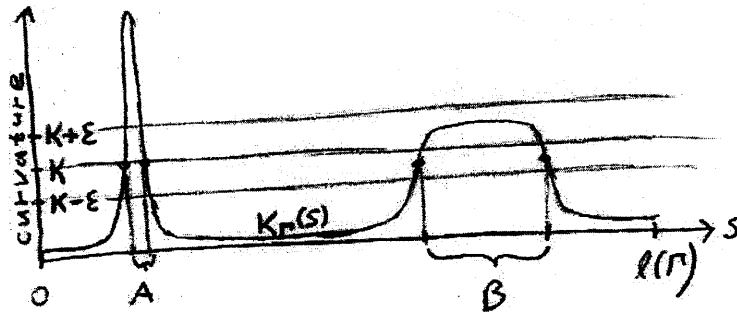
$$\Theta(\sigma, \epsilon) > r\kappa. \quad (4.11)$$

Then choose ℓ_0 so for $s < \ell_0$,

$$\langle \gamma'(s), P/|P| \rangle < \epsilon, \quad \langle \gamma(s), \gamma'(0) \rangle > 1 - \epsilon$$



(a)



(b)

Figure 4-15: Free thread curvature must be near maximum wire curvature.
We have shown that the free thread curvature κ must be near the curvature of the supporting wire. In this diagram we show what happens if κ is *not* close to the maximum of the wire curvature κ_r . Then there is a region A on the wire where the wire curvature exceeds the free thread curvature. As we saw in the proof of the Thread-Bearing-Wire Curvature Bound Lemma ??, we may introduce a new crescent here and reduce overall Dirichlet energy, violating the minimizing property of our supposed minimizer.

and

$$|\gamma(s)| < \sigma.$$

Returning to (4.11) we see for $0 < s < \ell_0$,

$$f''(s) > -\kappa + \frac{1}{r}\Theta(\sigma, \epsilon).$$

We see by (4.11) that on $(0, \ell_0)$,

$$f(s) \geq \frac{1}{2}\Theta(\sigma, \epsilon)s^2 \geq 0.$$

So the thread stays outside of the sphere $B(P, r)$ for length ℓ_0 as claimed. ■

Lemma 4.16. [Quadratic Trumpet] Let (X, ϕ_-) be an Alt crescent satisfying the conditions of Varying Frenet Frame Graph Lemma (Lem. 4.11). Then near either corner of the crescent, the surface is contained in a quadratic trumpet.

Proof. The wire, being a C^3 curve, stays in quadratic trumpet. So does the thread by the previous lemma. The slope bound of Varying Frenet Frame Graph Lemma (Lem. 4.11) ensures that the whole surface also initially stays in some quadratic trumpet. ■

Lemma 4.17. [Corner Slope Improvement] If the corner is contained inside a quadratic trumpet $\sqrt{y^2 + z^2} \leq Cx^2, x \in [0, x_m]$ for x_m sufficiently small relative to the geometry of Γ , then a double disc $v \cdot \hat{x} \leq \frac{2C}{5}$ does not intersect the Gauss image of the corner for $x < x_m/2$. This implies a slope bound $f_x \leq \frac{5}{2}C$ for $x < x_m/2$.

Proof. This is a straightforward computation (See **Figure 4-16**). Let x_1 be in the range 0 to $x_m/2$. One shows that planes passing through the cross-section $x = x_1$ of the trumpet with normals in the double spherical disc above (**Figure 4-17**) do not intersect the $x = 2x_1$ cross-section of the trumpet (**Figure 4-18**). As such, they intersect the boundary of the corner only on the thread and on the wire. They can intersect the wire at most once because if x_m is chosen sufficiently small relative to the geometry of Γ , one can ensure that $\kappa_\Gamma \leq C$ inside $x \leq x_m$. As such these planes cannot be tangent planes to the Alt minimizer at $x = x_1$, by the Normal Avoidance Lemma (Lem. 4.5). ■

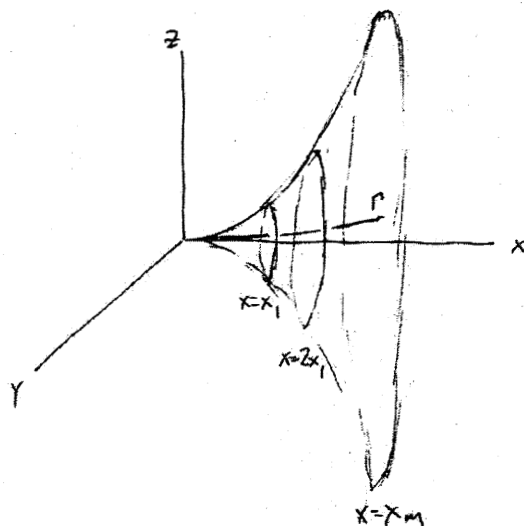


Figure 4-16: Figure for Corner Slope Improvement Lemma (Lem. 4.17).

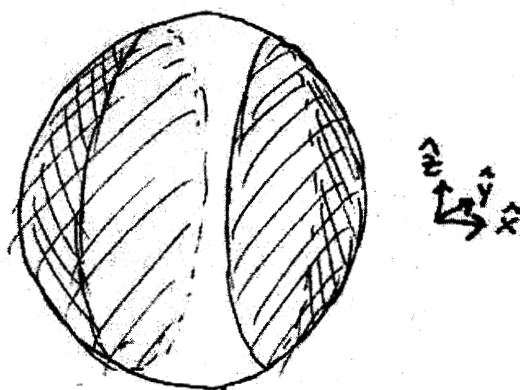


Figure 4-17: Figure for Corner Slope Improvement Lemma (Lem. 4.17).

4.6 Proof of Near-wire Crescent Theorem (Thm. 1.4)

We may now prove the first of the two main theorems of this thesis.

Proof–Theorem 1.4. We prove each claim of Near-wire Crescent Theorem in turn. Let $\Gamma(s_0)$ be a corner of a crescent of an Alt minimizer in a R -tubular neighborhood of Γ for $R < R(\Gamma)$. We show the claimed properties below. We obtain the constant $R(\Gamma)$ by taking a minimum of the $R(\Gamma)$ values arrived at in each lemma we quote below.

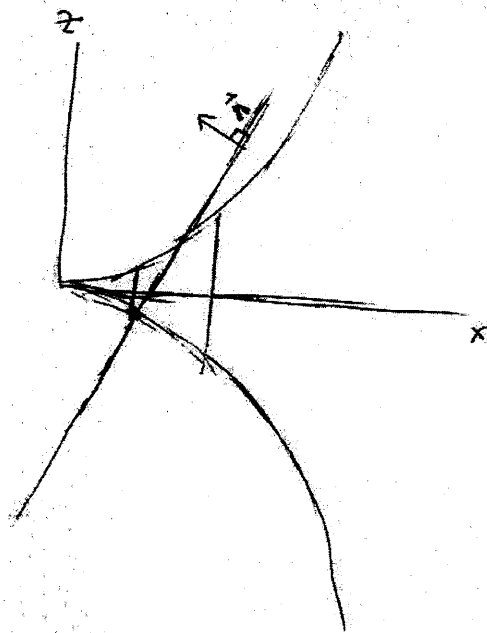


Figure 4-18: Figure for Corner Slope Improvement Lemma (Lem. 4.17).

First, we note that for sufficiently small R , the thread must be C^1 and only touch Γ tangentially (Varying Frenet Frame Graph Lemma (Lem. 4.11)). Then:

- (i) *The supporting wire is short.* We proved this in part (i) of Lemma ??.
- (ii) *Both corners are close to a maximum of wire curvature.* This follows from part (iii) of Lemma ??.
- (iii) *The crescent is a graph in the Frenet coordinates of $\Gamma(s_0)$.* We showed this in Varying Frenet Frame Graph Lemma (Lem. 4.11). The slope improvement in the x direction was shown in Corner Slope Improvement Lemma (Lem. 4.17).
- (iv) *The free thread curvature κ is near the wire curvature κ_Γ .* We showed this in part (ii) of Lemma ??.
- (v) *The Frenet frame of the thread is near that of the supporting wire.* We showed this in Varying Frenet Frame Graph Lemma (Lem. 4.11)

■

Chapter 5

C^1 Corner Theorem

By the end of this section, we prove the C^1 Corner Regularity Theorem (Thm. 1.5) and thus establish Conjecture 1.2. We reprint a copy of C^1 Corner Regularity Theorem (Thm. 1.5) below:

Theorem 5.1. [C^1 Corner Regularity] Let Γ be a generic embedded wire. There is a small R so any Alt minimizer μ lying in the R -tubular neighborhood has the following property. Let Σ be any crescent supported in the interior of Γ . Let N be a unit normal vector field to Σ .

- (i) The normal vector field is continuous up to each corner of Σ . The limit of N as one approaches a corner $\Gamma(s)$ is the Frenet binormal $\eta_\Gamma(s)$.
- (ii) The Gauss map for Σ is injective and is an embedding on its interior.
- (iii) The Gauss image of the thread and wire curves bounding Σ have the properties described in **Figure 5-1**.
- (iv) Consider the first eigenvalue λ_1 of the Laplacian on the Gauss image of Σ with Dirichlet boundary condition on the Gauss image of the wire and Neumann condition on the Gauss image. This eigenvalue is large:

$$\lambda_1 > C(\Gamma)R^{-1/3}. \tag{5.1}$$

Here is an outline of our proof. The first step is to study the normal field of a near-wire crescent along the thread. In Section 5.1, we show that the torsion of the

thread cannot be zero. This, combined with the slope improvement of Corner Slope Improvement Lemma (Lem. 4.17) gives the normal field on the thread an approximately monotonic behavior as it approaches the corner. We are thus able to show that it approaches a limit. We then make the observation (Section 5.2) that if the y slope of the surface is (up to an error term) the steepest at the thread boundary, then we are able to show that the entire surface is C^1 at the corner, and that its normal vector converges to the Frenet binormal of the wire at the corner. The rest of our work focuses on establishing this approximate slope inequality. In Section 5.6 we prove this crucial inequality by showing (Section 5.5) that the Gauss map of the near-wire crescent is injective, and is an embedding on the crescent interior. Showing this injectivity property requires a careful study of the Gauss map. Several other interesting observations result, which we detail in Section 5.7 and Section 5.8. Finally we prove the second main theorem of this thesis, C^1 Corner Regularity Theorem (Thm. 1.5), in Section 5.9.

5.1 A monotonicity property for the thread binormal

Lemma 5.2. [Corner Thread Monotonicity] Let (B, X) be a crescent of an Alt minimizer sufficiently small so that:

- (i) The entire crescent is a graph relative to the standard Frenet coordinates of the wire at one corner.
- (ii) The torsion of the supporting wire is always positive.
- (iii) Any plane intersects the supporting wire in at most three points.

Then the torsion of the thread along this crescent is everywhere positive.

Proof. We show that the torsion of the thread cannot be zero at any point p in the interior of the thread. If it were, Series Solutions to ThIP problem Theorem (Thm. B.6) shows that the tangent plane at such a point intersects the Alt minimizer in a graph that has valence at least 4 at p . The graph already touches the thread at p , so it cannot do so anywhere else. It can touch the wire at no more than three points. So this is a contradiction.

The torsion of the thread (which is continuous on the interior of the thread) must have a fixed sign. What sign is it? Consider the intersection graph between the tangent plane at an interior point p of the thread and the Alt minimizer. The graph has valence 3 at p , and this divides the Alt minimizer into 4 regions which are alternately above and below the plane. We can assign them signs: positive if they are above the plane and negative if they are below. Then the region which contains the thread between p and the far corner has the same sign as the thread torsion at p . On the other hand, any plane which intersects the wire in three places has the far corner above the plane. In this way we see that the torsion of the thread is always positive. ■

Lemma 5.3. [Corner Thread Normal Limit] Under the assumptions of the previous lemma, the thread is uniformly C^2 up to where it meets the wire at the two corners.

Proof. We already know (from Alt in [1]) that the *magnitude* of the curvature vector along the thread is bounded (in fact it is a constant κ .) What needs to be proved is that its *direction* has a limit as one approaches either corner.

Consider the corner at the origin. We will examine the function

$$f(s) = \gamma_{[z]}(s) = \langle \gamma(s), \eta_{\Gamma}(0) \rangle.$$

We have

$$f'(s) = \langle \gamma'(s), \eta_{\Gamma}(0) \rangle.$$

$$f''(s) = \langle \gamma''(s), \eta_{\Gamma}(0) \rangle.$$

$$f'''(s) = \langle \gamma'''(s), \eta_{\Gamma}(0) \rangle.$$

This gives $f(0) = f'(0) = 0$. Now

$$f'''(s) = \langle \kappa T(s) \eta_{\gamma}(s) - \kappa^2 \gamma'(s), \eta_{\Gamma}(0) \rangle.$$

Pick any $c > \kappa$. Then $f'''(s) + cs > \kappa T(s) \langle \eta_{\gamma}(s), \eta_{\Gamma}(0) \rangle$ which is positive because of our above argument about the sign of T (Corner Thread Monotonicity Lemma (Lem. 5.2)) and because of the general Lipschitz control on $\eta_{\gamma}(s)$ (Varying Frenet Frame Graph Lemma (Lem. 4.11)) and the fact that the Frenet frame of Γ varies at most $C(\Gamma)s$ from $\Gamma(0)$ to $\Gamma(s)$. This means that $f''(s) + \frac{1}{2}cs^2$ is increasing. Because of this expression's monotonicity, we know it has a limit as s goes to zero. But that means $f''(s)$ has a

limit as s goes to zero. And that means $\gamma''(s)$ has a limit as s goes to zero. We conclude that γ is uniformly C^2 up to the corner at $s = 0$. The limit of the thread binormal exists at the other corner follows by a similar argument. ■

5.2 A crucial slope inequality

The intuition behind Conjecture 1.2 is that the curvedness of the generic wire should encourage the normal field N of the surface to get close to the Frenet binormal of the wire as one approaches the corner. In this section we demonstrate how this is true for N on the thread boundary, provided one knows that the $z - y$ slope of the surface is approximately less in the interior than at the thread.

To demonstrate our crucial inequality, we need to adopt the coordinates given to us in the last section. Let (X, ϕ_-) be an Alt crescent. By Near-wire Crescent Theorem (Thm. 1.4), proved in the last section, the Alt crescent is a graph in the Frenet coordinates of the wire at a corner point. We may project the wire boundary of (X, ϕ_-) to the x - y plane to get the *wire shadow curve* $y = \underline{\Gamma}(x)$. Similarly we may project the thread boundary of the crescent to get the *thread shadow curve* $y = \underline{\gamma}(x)$. We may then write the crescent as the graph $z = f(x, y)$, where

$$\underline{\Gamma}(x) \leq y \leq \underline{\gamma}(x)$$

and x lies in some small interval $[0, x_{c+}]$. See **Figure 5-3**.

For (x, y) in $\text{dom } f$ and $0 < x < x_{c+}$, let $N(x, y)$ be the upward pointing normal to the crescent above (x, y) .

Lemma 5.4. [Corner Slope Inequality] Assume that on $\text{dom } f$ we have

$$f_y(x, y) < f_y(x, \underline{\gamma}(x)) + \epsilon(x) \quad (5.2)$$

where $\epsilon(x)$ approaches 0 as x goes to 0. Then as we move along the thread to the origin, the normal field N

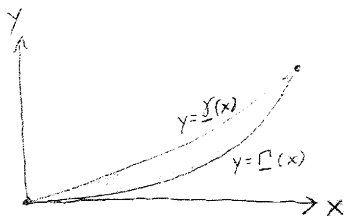


Figure 5-2: Domain of f .

approaches the Frenet binormal of the wire at the origin:

$$\lim_{x \rightarrow 0^+} N(x, \underline{\gamma}(x)) = (0, 0, 1).$$

Proof. Our control on $\gamma''(x)$ (quote main thm proved in last section) may be integrated to yield

$$\gamma(x) = \left(x, \left(\frac{1}{2} \kappa \cos \alpha + \epsilon(x) \right) x^2, \left(\frac{1}{2} \kappa \sin \alpha + \epsilon(x) \right) x^2 \right).$$

(Here and later in the proof, the function $\epsilon(x)$ may take different values in different equations.) On the other hand,

$$\Gamma(x) = \left(x, \frac{1}{2} \kappa_{\Gamma}(0) x^2 + O(x^3), O(x^3) \right).$$

Applying the Mean Value Theorem to the graph of f sliced by the $x - z$ plane through (x, y) , we find that there is a point (x, y') with

$$f_y(x, y') = \frac{(\kappa \sin \alpha + \epsilon(x)) x^2 - O(x^3)}{(\kappa \cos \alpha + \epsilon(x)) x^2 - \kappa_{\Gamma}(0) x^2} > \frac{\kappa \sin \alpha}{\kappa \cos \alpha - \kappa_{\Gamma}(0) + \epsilon_2(x)} - \epsilon_3(x). \quad (5.3)$$

If $\kappa \cos \alpha = \kappa_{\Gamma}(0)$, or if not and

$$\frac{\kappa \sin \alpha}{\kappa \cos \alpha - \kappa_{\Gamma}(0)} > \tan \alpha$$

then for sufficiently small x we contradict (5.2). The only way to obey (5.2) is to have $\alpha = 0$. ■

We see in the proof of this result that the nonzero curvature of the wire is crucial – it shortens the y -distance in the slope expression of (5.3) and forces the vectorfield N along the thread to stand straight up.

5.3 Coordinates

The Near-wire Crescent Theorem (Thm. 1.4) allows us to write a near-wire Alt crescent as a graph in the Frenet coordinates of a corner point in the interior of the wire. It also guarantees that the thread meets the wire in the interior only tangentially (at cusp-corners). In Section 5 we will be using these coordinates intensively.

Consider an Alt crescent (X, ϕ_-) lying within distance R of a generic wire Γ . Let R be small enough so that Near-wire Crescent Theorem (Thm. 1.4) applies. Assume that both of its corners lie in the interior of the wire. Then we may apply Near-wire Crescent Theorem (Thm. 1.4) at both corners. We have that (X, ϕ_-) is an Alt crescent supported on a piece of wire $\Gamma(s)$ for s in some interval $\text{Im } \phi_- = [s_0, s_1]$. We reparametrize Γ so this supporting wire is parametrized by $s \in [0, s_{c_+}]$ for $s_{c_+} \leq C(\Gamma)R^{1/12}$. Let us refer to $\Gamma(0)$ as the *base corner* and $\Gamma(s_{c_+})$ as the *positive corner*. We introduce Frenet coordinates at the base corner:

$$(x, y, z) \mapsto \Gamma(0) + x\Gamma'(0) + y\nu_\Gamma(0) + z\eta_\Gamma(0). \quad (5.4)$$

Most of our calculations will be done in these coordinates.

Assumption 5.5. We assume that $T_\Gamma(0) < 0$. The case that $T_\Gamma(0) > 0$ is just a reflection of this case.

We will find it convenient to convert between the s coordinate and the x coordinate using

$$x(s) = \Gamma_{[x]}(s) = s + O(s^3)$$

and

$$s(x) = (\Gamma_{[x]})^{-1}(x) = x + O(x^3).$$

See Section A.1.

Then the crescent is a graph $z = f(x, y)$ over a doubly-cusped domain

$$\text{dom } f = \{(x, y) \mid 0 < x < x_{c_+}; \underline{\Gamma}(x) \leq y \leq \underline{\gamma}(x)\}.$$

The domain is bounded by the *thread shadow curve* $y = \underline{\gamma}(x)$ and *wire shadow curve* $y = \underline{\Gamma}(x)$. Here we have by Near-wire Crescent Theorem (Thm. 1.4) that $x_{c_+} < C(\Gamma)R^{1/12}$. Also, by Theorem 2.12 we know that $f \in C^4(\Omega)$. See **Figure 5-3**.

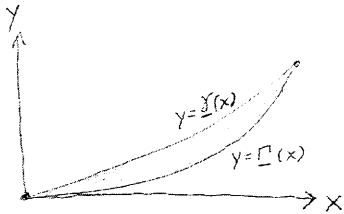


Figure 5-3: Domain of f .

We orient the Alt crescent so it has unit normal vectors pointing in the positive z

direction. They lie in the unit sphere (*the Gauss sphere*) in a neighborhood

$$\mathcal{N} = \{(x, y) \mid \sqrt{x^2 + y^2} < C(\Gamma)R^{1/12}\}$$

where x, y are the coordinates x, y from (5.4). See Near-wire Crescent Theorem (Thm. 1.4). We define the Gauss map $g \in C^3(\Omega, \mathbb{R}^2)$ which gives the x, y components of the normal vector at $(x, y, f(x, y))$ on the Alt crescent.

Definition 5.6. Occasionally we will use coordinates relative to the **positive corner**:

$$(x', y', z') \mapsto \Gamma(s_{c_+}) - x'\Gamma'(s_{c_+}) + y'\nu_\Gamma(s_{c_+}) + z'\eta_\Gamma(s_{c_+}).$$

Note the sign difference relative to (5.4). These are the coordinates which we would choose if we wanted the point $\Gamma(s_{c_+})$ to be our base corner, and if we reflected things to satisfy Assumption 5.5. The x' and y' coordinate axes are geodesics on the Gauss sphere near $(x, y, z) = (0, 0, 1)$. Their offset and tilt relative to the (x, y, z) coordinate system are governed by the amount that the Frenet frame of Γ has changed from $s = 0$ to $s = s_{c_+}$. Fortunately this is small ($O(R^{1/12})$). As a result, one sees that the level sets of x' are graphs over the y axis.

We define the *Gauss wire curve* $g_\Gamma \in C^3((0, x_{c_+}), \mathbb{R}^2)$ by

$$g_\Gamma(x) = g((x, \underline{\Gamma}(x))). \quad (5.5)$$

Similarly the *Gauss thread curve* $g_\gamma(x) \in C^3((0, x_{c_+}), \mathbb{R}^2)$ is

$$g_\gamma(x) = g((x, \underline{\gamma}(x))).$$

5.4 Gauss image constrained by wire-related curves

Lemma 5.7. The Gauss image of our near-wire crescent lies in the fourth quadrant,

$$x > 0, y < 0.$$

Moreover, the Gauss map is an immersion on $\text{dom } g$ except possibly on the $\underline{\Gamma}$ curve.

Proof. Given a prospective unit normal vector colinear with $(a, b, 1)$, with $|a|, |b| <$

$C(\Gamma)R^{1/12}$, we consider a plane perpendicular to it, defined as the zero set of

$$P(x, y, z) = ax + by + z - d.$$

By the Intersection Graph Lemma (Lem. 3.6), for this plane to be tangent to an interior point of a near-wire crescent, the function $P \circ \Gamma$ must have at least three zeroes on the supporting piece of wire. We may change coordinates using $x = \Gamma_{[x]}(s)$, to obtain the expansion

$$\Gamma(x) = \left(x, \frac{1}{2}\kappa_0^\Gamma x^2 + \frac{1}{6}\kappa_1^\Gamma x^3 + O(x^4), -\frac{1}{6}\kappa_0^\Gamma T_0^\Gamma x^3 + O(x^4) \right)$$

and the expression

$$w(x) = P(\Gamma(s)) = ax + \frac{1}{2}\kappa_0^\Gamma bx^2 + \left(-\frac{1}{6}\kappa_0^\Gamma T_0^\Gamma + \frac{1}{6}\kappa_1^\Gamma b \right) x^3 + O(x^4).$$

Applying Taylor's theorem to derivatives of Γ give

$$\begin{aligned} w'(x) &= a + \kappa_0^\Gamma bx + \left(-\frac{1}{2}\kappa_0^\Gamma T_0^\Gamma + \frac{1}{2}\kappa_1^\Gamma b \right) x^2 + O(x^3) \\ w''(x) &= \kappa_0^\Gamma b + (-\kappa_0^\Gamma T_0^\Gamma + \kappa_1^\Gamma b) x + O(x^2) \\ w'''(x) &= (-\kappa_0^\Gamma T_0^\Gamma + \kappa_1^\Gamma b) + O(x). \end{aligned} \tag{5.6}$$

We have $x \in [0, C(\Gamma)R^{1/12}]$ and $|a|, |b| < C(\Gamma)R^{1/6}$.

Because a and b are $O(R^{1/12})$, we see that w''' is positive on the supporting wire interval $x \in [0, C(\Gamma)R^{1/12}]$. Now we may apply the Generalized Descartes's Rule Lemma (Lem. A.3). We see that the only way to get three zeroes for $x > 0$ is to have

$$b < 0, \quad a > 0, \quad d < 0. \tag{5.7}$$

This shows that the Gauss image of our near-wire crescent lie over the fourth quadrant $x > 0, y < 0$. ■

Lemma 5.8. The Gauss thread curve g_γ is a graph over the negative y axis; it can be reparametrized as

$$y \mapsto (h_\gamma(y), y) \tag{5.8}$$

where $h_\gamma(y)$ is in $C^2([y_1^\gamma, y_0^\gamma])$ for $y_1^\gamma < y_0^\gamma \leq 0$. We have $h_\gamma(y_0^\gamma) = 0$ and $h_\gamma''(y) > 0$.

Proof. We saw in Section 3.2 that the Gauss image of the thread curve moves in the ν_γ direction with curvature in the γ' direction. By Near-wire Crescent Theorem (Thm. 1.4), the Frenet frame of the thread is within $R^{1/12}$ of the Frenet frame of Γ at $s = 0$. Moreover, by Corner Thread Monotonicity Lemma (Lem. 5.2), the thread torsion has definite sign. These facts prove the graph property and the second derivative property.

As for the last claim: we must show that the Gauss curvature of the surface does not vanish in the interior or on the $\underline{\gamma}$ curve. If it vanishes at some point (x, y) in the interior, then the tangent plane V through $(x, y, f(x, y))$ would give an intersection graph $G(V, X)$ with a node in Δ° having valence at least 6. But then the plane V would have to intersect the supporting wire at least 5 times. However, we saw above that no tangent plane to the surface may intersect the wire at more than 3 places. Similarly, if the Gauss curvature vanishes at some thread point $(x, \underline{\gamma}(x))$ then the tangent plane V through the surface at $(x, \underline{\gamma}(x), f(x, \underline{\gamma}(x)))$ would give rise to an intersection graph $G(V, X)$ with a node on $\partial_- \Delta$ having valence at least 4 (See Series Solutions to ThIP problem Theorem (Thm. B.6, p. 168)). This would then force there to be at least 4 intersections of V with the supporting wire: again a contradiction. ■

Here we converted between wire arclength s and the coordinate x using $s = x + O(x^3)$.

Lemma 5.9. The wire Frenet binormal curve η_Γ is a graph over the y axis. It may be parametrized as the curve

$$x \mapsto \left(-\frac{\kappa_\Gamma(0)}{2T_\Gamma(0)}x^2 + O(x^3), x + O(x^2) \right)$$

with derivative

$$x \mapsto \left(-\frac{\kappa_\Gamma(0)}{T_\Gamma(0)}x + O(x^2), 1 + O(x) \right).$$

Proof. Using the calculations of Section A.1 we obtain

$$(\eta_\Gamma)_s(s) = \begin{pmatrix} \frac{\partial}{\partial s} & -\kappa_\Gamma(s) & 0 \\ \kappa_\Gamma(s) & \frac{\partial}{\partial s} & T_\Gamma(s) \\ 0 & -T_\Gamma(s) & \frac{\partial}{\partial s} \end{pmatrix} \begin{pmatrix} 0 \\ 0 \\ 1 \end{pmatrix} = \begin{pmatrix} 0 \\ T_\Gamma(s) \\ 0 \end{pmatrix}$$

which is to say $(\eta_\Gamma)_s(s) = T_\Gamma(s)\nu_\Gamma(s)$. Moreover,

$$\begin{aligned} (\eta_\Gamma)_{ss}(0) &= \begin{pmatrix} \frac{\partial}{\partial s} & -\kappa_\Gamma(0) & 0 \\ \kappa_\Gamma(0) & \frac{\partial}{\partial s} & T_\Gamma(0) \\ 0 & -T_\Gamma(0) & \frac{\partial}{\partial s} \end{pmatrix} \begin{pmatrix} 0 \\ T_\Gamma(0) \\ 0 \end{pmatrix} \\ &= \begin{pmatrix} -\kappa_\Gamma(0)T_\Gamma(0) \\ T_\Gamma'(0) \\ -T_\Gamma(0)^2 \end{pmatrix} \end{aligned}$$

So in our x - y coordinates for the Gauss sphere, we obtain

$$\begin{aligned} \eta_\Gamma(s(x)) &= \left(-\frac{1}{2}\kappa_\Gamma(0)T_\Gamma(0)s^2, T_\Gamma(0)s + \frac{1}{2}T_\Gamma'(0)s^2 \right) + O(s^3) \\ \eta_\Gamma(s(x)) &= \left(-\frac{1}{2}\kappa_\Gamma(0)T_\Gamma(0)x^2, T_\Gamma(0)x + O(x^2) \right) \end{aligned}$$

■

As for the Gauss image of the wire, we draw in $\eta_\Gamma(s)$ in our x - y coordinates. Each normal vector $N(\Gamma(s))$ is perpendicular to $\Gamma'(s)$, so it lies in the great circle through $\eta_\Gamma(s)$ and $\nu_\Gamma(s)$. This motivates defining a “ruling map”

$$\Xi(x, v) = \exp_{\eta_\Gamma(s(x))}(v\nu_\Gamma(s(x))).$$

Here \exp is the exponential map of the sphere as a Riemannian manifold. This gives us a kind of ruling of the Gauss sphere near the north pole. We obtain the following lemma.

Lemma 5.10. The ruling map is an immersion except on the critical curve $\eta_\Gamma(s)$, where the rank of its differential drops to 1. Moreover, in our north pole neighborhood \mathcal{N} , the map is 1-1 on the η_Γ curve, it is 2-1 on the negative x side of η_Γ , and it does not hit the region on the positive x side of η_Γ . For each $\eta_\Gamma(s) \in \mathcal{N}$, $s \in (0, s_{c_+})$, we get a geodesic segment lying in \mathcal{N} defined by $t \mapsto \Xi(s, t)$; the geodesic is a graph over the y -axis which has positive x coordinate for $t \geq 0$. The Gauss wire curve has the property that it factors through the ruling map:

$$g_\Gamma(\hat{x}) = \Xi(\hat{x}, \nu_\Gamma(\hat{x})) \tag{5.9}$$

for some function $\nu_\Gamma \in C^0((0, x_{c_+}), \mathbb{R})$.

If $v_\Gamma(\hat{x}) \neq 0$ then consider affine coordinates \tilde{u}, \tilde{v} at $(\hat{x}, v_\Gamma(x))$ in $\text{dom } \Xi$ with the \tilde{u} -axis pointing along the graph of v_Γ in the positive \hat{x} direction and \tilde{v} pointing away from the \hat{x} -axis. Then $d_{(\hat{x}, v_\Gamma(x))}$ identifies these with affine coordinates u, v at $g_\Gamma(\hat{x})$. Locally the ruling geodesic $s \mapsto \Xi(x_{c_+}, s)$ can be written as a graph $v = h(u)$. Locally, the g_Γ curve crosses this graph from below to above (in the sense of v) as x increases past \hat{x} .

5.5 Gauss map is injective and is an embedding on the interior

Lemma 5.11. The Gauss map is an immersion on its domain except possibly on a set of measure zero on the $\underline{\Gamma}$ curve.

Proof. If on the contrary $d_{(x, \underline{\Gamma}(x))}g$ were not injective for an interval $x \in (x_0, x_1)$ then we know that $v_\Gamma(x) = 0$ on this interval. But then on this interval, $g_\Gamma(x) = \eta_\Gamma(s(x))$. By the above lemma on η_Γ , we saw that $(\eta_\Gamma(s(x)))_x$ is nonzero in our polar neighborhood \mathcal{N} . So in fact dg has at least rank 1 on our interval. But that suffices to show dg has full rank, since f is a minimal surface. ■

Lemma 5.12. The Gauss wire curve lies in S_Ξ .

Proof. Apply Lemma 5.7 at both the base corner and the positive corner; then note Lemma 5.10. ■

Our task is to sort through these many conditions on the Gauss map and control it well enough to be able to say something about limits of the normal vectors as we approach the corner.

Lemma 5.13. The Gauss thread curve stays on the negative x side of the wire binormal curve η_Γ .

Proof. Pick any point $g_\gamma(\hat{x}) = (x_0, y_0)$ on the Gauss thread curve, $0 < \hat{x} < x_{c_+}$. We know from Lemma 5.8 that $x_0 > 0$. Using the Corner Slope Improvement Lemma (Lem. 4.17), we may find a $\hat{x}_0 = C(\Gamma)x_0$ so g maps $x < \hat{x}_0$ to $x < x_0$ on the Gauss sphere.

Now we may apply Lemma 5.8 relative to the x', y', z' coordinates of the positive corner. Translating back into x, y coordinates, we may conclude that there is a geodesic

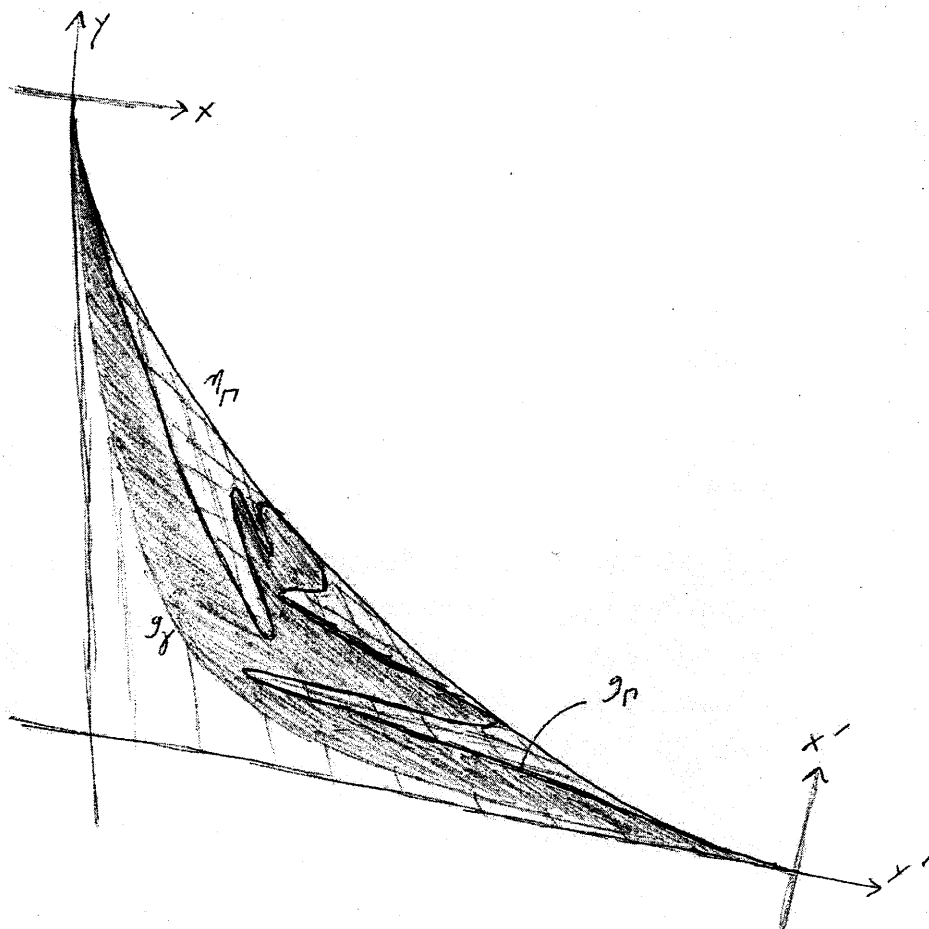


Figure 5-1: Gauss image control. The above diagram takes place in a small neighborhood of $\eta_{\Gamma}(P)$ (the Frenet binormal of the wire at the corner point). In this neighborhood, we may project the sphere to the tangent plane at η_{Γ} to get x and y coordinates on the sphere. We may do the same at the other corner of the crescent to get x' and y' coordinates. The Gauss image of the thread is a graph over the x axis in x - y coordinates and also a graph over the x' axis in x' - y' coordinates. Its geodesic curvature has a definite sign. The Gauss image of the thread satisfies something close to a graph condition: it may be parametrized as $\exp_{\eta_{\Gamma}(s)}(v(s)\nu_{\Gamma}(s))$ for some continuous function $v(s)$.

Figure 5-4: Gauss image constrained by quadrants. In Lemma 5.7 we show that the Gauss image is constrained to the fourth quadrant of our x - y coordinates at one corner. Applying this lemma to the other corner as well constrains the image as shown. The Gauss wire curve factors through the ruling shown.

$x' = x'_0$ separating (x_0, y_0) from the positive corner's Frenet binormal $\eta_\Gamma(s_{c_+})$. Then applying the Corner Slope Improvement Lemma (Lem. 4.17), we may find an $\hat{x}_+ = x_{c_+} - C(\Gamma)x'_0$ so g maps $x > \hat{x}_+$ to the far side of the $x' = x'_0$ geodesic from (x_0, y_0) . Let U be $\text{dom } g$ restricted to $\hat{x}_0 \leq x \leq \hat{x}_+$. We parametrize the horizontal segment through (x_0, y_0) as $\sigma(s) = (x_0 + s, y_0)$. Now we may apply the Curve Lift Lemma (Lem. A.4, p. 149) to obtain a lifted curve $\hat{\sigma} \in C^0([0, s^*], U)$, $s^* > 0$, with

$$g(\hat{\sigma}(s)) = \sigma(s).$$

We know by Lemma A.4 that $\hat{\sigma}(s^*)$ lies in ∂U . It can't lie in the $x = \hat{x}_0, \hat{x}_+$ boundaries because both boundaries map to curves which are graphs over the y -axis having values less than x_0 at $y = y_0$. (See Definition 5.6.) So $\sigma([0, C(\Gamma)R^{1/12}])$ is disjoint from the Gauss image of these parts of ∂U . Moreover, $\hat{\sigma}(s^*)$ can't hit the $\underline{\gamma}$ part of ∂U because g_γ is a graph over the y axis. We conclude that $q = \hat{\sigma}(s^*)$ lies in the Gauss wire curve. By Lemma 5.10, this wire point q must lie on the curve η_Γ or to the negative x side of it. Since $s^* > 0$, the result follows. ■

Lemma 5.14. The Gauss wire curve does not self-intersect. In other words, the Gauss map g is injective on the $\underline{\Gamma}$ curve.

Proof. The idea of this proof is to posit such an intersection, and look at what it means for the two ruling lines which the wire points sit on. The remainder of these ruling lines do not intersect on the Gauss sphere. However, we will show that we can lift these disjoint segments to segments in the domain of the Gauss map which do intersect. This will yield a contradiction. Let us now become specific.

Assume to the contrary that the Gauss wire curve does intersect at some $q = (x_q, y_q) = g(a, \underline{\Gamma}(a)) = g(b, \underline{\Gamma}(b))$, $0 < a < b < x_{c_+}$. By Lemma 5.10, we may write

$$g(a, \underline{\Gamma}(a)) = \Xi(a, v_\Gamma(a)), \quad g(b, \underline{\Gamma}(b)) = \Xi(b, v_\Gamma(b)).$$

Because Ξ is injective on $v = 0$, we know that we must have $v_\Gamma(a), v_\Gamma(b) \neq 0$. In fact the only way for there to be an intersection is $v_\Gamma(a) < 0, v_\Gamma(b) > 0$. In any case, q must lie in the interior of S_Ξ .

Our first step is to cut off the corners of the domain of g appropriately. We begin

at the base corner. Consider the geodesic

$$\sigma_a(s) = \Xi(a, s)$$

passing through q at $s = v_\Gamma(a)$ and exiting our polar neighborhood \mathcal{N} at $s = s_-^a$. As noted in Lemma 5.10, this geodesic is a graph over the y axis which has positive x coordinate for $s \in [a, s_+^a]$. Let $x_0 > 0$ be the lowest x coordinate it attains on this interval. Then by the Corner Slope Improvement Lemma (Lem. 4.17), there is an $\hat{x}_0 = C(\Gamma)x_0 \in (0, a)$ so that the Gauss map sends $x < \hat{x}_0$ to $x < x_0/2$ on the Gauss sphere. As such, the Gauss image of $x = \hat{x}_0$ is disjoint from the geodesic segment of $\sigma_a, s \in [v_\Gamma(a), s_+^a]$.

Working relative to x', y' coordinates at $\eta_\Gamma(s_{c_+})$, repeat the same process for the geodesic

$$\sigma_b(s) = \Xi(b, s),$$

which passes through q at $s = v_\Gamma(b)$ and exits \mathcal{N} at $s = s_+^b$. We obtain a cutoff value $\hat{x}_+ \in (b, x_{c_+})$ so the Gauss map sends $x = \hat{x}_+$ to $x' \leq x'_+$ so that it does not intersect $\sigma_b, s \in [s_0^b, s_+^b]$.

Now let U be the compact subdomain of $\text{dom } g$ with $x \in [\hat{x}_0, \hat{x}_+]$. Noting the Lemma 5.10, we can apply the Curve Lift Lemma (Lem. A.4, p. 149) to lift $\sigma_a : [v_\Gamma(a), s_1^a] \rightarrow U$ and $\sigma_b : [v_\Gamma(b), s_1^b] \rightarrow U$ to positive length curves $\hat{\sigma}_a, \hat{\sigma}_b$ in U which terminate in ∂U .¹ Because of how the $x = \hat{x}_0$ cutoff was constructed, $\hat{\sigma}_a$ cannot terminate in $x = \hat{x}_0$. If it terminates on the $\underline{\gamma}$ curve then because σ_a is a graph over the y axis, moving in the negative y direction, and because it has positive length, it must meet the thread curve at $y < y_q$. Let Θ_a be the set of $x \in [\hat{x}_0, \hat{x}_+]$ where $g_\gamma(x)$ has y value less than y_q . (This set could be empty.) We conclude that $\hat{\sigma}_a$ terminates on the $\underline{\gamma}$ curve for $x \in \Theta_a$, or it terminates on the $x = \hat{x}_+$ boundary of U .

Let us compare to the lifted curve $\hat{\sigma}_b$. Because of how the $x = \hat{x}_+$ cutoff was constructed, $\hat{\sigma}_b$ cannot terminate in $x = \hat{x}_+$. If it terminates on the $\underline{\gamma}$ curve then because σ_b is a graph over the y axis, moving in the positive y direction, and because it has positive length, it must meet the thread curve at $y > y_q$. Let Θ_b be the set of $x \in [\hat{x}_0, \hat{x}_+]$ where $g_\gamma(x)$ has y value more than y_q . (This set could be empty.) We conclude that $\hat{\sigma}_b$ terminates on the $\underline{\gamma}$ curve for $x \in \Theta_b$, or it terminates on the $x = \hat{x}_0$

¹It should be clear that this lemma applies. We note that the curves σ_a, σ_b do not intersect the curve η_Γ and so we are ensured that the Gauss map is an immersion on the preimage of these curves.

boundary of U .

Because of the Gauss thread curve is a graph over the y -axis, every element of Θ_a exceeds every element of Θ_b . Now we see in **Figure 5-5** that the curves $\hat{\sigma}_a$ and $\hat{\sigma}_b$ must cross:

$$\hat{\sigma}_a(s_a^*) = \hat{\sigma}_b(s_b^*)$$

for some $s_a^* \in (v_\Gamma(a), s_1^a]$ and $s_b^* \in (v_\Gamma(b), s_1^b]$. But then we may push down by g to obtain

$$\sigma_a(s_a^*) = \sigma_b(s_b^*).$$

But this is a contradiction, because the geodesics σ_a and σ_b do not touch after their initial intersection at q ! ■

Lemma 5.15. The Gauss wire curve does not touch the supporting ruling segment of any Gauss wire point $g_\Gamma(\hat{x})$. In other words, g_Γ does not intersect $\Xi(\hat{x}, [0, v_\Gamma(\hat{x})])$ when $v_\Gamma(\hat{x}) > 0$ or $\Xi(\hat{x}, (v_\Gamma(\hat{x}), 0])$ when $v_\Gamma(\hat{x}) < 0$.

Proof. We show the case $v_\Gamma(\hat{x}) < 0$; the other case follows similarly. Say to the

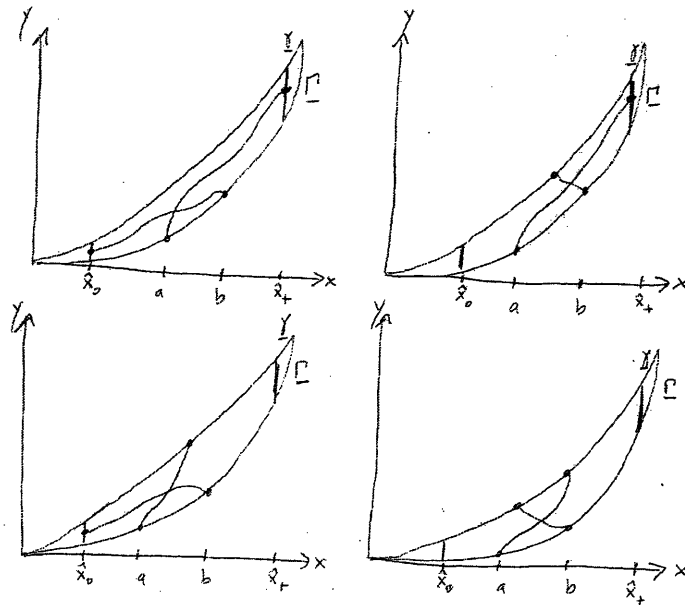


Figure 5-5: Lifted curves cross. Based on the arguments of Lemma 5.14, the lifted curves $\hat{\sigma}_a$ and $\hat{\sigma}_b$ must cross.

contrary that

$$\Xi(a, v) = \Xi(c, v_\Gamma(c)).$$

Then we would have to have $v_\Gamma(c) > 0$, for the ruling map is injective on pieces of its domain where v has a single sign. Well, v_Γ is continuous, so on (a, c) it must hit zero for the first time at some intermediate $b \in (a, c)$. Let Z be the region bounded by $g_\Gamma|_{[a,b]}$, the curve $\eta_\Gamma|_{[s(a),s(b)]}$, and the ruling geodesic from $\eta_\Gamma(s(x))$ to $g_\Gamma(a)$. There are two cases:

CASE I. The Gauss wire curve enters region Z after touching the η_Γ curve at $\eta_\Gamma(s(b))$. See **Figure 5-6**. In this case, take any $b' \in (b, c)$ near b . Introduce a smooth curve $\sigma(s)$ which for $s \geq 0$ follows the ruling supporting $g_\Gamma(b')$ for a short distance, then turns and moves vertically so it exits the region Z by crossing the η_Γ curve. By making this happen close enough to $g_\Gamma(b')$ we can ensure that σ does not touch the Gauss thread curve for $s \geq 0$ (see Lemma 5.13). Continue σ for $s \leq 0$ by having it turn and move vertically in negative y , never touching η_Γ . Form a subdomain U of $\text{dom } g$ by cutting off $\text{dom } g$ near $x = 0$ and $x = x_{c+}$ so that the Gauss image of the cutoff curves do not touch $\sigma(s), s \geq 0$ and so $(b', \underline{\Gamma}(b'))$ lies in U . We would like to apply the Curve Lift Lemma (Lem. A.4, p. 149) to lift σ to a curve $\hat{\sigma} : [0, s^*] \rightarrow U$ where $s^* > 0$ and $\hat{\sigma}(s^*) \in \partial U$. Let us check that the conditions of Curve Lift Lemma (Lem. A.4, p. 149) are met. We note that the Gauss map is an immersion on the preimage of $\text{Im } \sigma$ lying in U . (Indeed for this to be false we would need v_Γ to vanish corresponding to the point where σ crosses η_Γ , but to the contrary it is positive there by construction.) Moreover, Lemma 5.10 guarantees that the Possibly Nontransverse condition (a_2) is met. Checking the other conditions of Curve Lift Lemma (Lem. A.4, p. 149) is straightforward. But then pushing down by g , this means that σ intersects $g(\partial U)$ at some $s^* > 0$. This is in fact impossible by our construction, and will lead to a contradiction. Let us check: by construction, it can't touch the Gauss image of the cutoff boundaries or the $\underline{\gamma}$ boundary.

- (i) For it to be touched by $g_\Gamma(x)$ for $v_\Gamma(x) < 0$, it we would have to have $x \in [a, b]$, but those Gauss wire curve points are in a part of ∂Z which σ never touches for positive s .
- (ii) For it to be touched by $g_\Gamma(x)$ for $v_\Gamma(x) = 0$, this would have to happen where σ crosses the η_Γ curve, but that happens at $\eta_\Gamma(x')$ for $x' \in (a, b)$ and b was chosen so it was the first place on (a, c) where v_Γ vanishes.

(iii) For it to be touched by $g_{\Gamma}(x)$ for $v_{\Gamma}(x) > 0$, we would have to have $x \in (b, b')$. Let τ be the pieces of wire curve $g_{\Gamma}(x), x \in (b, b'), v_{\Gamma}(x) > 0$. Then τ is a graph over a subset of (b, b') with respect to the positive v ruling by Ξ . The curve $\sigma, s > 0$, is also a graph in this sense, and has been constructed to have strictly larger v values. So there is no touching in this case either.

We have achieved a contradiction in this case.

CASE II. The Gauss wire curve does not enter the region Z after touching the η_{Γ} curve at $\eta_{\Gamma}(s(b))$. See **Figure 5-7**. In this case, it is impossible for the Gauss wire curve to move subordinate to the ruling Ξ and reach $\Xi(a, v)$ without crossing $g_{\Gamma}(x), x \in [a, b]$. This is prohibited of course by Lemma 5.14. We have achieved a contradiction in this case. ■

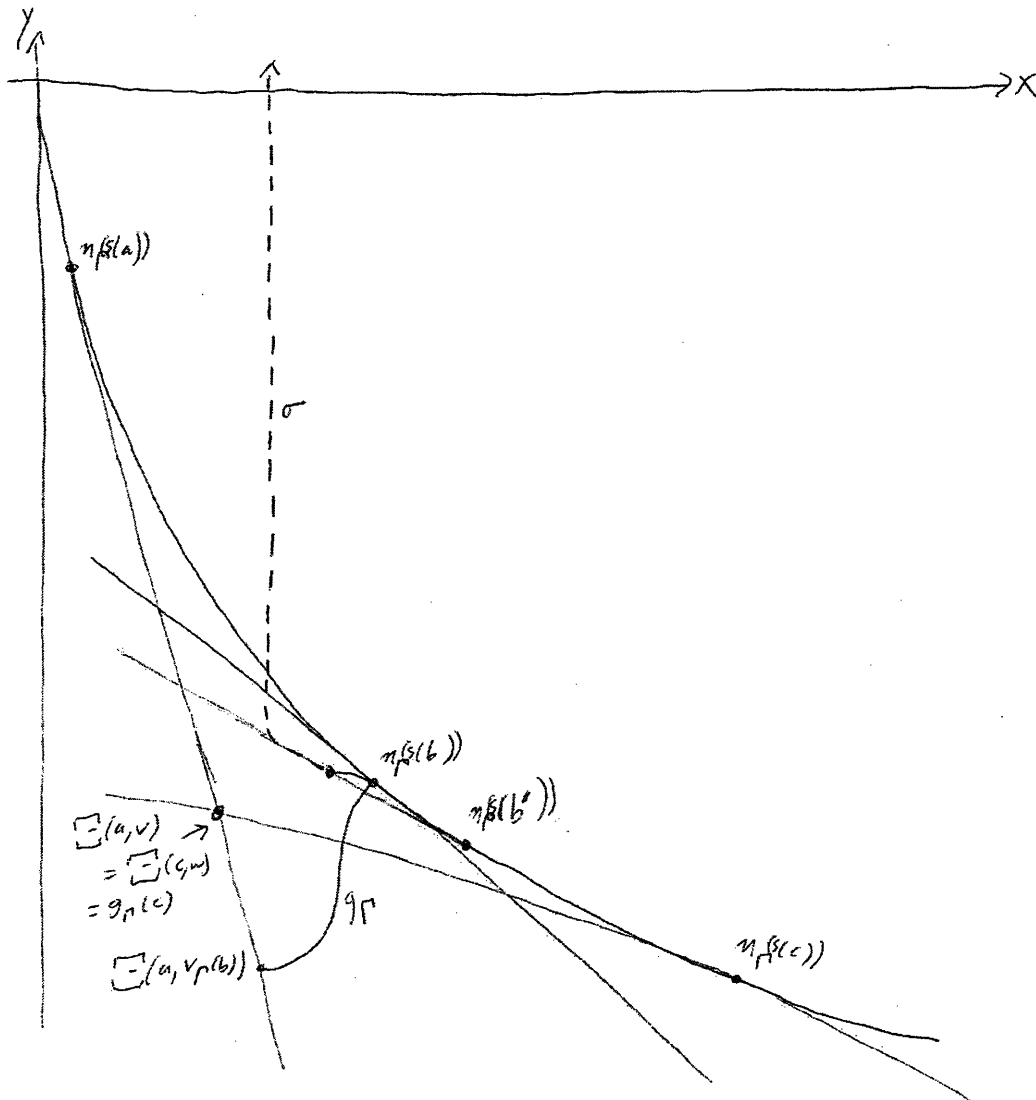


Figure 5-6: Gauss wire curve cannot cross supporting ruling segment: I.

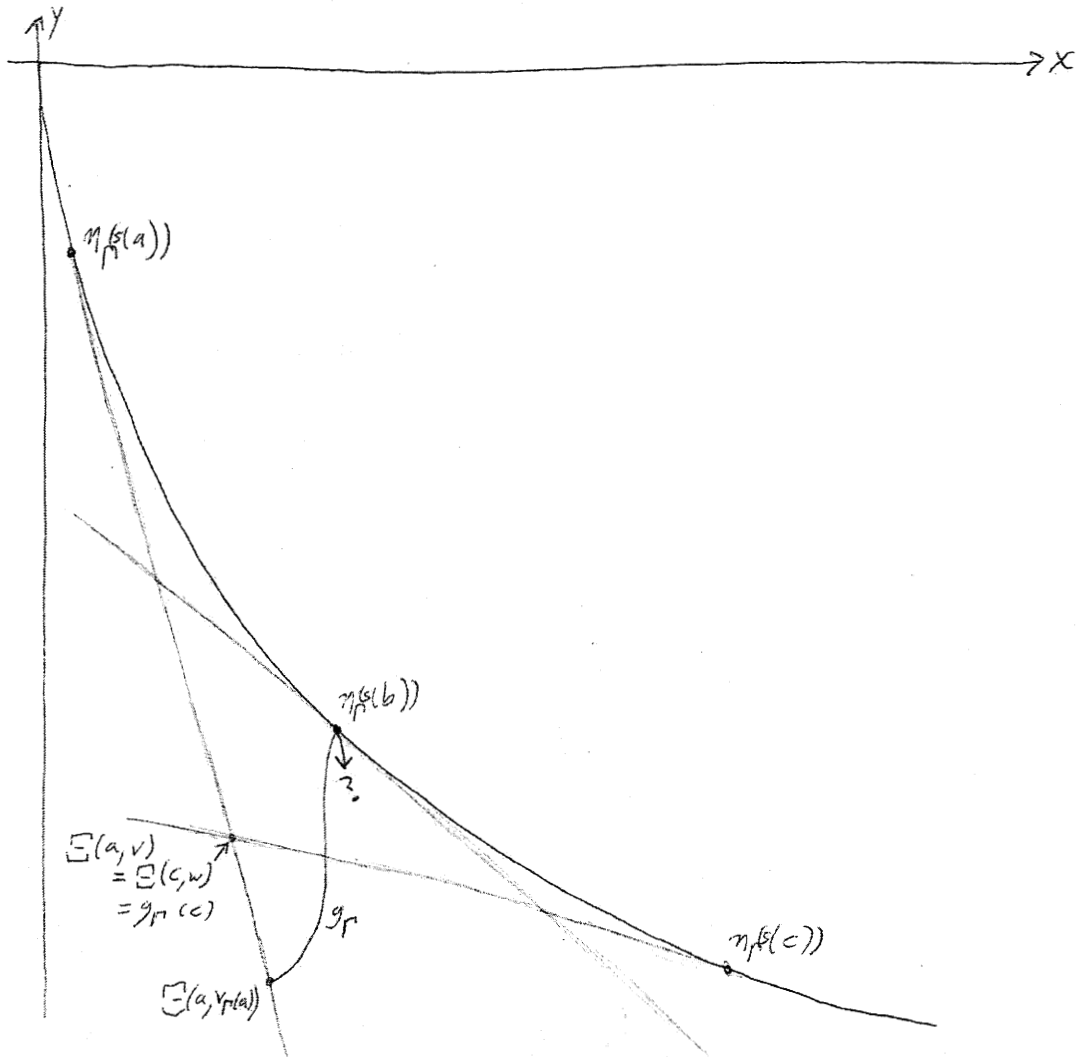


Figure 5-7: Gauss wire curve cannot cross supporting ruling segment: II.

Lemma 5.16. The Gauss thread curve does not intersect the Gauss wire curve.

Proof. If such an intersection happened, it would have to happen off the η_Γ curve, by Lemma 5.13. Now see **Figure 5-8**. Given such an intersection at $g_\Gamma(a)$, we define a smooth curve $\sigma(s)$ which for $s \geq 0$ follows the supporting geodesic and then turns and crosses η_Γ and then exits the polar neighborhood \mathcal{N} . Continue σ for $s \leq 0$ so it never touches η_Γ and exits the polar region \mathcal{N} . Construct a subdomain U of $\text{dom } g$ by cutting off near $x = 0$ and $x = x_{c_+}$ so that the Gauss image of the boundaries formed miss the curve $\sigma(s), s \geq 0$, and so that U contains $(a, \underline{\Gamma}(a))$. We may then apply the Curve Lift Lemma (Lem. A.4, p. 149) to lift σ to a curve $\hat{\sigma} : [0, s^*] \rightarrow U, s^* > 0$, which terminates in ∂U . By Lemma 5.15, the σ curve does not touch the wire for $s > 0$. The σ curve cannot touch the thread for $s > 0$, because if it did, the thread curve would be touching a geodesic at two points. As a curve of positive curvature, it would then have to stay on the side of ruling geodesic away from the y axis. It would then have to touch η_Γ , violating Lemma 5.13. Finally, by construction the curve $\sigma(s), s \geq 0$ does not touch the Gauss image of the cutoff boundaries of U . So we have a contradiction.

■

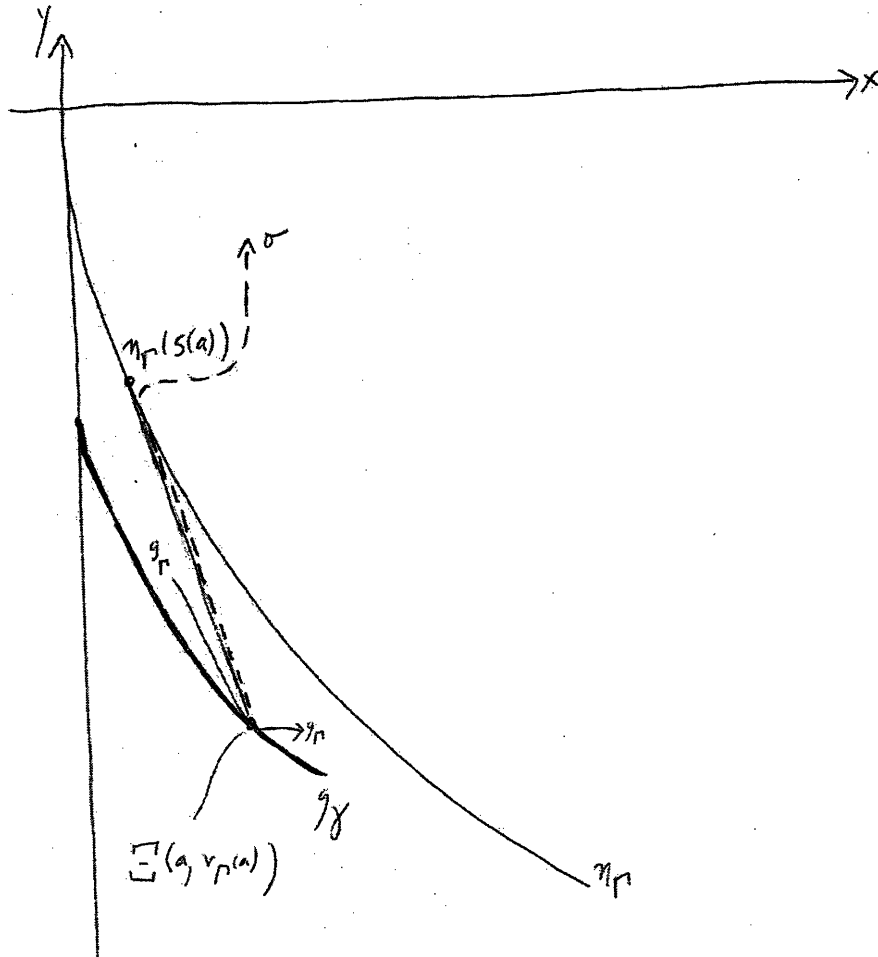


Figure 5-8: Gauss wire curve cannot intersect Gauss thread curve.

Lemma 5.17. The Gauss map does not map to points on the negative x side of the g_γ curve.

Proof. Say on the contrary that $g(\hat{q}) = q, \hat{q} \in (\text{dom } g)^o$ as in **Figure 5-9**. Then form a smooth curve σ which for $s \geq 0$ moves horizontally parallel to x (crossing the Gauss thread curve at $g_\gamma(b)$) until it first hits a wire point, then turns and follows the ruling geodesic supporting that wire point back to the η_Γ curve, then turns and crosses η_Γ and eventually exits the polar neighborhood \mathcal{N} . For $s \leq 0$, continue the curve so it never touches η_Γ and then exits \mathcal{N} . Form a subdomain U of $\text{dom } g$ by cutting off $\text{dom } g$ near $x = 0$ and $x = x_{e_+}$ so the Gauss image of the cutoff lines miss $\sigma(s), s \geq 0$ and so U contains $(b, \underline{\gamma}(b)), (a, \underline{\Gamma}(a))$. We may now apply the Curve Lift Lemma (Lem. A.4, p. 149) to lift σ to a curve $\hat{\sigma}_1 : [0, s_1^*] \rightarrow U, s_1^* > 0$, which starts at \hat{q} and terminates in ∂U . We may also lift σ to a curve $\hat{\sigma}_2 : [0, s_2^*] \rightarrow U, s_2^* > 0$, which starts at $(b, \underline{\gamma}(b))$ and ends in ∂U . But then looking at **Figure 5-9**, we see that

$$g(\hat{\sigma}_1(s_1^*)) = g(\hat{\sigma}_2(s_2^*)) = g_\Gamma(a).$$

By the injectivity of g on the $\underline{\Gamma}$ curve (Lemma 5.14), we conclude that $\hat{\sigma}_1(s_1^*) = \hat{\sigma}_2(s_2^*)$. But then by looking at the local picture, we can continue backwards on both curves to conclude that they are the same curve. But then $q = g_\gamma(a)$, which is a contradiction. Looking at the local picture, we can continue backwards on both curves to conclude that they are the same curve. But then $q = g_\gamma(a)$, which is a contradiction. ■

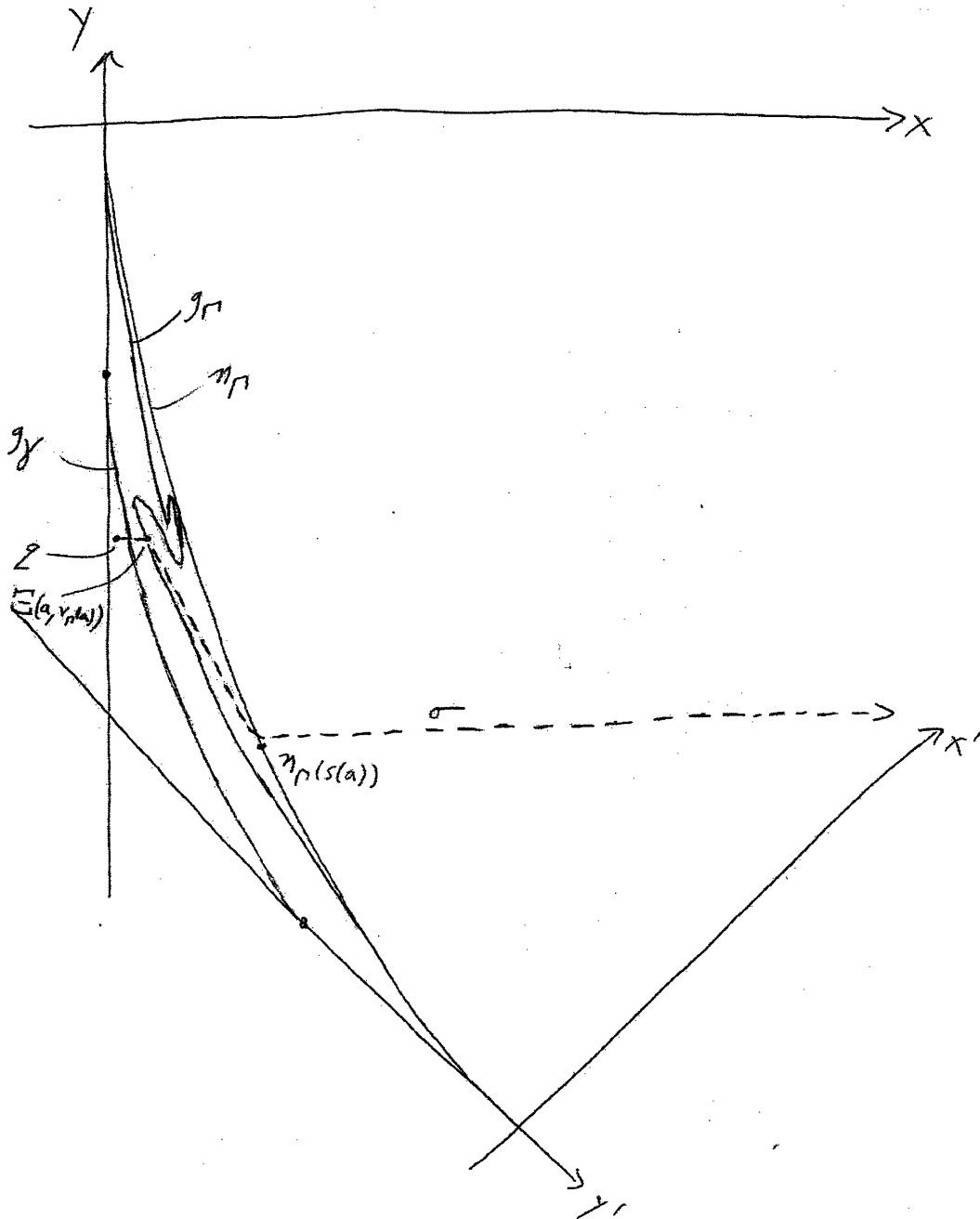


Figure 5-9: The Gauss thread curve bounds the Gauss image to one side..

Lemma 5.18. The Gauss map is injective.

Proof. Say there are two points $\hat{p}_1, \hat{p}_2 \in \text{dom } g$ with $g(\hat{p}_1) = g(\hat{p}_2) = p$. We will show that they must be the same point. There are two cases. The second case is that p lies on η_Γ and g maps to p non-immersively. Otherwise we have the first case, which we prove now. For $s \geq 0$ let $\sigma(s)$ be a segment from p moving approximately parallel to the x axis in the positive direction so that does not intersect η_Γ at the image of a point where g is not an immersion. (This is possible because there are only countably many such points; see Lemma 5.11.) Modify σ so if it hits the image of the Gauss wire curve, it turns smoothly and follows the supporting ruling segment of Ξ back to the η_Γ curve and then turns to cross that curve smoothly and then move parallel to the x axis until it exits the polar neighborhood \mathcal{N} . In this way the curve σ touches the Gauss wire curve at most once for $s > 0$ (See Lemma 5.15). It cannot touch the thread for $s > 0$ because by Lemma 5.17 the point p is either on the thread or to the positive x side of the thread, and σ moves in the positive x direction with y changing little enough so it does not touch the graph of the Gauss thread curve.

This curve has been chosen so that the Gauss map is immersive on $g^{-1}(\text{Im } \sigma \setminus \{\sigma(0)\})$. Cut off the domain of g near $x = 0$ and $x = x_{c+}$ to make a subdomain U so by the Corner Slope Improvement Lemma (Lem. 4.17), the curve σ does not intersect the Gauss image of the cutoff boundaries of U . We may apply Curve Lift Lemma (Lem. A.4, p. 149) to lift this curve by g to \hat{p}_1 and \hat{p}_2 . This gives two curves $\hat{\sigma}_1$ and $\hat{\sigma}_2$. By Curve Lift Lemma (Lem. A.4, p. 149), these curves must both touch the set $g(\partial U)$ at positive arclength values. By construction they may only touch the $\underline{\Gamma}$ or $\underline{\gamma}$ boundaries of U . Because σ travelled in the direction of increasing x , it cannot touch the Gauss thread curve for positive arclength parameter. So both lifted curves must terminate at points lying over a wire point. The curve σ was constructed so there is at most one such point, some point $g_\Gamma(x^*)$. But then because the Gauss wire curve is simple (Lemma 5.14), we conclude that the curves $\hat{\sigma}_1$ and $\hat{\sigma}_2$ terminate in the same point in $\text{dom } g$. Then by the uniqueness property of Curve Lift Lemma (Lem. A.4), we may conclude that the curves $\hat{\sigma}_1$ and $\hat{\sigma}_2$ are identical. In particular, their starting points \hat{p}_1 and \hat{p}_2 are the same.

We return to the second case, that p lies on $\eta_\Gamma(s(a))$ and g is not immersive at $(a, \underline{\Gamma}(a))$. Then because the Gauss map is an injection on the $\underline{\Gamma}$ boundary (Lemma 5.14), we know at least one of the points \hat{p}_1, \hat{p}_2 is not on the $\underline{\Gamma}$ curve. Without loss of generality, assume it is \hat{p}_1 . Then draw a curve τ in the Gauss sphere starting at p and moving

exactly horizontally in the direction of increasing x . Use Corner Slope Improvement Lemma (Lem. 4.17) to cut off the domain of g near its cusps so the image of the cutoff curves is away from the curve τ . Because \hat{p}_1 is not on the Γ boundary of $\text{dom } g$, the map g is immersive at \hat{p}_1 . We may use Curve Lift Lemma (Lem. A.4, p. 149) to lift τ to a curve $\hat{\tau}$ in $\text{dom } g$. Then τ must hit a boundary of the cutoff domain of g after positive length. But it does not hit any points of the Gauss image of this set. This is a contradiction. This completes the second case. ■

Lemma 5.19. Let y_γ^0 be the limit of the y -component of $g_\gamma(x)$ at $x = 0$. There is a positive continuous decreasing function $\delta : (0, x_{c+}) \rightarrow \mathbb{R}$ so

$$g_{[y]}(x, y) \geq y_\gamma^0 - \delta(x).$$

Proof. Given (\hat{x}, \hat{y}) in $\text{dom } g$, we know by the Corner Slope Improvement Lemma (Lem. 4.17) that $g(\hat{x}, \hat{y})$ lies in $x < C(\Gamma)\hat{x}$. By Lemmas 5.17 and 5.13 we see that $g(\hat{x}, \hat{y})$ lies in the shaded region shown in **Figure 5-10**. Here the intersection point between g_γ and the vertical line may be taken to be the highest such intersection. The fact that g_γ cannot lie on the y axis (Lemma 5.7) shows that such an intersection must exist for sufficiently small \hat{x} . The continuity of g_γ forces the intersection to be some vertical distance $\delta(\hat{x})$ from y_γ^0 , where $\delta(\hat{x})$ vanishes as \hat{x} goes to zero. ■

5.6 Obtaining the crucial slope inequality

Lemma 5.20. The Gauss map has a limit at the base corner, and that limit is the Frenet binormal of the wire at the base corner. In other words, the limit $\lim_{p \rightarrow (0,0)} g(p)$ exists and equals $(0, 0)$.

Proof. By the Corner Thread Monotonicity Lemma (Lem. 5.2) and the Corner Slope Improvement Lemma (Lem. 4.17) we know that the Frenet frame of the thread approaches a limit at the base corner. Let $\eta_\gamma(0) = (-\sin \alpha)\nu_\Gamma(0) + (\cos \alpha)\eta_\Gamma(0)$ be the binormal in this limiting frame. Then $\sin \alpha = -y_0^\gamma$ from the previous lemma. Let (x, y) be in $\text{dom } f$. Then the previous lemma says

$$\frac{-f_y(x, y)}{\sqrt{1 + f_x(x, y)^2 + f_y(x, y)^2}} > y_0^\gamma - \delta(x).$$

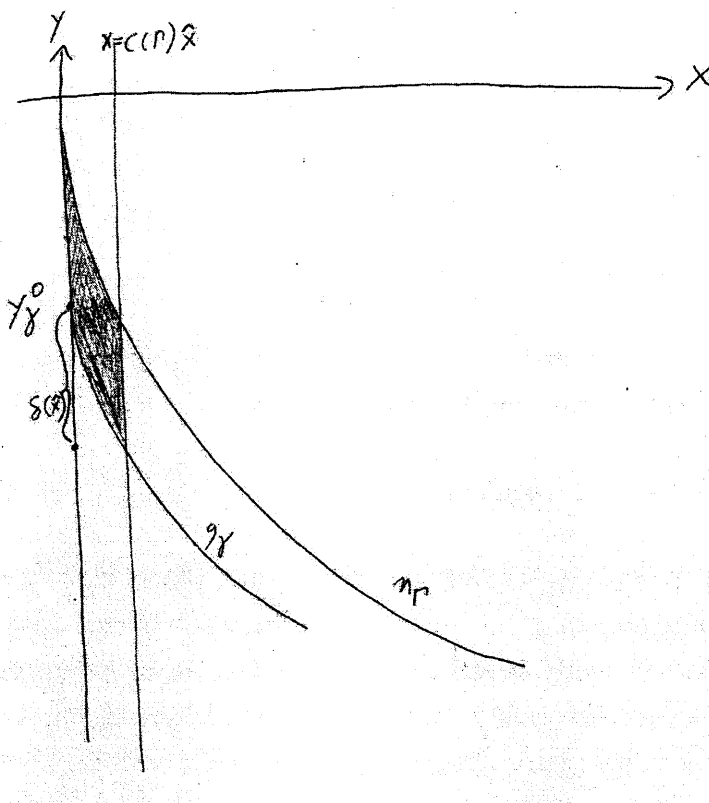


Figure 5-10: Gauss thread curve bounds y -slopes.

Using the fact that $f_y(x, y)$ lies in $(0, C(\Gamma)R^{1/12})$ and $f_x(x, y) \in (-C(\Gamma)x, 0)$ we may obtain

$$\frac{-f_y(x, y)}{\sqrt{1 + f_y(x, y)^2}} > y_0^\gamma - \delta_2(x)$$

for $\delta_2(x) > 0$ continuously approaching 0 as x goes to 0. Now we may use the fact that the function

$$a \mapsto \frac{a}{\sqrt{1 + a^2}} = \sin \tan^{-1}(a)$$

is a monotonically increasing map from \mathbb{R} to $(-1, 1)$ to show

$$\begin{aligned} \frac{-f_y(x, y)}{\sqrt{1 + f_y(x, y)^2}} &> y_0^\gamma - \delta_2(x) \\ \sin \tan^{-1} f_y(x, y) &< \sin \alpha + \delta_2(x) \\ f_y(x, y) &< \tan \alpha + \delta_3(x) \end{aligned} \tag{5.10}$$

Well, again noting the Corner Slope Improvement Lemma (Lem. 4.17), we show that $f_y(x, \underline{\gamma}(x))$ approaches $\tan \alpha$. We have now shown the crucial inequality (5.2) and may apply Corner Slope Inequality Lemma (Lem. 5.4) to obtain the result. ■

In this section we have proved:

Lemma 5.21. The Gauss image is a simply-connected domain bounded by the Gauss thread curve and Gauss wire curve, meeting at the wire Frenet binormal points $\eta_\Gamma(0)$ and $\eta_\Gamma(s_{c_+})$.

5.7 Laplacian on Gauss image with Dirichlet-Neumann boundary conditions

Lemma 5.22. The first eigenvalue of the Laplacian on $\text{Im } g$ with Dirichlet condition on the Gauss wire curve and Neumann condition on the Gauss thread curve is large:

$$\lambda_1 \geq C(\Gamma)R^{-1/3}$$

Proof. Consider a test function $\varphi \in C^0(\overline{\text{Im } g})$ with $\varphi = 0$ on the Gauss wire curve, and

$$I = \int_{\text{Im } g} G(\nabla^G \varphi, \nabla^G \varphi) \text{dvol } G \tag{5.11}$$

defined and finite. Here G is the metric on the sphere in our x, y coordinates:

$$G(u, v) = \langle \pi(u), \pi(v) \rangle$$

where

$$\pi(u_1, u_2) = (u_1, u_2, \sqrt{1 - u_1^2 - u_2^2}).$$

For $|x|, |y| < \epsilon$ we have in $\partial x, \partial y$ coordinates that G is the matrix

$$G = \begin{pmatrix} 1 + x^2 & xy \\ xy & 1 + y^2 \end{pmatrix} + O(\epsilon^4)$$

We see that

$$\text{dvol } G = \sqrt{\det G} = 1 + \epsilon^2 + O(\epsilon^4) \tag{5.12}$$

and

$$G(u, u) = (1 + 2\epsilon^2 + O(\epsilon^4))(u_1^2 + u_2^2). \quad (5.13)$$

The domain of g lies in the first quadrant with $x \leq C(\Gamma)R^{1/12}$ and $y \leq C(\Gamma)R^{1/6}$. In Lemma 5.8, equation (5.8) we showed that the Gauss thread curve is a graph $x = h_\gamma(y)$. The Gauss wire curve is trapped between this graph and the graph of the wire Frenet binormal curve η_Γ . We may extend our test function φ by zero so it is defined for all points to the right of $\text{dom } h_\gamma$ from $x = h_\gamma(y)$ to $x = H$ where $H = C(\Gamma)R^{1/6}$ is the maximum x -value of the wire Frenet binormal curve.² Now we may estimate I of (5.11) as

$$\begin{aligned} I &\geq \int_{y \in \text{dom } h_\gamma} \int_{x=h_\gamma(y)}^H (\varphi_x^2 + \varphi_y^2) dx dy \\ &\geq \int_{y \in \text{dom } h_\gamma} \left(\int_{x=h_\gamma(y)}^H \varphi_y^2 dx \right) dy \end{aligned}$$

We may treat the inner integral using the eigenvalue estimate $\int_0^b w_y^2 dy \geq \frac{\pi^2}{4b^2} \int_0^b w^2$ for $w(0) = 0$. In our case, the longest that the interval $[h_\gamma(x), H]$ can be is $H = C(\Gamma)R^{1/6}$. So we may continue,

$$\begin{aligned} I &\geq \int_{y \in \text{dom } h_\gamma} C(\Gamma)R^{-1/3} \left(\int_{x=h_\gamma(y)}^H \varphi^2 dx \right) dy \\ &= C(\Gamma)R^{-1/3} \int_{\text{Im } g} \varphi^2 dx dy \\ &\geq C(\Gamma)R^{-1/3} \int_{\text{Im } g} \varphi^2 d\text{vol } G \end{aligned}$$

In the last step we used (5.12). ■

²This calculation of H follows from the fact that the wire Frenet binormal curve is a graph of a function which is approximately quadratic over an interval of length $C(\Gamma)R^{1/12}$.

5.8 Lower bound on thread torsion near corner

Lemma 5.23. For $0 < x(s) < x_{c_+}$, define $\kappa_{g_\gamma}(s) = \kappa/T_\gamma(s)$. Then

$$\int_{s_1=0}^s \int_{s_2=0}^s \kappa_{g_\gamma}(s_2) ds_2 ds_1 < \kappa_\Gamma(0)/T_\Gamma(0)s^2 + O(s^3).$$

In particular, if $T_\gamma(s)$ has a limit T_0 as s goes to zero, then

$$\frac{T_0}{T_\Gamma(0)} \geq \frac{\kappa}{\kappa_\Gamma(0)}. \quad (5.14)$$

Proof. This follows directly from the fact that the Gauss thread curve and the wire binormal curve are both graphs over the negative y axis, they start at the origin, and the wire binormal curve stays on the positive x side of the Gauss thread curve. One must also note that the curvature of the Gauss thread curve is κ/T_γ . (See section 3.2.)

■

REMARK. We already have a large class of examples of *extensible thread-wire surfaces*. We do not show that these are Alt minimizers, although we expect that they are when their thread and wire boundaries are close. We can compute exactly the ratio between thread torsion and wire torsion for extensible thread-wire surfaces at wire-oscillating corners. It is interesting to compare this calculation with the bound of the above result. The regime where we should compare is when the thread curvature is close to the wire curvature, as must be the case for the near-wire Alt minimizers treated by Lemma 5.23. Plugging $\kappa = \kappa_\Gamma(0) + \epsilon$ into our exact computation for extensible surfaces (equation (7.1)) gives

$$\begin{aligned} \frac{T_0}{T_\Gamma(0)} &= \frac{\kappa_\Gamma(0)}{3\kappa_\Gamma(0) - 2\kappa} \\ &= 1 + 2\epsilon + O(\epsilon^2). \end{aligned}$$

On the other hand, equation (5.14) gives

$$\frac{T_0}{T_\Gamma(0)} \geq 1 + \epsilon.$$

So if one showed that the extensible thread-wire surfaces were Alt minimizers, their torsion ratios would be consistent with Lemma 5.23. One is naturally interested to

know if the thread torsion always attains a limit for near-wire Alt minimizers – and if so, how the thread torsion/wire torsion ratio behaves.

5.9 Proof of C^1 Corner Regularity Theorem (Thm. 1.5)

Together the results of this section prove C^1 Corner Regularity Theorem (Thm. 1.5). Claim (i) of the theorem, that the normal field converges to the Frenet binormal of the wire, is proved as Lemma 5.20. Claim (ii), that the Gauss map is injective and an embedding on its interior, is proved as Lemma 5.11 and Lemma 5.18. Claim (iii), that the Gauss map has the properties described in **Figure 1-4**, is proved as Lemma 5.7, Lemma 5.8, and Lemma 5.10. Also see Section 3.2 for the calculation of the curvature of the Gauss thread curve.

Chapter 6

Sufficient $C^{1,1}$ control implies crescent finiteness

This section is important because it justifies why we are studying near-wire crescents. The main outcome of this section is a proof of Lemma 1.3.

In Section 6.1 we show that if near-wire crescents were guaranteed to straddle maxima of wire curvature, then the Crescent Finiteness Conjecture (Conj. 1.1) would follow. The game is then to show that near-wire crescents straddle maxima of wire curvature. The first theorem of this thesis—Near-wire Crescent Theorem (Thm. 1.4)—fell short of this goal. It was only able to show that near-wire maxima lay *close* to maxima of wire curvature. It left open the possibility that even *infinitely many* crescents might lie near a single maximum of wire curvature. Our job is to reduce this bound to one, by showing that near-wire crescents straddle maxima of wire curvature.

Subject to a $C^{1,1}$ bound, we do this in Section 6.2. We analyze the intrinsic geometry of the crescent.¹By examining a family of curves with constant geodesic curvature, we show that near-wire crescents contain maxima of wire curvature.

¹The author also considered another method, which is extrinsic. Using a “twisting slide map” which transforms all of space near the wire, one can try to show that a crescent supported on a wire with monotonic curvature may be improved as an Alt competitor. This method is limited because it requires that the torsion not be too large relative to κ'' at a maximum of wire curvature.

6.1 Counting crescents using maxima of wire curvature

Lemma 6.1. Let Γ be an embedded, generic wire. Assume that there is an $R(\Gamma) > 0$ so any Alt crescent on Γ in a $R(\Gamma)$ tubular neighborhood of Γ contains a maximum of wire curvature κ_Γ in the interior of its supporting wire. Then for any length scale W small relative to the geometry of Γ , the following holds. For any Alt minimizer (B, M) supported on Γ ,

$$\#\text{crescents} < n + \ell(\Gamma)/W$$

and any crescent in (B, M) with supporting wire shorter than length W contains a maximum of κ_Γ . Here n is the number of maxima of κ_Γ .

Proof. Given $W > 0$, there is an $R(W) > 0$ so the convex hull of any arc $\tilde{\Gamma}$ of Γ of shorter than W lies in the union of normal discs of radius R associated to the arc $\tilde{\Gamma}$. By TWS Convex Hull Theorem (Thm. 3.4), any crescent with supporting wire shorter than W will be contained in a tubular neighborhood of radius R . Picking W small, we may make $R(W)$ small. Thus for sufficiently small W , we may force every Alt crescent supported on a wire of length less than W to contain a maximum of wire curvature, by assumption. The supporting arcs of wire for crescents of a single Alt minimizer do not overlap. Thus for small W , there are at most n crescents with supporting wire shorter than W . On the other hand, there are at most $\ell(\Gamma)/W$ crescents with supporting wire equal to or longer than W . ■

6.2 Proof of Lemma 1.3

In this section we examine a crescent which has a normal field attaining limits at its corners which match the Frenet binormal of the wire there. We look at its intrinsic geometry as a Riemannian manifold with boundary, and show that the wire must attain a maximum of wire curvature on the interior of the supporting piece of wire. This proves Lemma 1.3 from the Introduction.

The basic inspiration is the planar case. See **Figure 6-1**.

Lemma 6.2. Let Γ be an embedded, generic wire. Let R be sufficiently small so that Near-wire Crescent Theorem (Thm. 1.4) applies. There is a constant $C(\Gamma)$, so any Alt

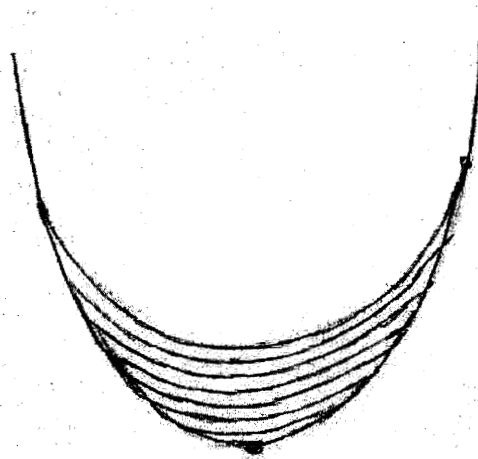


Figure 6-1: Planar crescents always contain a maximum of wire curvature. We may continue the thread curve as a family of constant curvature curves; this helps us find the maximum of wire curvature. In Section ?? we adapt this idea to the nonplanar case.

crescent (X, ϕ_-) lying in $\text{Tub}_R(\Gamma)$ is supported by a piece of Γ on which κ_Γ attains an interior maximum, provided the following holds:

- **Corner property:** The Alt crescent may be written as a graph $z = f(x, y)$ in the Frenet coordinates of the wire at one of the corner points. Moreover, the function f is $C^{1,1}$ with $D^2 f$ bounded by $C(\Gamma)$.

If this curvature control held for all Alt minimizers sufficiently near the wire, we could then invoke:

We use **Figure 6-2** as our guide. Here (Σ, g) is the Alt crescent, considered as a Riemannian manifold with boundary. We parametrize the supporting wire by $\Gamma : [0, b_\Gamma] \rightarrow \mathbb{R}^3$ and the free thread by $\gamma : [0, b_\gamma] \rightarrow \mathbb{R}^3$, both by their own arclength. We also employ the Frenet coordinate functions x, y, z of Γ at $s = 0$. So for example, $x(P_+)$ is the x -coordinate of the far corner.

Definition 6.3. The **horizontal corner distance** of a point q in Σ is

$$d_{P_\pm}(q) = \min(x(q), x(P_+) - x(q)).$$

Lemma 6.4. In the context of Lemma 6.2, there exists a continuous bijection $c : (0, b_\Gamma) \rightarrow (0, b_\gamma)$ and a constant $C_1(\Gamma) \ll 1$ with the following properties:

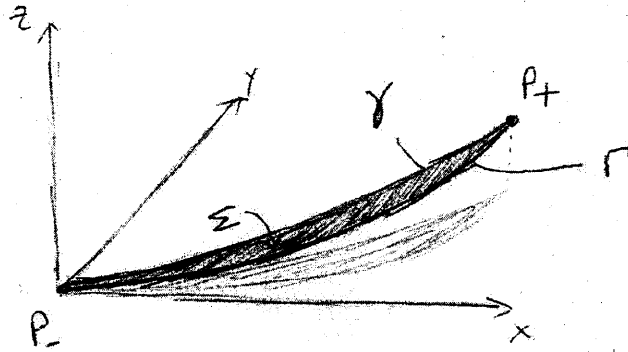


Figure 6-2: The geometric set-up.

- (i) Consider the point $p = \Gamma(s)$ and the truncated manifold $\Sigma(s) = \Sigma \cap \{d_{P_{\pm}} > C_1(\Gamma)d_{P_{\pm}}(p)\}$. The closest point on $\text{Im } \gamma \cap \Sigma'$ to p , measured intrinsically within $\Sigma(s)$, is $\gamma(c(s))$.
- (ii) There is a unique shortest path from $\Gamma(s)$ to $\gamma(c(s))$ within $\Sigma(s)$. It is an embedded geodesic (parametrized by arclength as $t \mapsto \tau^s(t)$) which touches the boundary of $\Sigma(s)$ only at its initial and terminal points. The geodesic meets γ perpendicularly.
- (iii) The function $h(s) = \ell(\tau^s)$ satisfies a bound

$$h(s) < C(\Gamma)\kappa \min(s, b_{\Gamma} - s)^2.$$

See **Figure 6-3**.

Proof. The idea of the proof is to set $C(\Gamma)$ so that, because of the quadratic tapering of the surface at each corner, there is no need to wander that close to the corner. Specifically, given s we consider the path shown in **Figure 6-5** which moves along the $x = x(\Gamma(s))$ slice of Σ in the positive y direction. This path has length at most $C_1(\Gamma)\kappa x^2$ from the constant slope control for Σ as a graph over x - y . So if we pick $C(\Gamma) = C_1(\Gamma)\kappa x(P_+)/4$ in the lemma, we will guarantee that any path that wanders more than halfway from $x(\Gamma(s))$ to the cutoff x -value will automatically lose in the length-minimization competition. Standard differential geometry shows that a length-minimizing curve exists (and that it is embedded). The preceding argument shows that the minimizing curve does not abut the constraint. We may then do standard

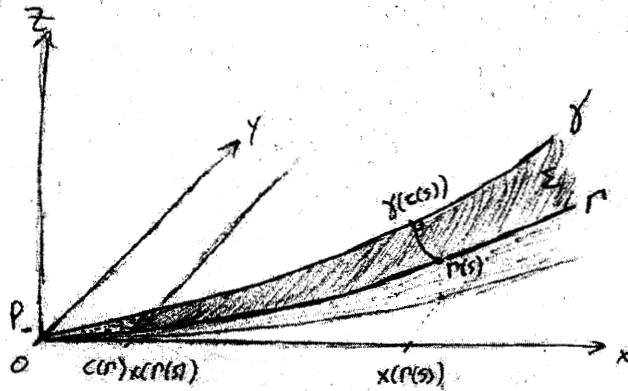


Figure 6-3: The function c defines a bijection between the wire and thread, based on finding a closest thread point to a given wire point.

calculus of variations to see that it is a geodesic. It is also clear that it must hit γ perpendicularly; otherwise there is a first order variation which decreases its length.

The path τ^s found above is the unique minimizer of length. Indeed, if there are two minimizers τ, τ' we get a picture like that in **Figure ??**. In part (a) of the figure we see the case that τ and τ' only intersect at $\Gamma(s)$, forming a region U . We may then write Gauss-Bonnet's theorem for this region:

$$-\kappa r + \pi/2 + \pi - \theta + \pi/2 = 2\pi - \int_U K_\Sigma d\text{vol } \Sigma.$$

Here $r > 0$ is the length of the thread connecting the end of τ to τ' , and $\theta \in [0, \pi]$ is as shown. But then $-\kappa r - \theta = -\int_U K_\Sigma d\text{vol } \Sigma$ which contradicts the fact that the Gauss curvature of a minimal surface is non-positive. On the other hand, if the minimizers τ, τ' cross, we just repeat the above analysis on the region they define which abuts the thread (**Figure ??b**). Thus we conclude that there is a unique minimizer τ^s .

We see that the geodesics τ^s must vary continuously with s . If two limits were obtainable in approaching some $s = s_1$, then we would be able to obtain two minimizers for that s value, which would contradict the uniqueness property.

The reference competitor shown in **Figure 6-5**, whose length we calculated above, shows (iii) of Lemma 6.4.

The function c must be surjective. Indeed, by (iii) we see that for small s the geodesic τ_s is of size $C(\Gamma)\kappa s^2$ and so must connect to a point $\gamma(c(s))$ with $c(s) <$

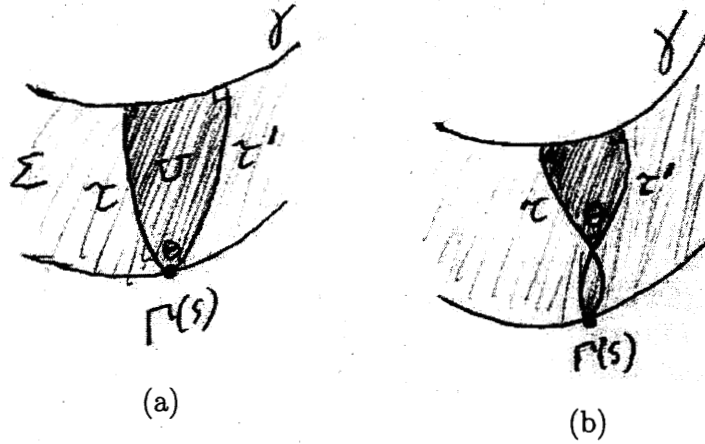


Figure 6-4: Uniqueness of length minimizer τ^s

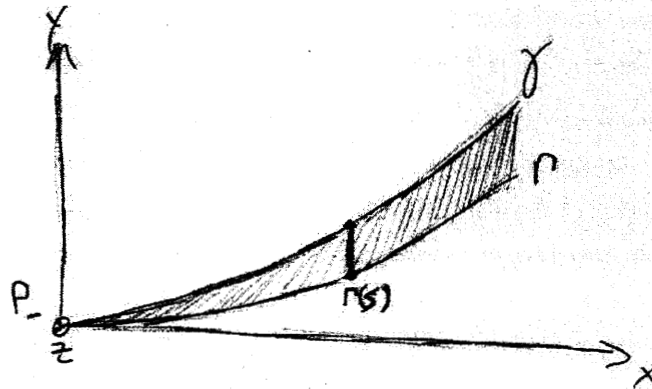


Figure 6-5: A top view of a simple-minded competitor in the minimization of Lemma 6.4.(i).

$C(\Gamma)\kappa s^2$. Making a similar argument for the other corner of Σ , we see that c attains arbitrarily high and low values in $(0, b_\gamma)$. By the intermediate value theorem, it is surjective.

On the other hand, c is injective. Indeed, if τ^{s_1} and τ_{s_2} reach the same point $\gamma(c(s_1)) = \gamma(c(s_2))$, then they both meet the thread here normally. By the uniqueness of geodesics, $\tau^{s_1} = \tau^{s_2}$ so $\Gamma(s_1) = \Gamma(s_2)$. ■

Lemma 6.5. In the context of Lemma 6.2, the function $h(s)$ attains its maximum at some interior point $s = s_0$. Here the geodesic τ^s meets both the wire and thread perpendicularly.

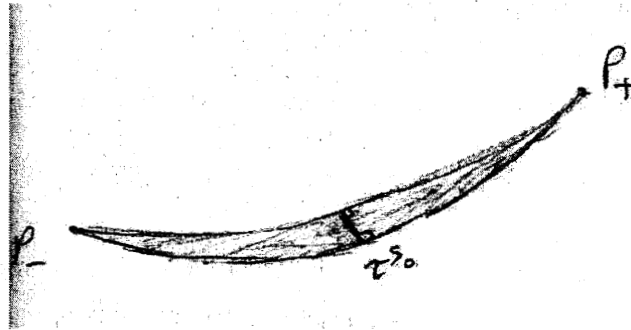


Figure 6-6: The geodesic τ^{s_0} .

See **Figure 6-6**.

Proof. We know that we cannot have $h(s) \equiv 0$ because then the constant curvature thread would coincide with the wire for positive length. This violates the Genericness Assumption 2.15. Then from Lemma 6.4.(iii), we know that it attains a positive maximum, and it does so at an interior point s_0 in $(0, b_\Gamma)$. Certainly the geodesic τ^{s_0} must meet the wire perpendicularly. If it does not, we can calculate the first variation of the geodesics emanating from γ normally and show that h attains higher values nearby. ■

Lemma 6.6. In the context of Lemma 6.2, at the corners we have the curvature inequality

$$\kappa_\Gamma(0) \leq \kappa, \quad \kappa_\Gamma(b^\Gamma) \leq \kappa.$$

Proof. Because of the corner assumption, we know that the Frenet frame of the thread coincides with that of Γ at the corner P_- . Then the curvature inequality follows from the fact that the thread stays on the positive y side of Γ . See **Figure 6-2**. ■

We may now tackle the main lemma of this section.

Proof–Lemma 6.2. Assume to the contrary that the supporting wire does not attain a maximum of its curvature on the interior. Then by Lemma 6.6,

$$\kappa_\Gamma \leq \kappa \tag{6.1}$$

on the entire supporting wire.

Definition 6.7. We define a family of constant-curvature curves on Σ as follows: For each point $\tau^{s_0}(y)$, let $\rho_y(x)$ be the curve of constant curvature defined by $|\rho'_y| = 1$ and

$$\nabla_{\rho'_y} \rho'_y = \kappa \text{Rot}(\rho'_y). \quad (6.2)$$

Here Rot rotates any tangent vector on Σ by $\pi/2$ in a continuous way compatible with $\text{Rot}\gamma' = \nu_\gamma$ on the thread.

Equation (6.2) is locally a second order ODE.

Lemma 6.8. Assume the curvature condition of Lemma 6.2. Let $\rho : [0, b] \rightarrow \Sigma$ be any curve in Σ with constant geodesic curvature κ . Then the projection $\underline{\rho}$ of ρ to x - y plane is a curve with curvature at most $C(\Gamma) + \kappa$. The lengths of ρ and $\underline{\rho}$ are comparable as R gets small. If $\ell(\underline{\rho}) < C(\Gamma)R^{1/12}$ then $\underline{\rho}$ is a graph over the tangent line to $\underline{\rho}$ at $s = 0$ and it continues along this line for a length comparable to $\ell(\rho)$ as R gets small.²

Proof. Consider the curve ρ , parametrized by arclength. We have

$$\rho'' = \kappa\nu + C(\Gamma)N$$

where ν is tangent to Σ and N is normal to it. By Near-wire Crescent Theorem (Thm. 1.4) we know that the binormal of ρ is constrained to be within $C(\Gamma)R^{1/12}$ of $(0, 0, 1)$. We may thus apply Lemma A.1 (p. 145) to obtain

$$\kappa_{\underline{\rho}} = (\kappa + C(\Gamma)) \quad (6.3)$$

The curve $\underline{\rho}'$ is a path on the unit sphere of length $\int_{s=0}^{\ell} (\underline{\rho}') |\kappa_{\underline{\rho}}| ds$; by above this is of size $C(\Gamma)R^{1/12}$. We conclude that $\langle \underline{\rho}'(s), \underline{\rho}'(0) \rangle > 1 - C(\Gamma, \epsilon_{\text{curv}})R^{1/12}$, so the curve $\underline{\rho}$ is indeed a graph and travels length $\ell(\underline{\rho})(1 + O(R^{1/12}))$ in the $\underline{\rho}'(0)$ direction. Finally, the slope control of Near-wire Crescent Theorem (Thm. 1.4) shows that this curve $\underline{\rho}(s)$ corresponds to a piece of ρ of length $\ell(\underline{\rho})(1 + O(R^{1/12}))$. ■

We may piece the constant curvature curves together to get a map $\Xi : (x, y) = \rho^y(x)$. The domain of this map contains $\{0\} \times [0, \ell(\tau^{s_0})]$; how much it extends in the x direction can vary as a function of y . The curve $x \mapsto \Xi(x, 0)$ parametrizes the thread curve up to each corner.

²By “comparable,” we mean their ratio approaches 1 as R goes to zero.

Subclaim 6.9. Given $\delta > 0$, there is a subdomain A_δ of $\text{dom } \Xi$, obtained by restricting each curve $\rho^y(x)$ to an interval of x values, such that

- (i) The map Ξ is an embedding on A_δ .
- (ii) The left boundary of A_δ maps to within horizontal distance δ of the base corner.
- (iii) The right boundary of A_δ maps to within horizontal distance δ of the positive corner.
- (iv) We have

$$h(C_1(\Gamma)\delta) > C_2(\Gamma).$$

Proof. Define A_δ as follows. For each $y \in (0, \ell(\tau^{s_0}))$, continue $\rho^y(x)$ in each direction until any of these holds:

- (i) The curve $\rho^y(x)$ hits $\partial \text{dom } f$.
- (ii) The curve $\rho^y(x)$ hits corner horizontal distance δ .

Using the graph property of Lemma 6.8 and the control of Σ as a graph over a domain between two graphs over the x axis, we may conclude that each ρ^y is well-defined in the set A^δ . Moreover, each ρ^y is a curve of length $O(R^{1/12})$ and its projection to the x - y plane is a graph over the x axis. We may now apply Lemma A.5 (p. 152).

Finally, we show that every ρ^y only terminates via condition (ii) above. Indeed, if one of them hits the lower boundary we can work backwards and violate the immersion property. If a ρ^y hits the upper boundary, we can work backwards to violate the property (6.1).

Then we can find a constant $C(\Gamma)$ so at horiz distnace $C(\Gamma)\delta$, the shortest path must pass through all of our ρ curves. (This uses the quadratic shape of the projection of Σ to the x - y plane.) We can then calculate this shortest length using the metric pulled back via Ξ . We can then use (A.12) to show you get at least a const amount of distance. ■

The last item of this subclaim contradicts Lemma 6.4. Thus we have achieved a contradiction, and we have proved by contradiction that κ_Γ must achieve a maximum on the supporting wire of the crescent. ■

Chapter 7

Examples

7.1 Extensible thread-wire surfaces

Let $\gamma : [0, b] \rightarrow \mathbb{R}^3$ be a regular real-analytic curve with constant curvature $\kappa \neq 0$. Let $\eta_\gamma(t)$ be the Frenet binormal to γ at $\gamma(t)$. Then we may apply Björling's formula to define a minimal surface which passes through γ :

$$X(u, v) = \text{Real} \left(\gamma(u + iv) - i \int_0^{u+iv} \gamma'(z) \times \eta_\gamma(z) dz \right).$$

Here we have used the expansion of γ to extend it as a map $\mathbb{C} \rightarrow \mathbb{C}^3$. The integral is a complex path integral. The \times operator is the extension of the usual cross product on \mathbb{R}^3 to a product on \mathbb{C}^3 . The parametrization X is defined in a neighborhood U of the real segment $[0, b]$ in the complex plane. Moreover, the minimal surface defined by X has the property that γ sits in it with $\eta_\gamma(t)$ agreeing with the normal to the surface at $\gamma(t)$.

Now let Γ be the curve parametrized by X restricted to any simple curve in U which forms a connected region U_Γ against the curve $[0, b]$. Then the surface $\Sigma(\gamma, \Gamma)$ parametrized by $X|_{U_\Gamma}$ is what we may call a *stationary thread-wire surface*. The curve Γ is its supporting wire, and the portion of γ bounding it is its free thread. We do not formalize the concept of stationary thread-wire surface in this thesis. The surface $\Sigma(\gamma, \Gamma)$ has the property that it lies inside a real-analytic surface.

The case where Γ meets γ tangentially at a corner point P is of particular interest to us. In this case, we know that the expansion for X at P converges near P . We may

then apply the analysis of Appendix B to this expansion. So long as the ratio $\kappa/\kappa_\Gamma(P)$ does not assume the critical value $3/2$ (see Definition B.5, p. 168), we find that there is a nice formula relating thread torsion to wire torsion:

$$T_\gamma(P) = \frac{\kappa_\Gamma(P)T_\Gamma(P)}{3\kappa_\Gamma(P) - 2\kappa}. \quad (7.1)$$

Since the analysis of Appendix B is quite complex, we prove (7.1) in a more direct and readable way:

Lemma 7.1. Let M be an isolated crescent of an Alt minimizer supported on wire Γ with thread γ . Assume that there exists a minimal surface \tilde{M} which contains M in its interior. Let P be a corner point of M . Let N_M be a unit normal field on M near P . Let $N_{\tilde{M}}$ be an extension to \tilde{M} near P . Then

$$\lim_{M \ni p \rightarrow P} N_M(p) = \lim_{\tilde{M} \ni p \rightarrow P} N_{\tilde{M}}(p) = N_{\tilde{M}}(P) = \pm \eta_\Gamma \quad (7.2)$$

where η_Γ is the third vector in the Frenet frame of Γ . Moreover

$$2\kappa T + \kappa_\Gamma T_\Gamma - 3T\kappa_\Gamma = 0. \quad (7.3)$$

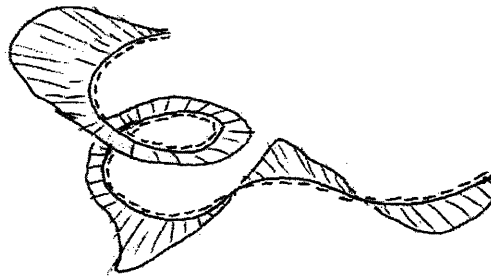


Figure 7-1: Extensible thread-wire surfaces. The solid/dashed curve is meant to be a space curve γ of constant curvature. By applying Björling's formula to this curve, we may create a minimal surface on one side of γ which has normal vector field agreeing with the Frenet binormal of γ along γ . Then one chooses a wire curve (within a radius of convergence) to bound the other side of the surface. The result is a stationary thread-wire surface. If one were to extend the surface in the other direction, so it extends along $-\dot{\gamma}$ one could create a thread-wire surface which is not a local minimum of area.

If $\kappa \neq \frac{3}{2}\kappa_\Gamma$ then we have:

$$T = \frac{\kappa_\Gamma T_\Gamma}{3\kappa_\Gamma - 2\kappa}. \quad (7.4)$$

Proof. Let $\gamma(t)$ parameterize (by arclength) the thread boundary along one side of the corner, with $\gamma(0) = P$. Let $\Gamma(t)$ parameterize (by arclength) the wire boundary along the other side of the corner, with $\Gamma(0) = P$. Consider the Frenet frame of $\gamma(t)$. Two of the vectors, $\dot{\gamma}(t)$ and $\ddot{\gamma}(t)$, lie in the tangent space $T_{\gamma(t)}\tilde{M}$. This means the third, $\eta_\gamma(t)$ points orthogonally to \tilde{M} . Without loss of generality, we may assume $\eta_\gamma(t) = N_{\tilde{M}}(\gamma(t))$. Now it was noted previously in this paper (and it is easy to calculate) that along γ , the second fundamental form is

$$\Pi = \begin{pmatrix} 0 & -T \\ -T & 0 \end{pmatrix}$$

with respect to the $\dot{\gamma}, \nu$ basis for $T_{\gamma(t)}\tilde{M}$. We may then consider how the Frenet frame of Γ relates to M at P . We have

$$\ddot{\Gamma}(0) = \Pi(\dot{\Gamma}(0), \dot{\Gamma}(0)) = \Pi(\dot{\gamma}(0), \dot{\gamma}(0)) = 0.$$

So the Frenet frame of Γ at P also has both $\dot{\Gamma}$ and ν_Γ lying in the tangent space of \tilde{M} . This shows (7.2).

Now let us investigate higher order behavior. We adopt the Frenet frame of Γ at the corner as coordinates for all of \mathbb{R}^3 . Let \tilde{M} be parameterized as a graph $(x, y, f(x, y))$. Near 0 we have a real analytic expansion

$$f(x, y) = -Txy + \sum_{n=3}^{\infty} \sum_{i=0}^n b_{n,i} x^i y^{n-i}.$$

We may expand arclength parameterizations of the wire (Γ) and thread (γ) in these

coordinates. See Section A.1.

$$\begin{aligned} & \Gamma(s) - \Gamma(0) \tag{7.5} \\ = & \left(s - \frac{\kappa_\Gamma^2}{6}s^3 - \frac{\kappa_\Gamma \dot{\kappa}_\Gamma}{8}s^4 - \frac{30\kappa_\Gamma^2 + 30\kappa_\Gamma \ddot{\kappa}_\Gamma + \kappa_\Gamma(\ddot{\kappa}_\Gamma - \kappa_\Gamma^3 - \kappa_\Gamma T^2)}{120}s^5 + O(s^6), \right. \\ & \frac{\kappa_\Gamma}{2}s^2 + \frac{\dot{\kappa}_\Gamma}{6}s^3 - \frac{\kappa_\Gamma^3 - \ddot{\kappa}_\Gamma + \kappa_\Gamma T^2}{24}s^4 - \frac{60\kappa_\Gamma^2 \dot{\kappa}_\Gamma - \ddot{\kappa}_\Gamma + T(3\kappa_\Gamma T + 21\kappa_\Gamma \dot{T}_\Gamma)}{120}s^5 + O(s^6), \\ & \left. - \frac{\kappa_\Gamma T}{6}s^3 - \frac{2\dot{\kappa}_\Gamma T + \kappa_\Gamma \dot{T}_\Gamma}{24}s^4 + \frac{T(\kappa_\Gamma^3 - 3\ddot{\kappa}_\Gamma + T^2 \kappa_\Gamma) - 30\kappa_\Gamma \dot{T}_\Gamma - \kappa_\Gamma \ddot{T}_\Gamma}{120}s^5 + O(s^6) \right) \end{aligned}$$

$$\begin{aligned} \gamma(s) - \gamma(0) = & \left(s - \frac{\kappa^2}{6}s^3 + \frac{\kappa(\kappa^3 + \kappa T^2)}{120}s^5 + O(s^6), \tag{7.6} \right. \\ & \frac{\kappa}{2}s^2 - \frac{\kappa^3 + \kappa T^2}{24}s^4 - \frac{7\kappa T \dot{T}}{40}s^5 + O(s^6), \\ & \left. - \frac{\kappa T}{6}s^3 - \frac{\kappa \dot{T}}{24}s^4 + \frac{T(\kappa^3 + T^2 \kappa) - \kappa \ddot{T}}{120}s^5 + O(s^6) \right) \end{aligned}$$

We impose the following conditions:

(i) The surface \tilde{M} satisfies the minimal surface equation

$$(1 + f_x^2)f_{yy} - 2f_x f_y f_{xy} + (1 + f_y^2)f_{xx} = 0. \tag{7.7}$$

(ii) The wire lies in \tilde{M} .

$$f(x, \Gamma_{(y)}(s_\Gamma(x))) = \Gamma_{(z)}(s_\Gamma(x)) \tag{7.8}$$

(iii) The thread lies in \tilde{M} :

$$f(x, \gamma_{(y)}(s_\gamma(x))) = \gamma_{(z)}(s_\gamma(x)) \tag{7.9}$$

(iv) The thread has constant curvature. This has already been reflected in the way that we wrote the arclength parameterization without any curvature derivative coefficients.

(v) The curvature vector $\ddot{\gamma}$ of the thread is parallel to the side normal ν of the thread in \tilde{M} . Really, since the curvature vector of the thread is already perpendicular

to the thread, we just need for $\tilde{\gamma}$ to lie in the tangent plane of \tilde{M} . We can write this as a determinant condition

$$\begin{vmatrix} 1 & 0 & f_x(\gamma(x)(s), \gamma(y)(s)) \\ 0 & 1 & f_y(\gamma(x)(s), \gamma(y)(s)) \\ \ddot{\gamma}(x)(s) & \ddot{\gamma}(y)(s) & \ddot{\gamma}(z)(s) \end{vmatrix} = 0. \quad (7.10)$$

Let us see how these conditions look when we use expansions for the wire, thread and surface out to fourth order in x, y .

(i) Surface is minimal.

$$\begin{aligned} 0 &= H \\ &= (2b_{3,1} + 6b_{3,3})x + (6b_{3,0} + 2b_{3,2})y \\ &\quad + (12b_{4,4} + 2b_{4,2})x^2 + (6b_{4,3} + 2T^3 + 6b_{4,1})xy + (2b_{4,2} + 12b_{4,0})y^2 + O(|(x, y)|^3). \end{aligned}$$

(ii) Wire lies in surface.

$$0 = \left(\frac{\kappa_\Gamma T}{6} - \frac{\kappa_\Gamma T}{2} + b_{3,3} \right) s^3 + \left(\frac{\kappa_\Gamma \dot{T}}{24} + \frac{b_{3,2}\kappa_\Gamma}{2} + b_{4,4} \right) s^4 + O(s^4).$$

(iii) Thread lies in surface.

$$0 = \left(-\frac{\kappa T}{3} + b_{3,3} \right) s^3 + \left(\frac{\kappa \dot{T}}{24} + \frac{b_{3,2}\kappa}{2} + b_{4,4} \right) s^4 + O(s^4).$$

(iv) Thread curvature points tangentially to the surface.

$$\begin{aligned} 0 &= \left(-b_{3,2}\kappa - \frac{1}{2}\dot{T}\kappa \right) s^2 \\ &\quad + \left(-\frac{1}{2}\kappa T^3 - b_{4,3}\kappa + 3\kappa^2 b_{3,3} - \frac{7}{6}\kappa^3 T - b_{3,1}\kappa^2 \right) s^3 \\ &\quad + \left(\frac{11}{6}b_{3,2}\kappa^3 + \frac{1}{2}b_{3,2}T^2\kappa - \frac{3}{4}b_{3,0}\kappa^3 - b_{4,2}\kappa^2 + 4\kappa^2 b_{4,4} \right) s^4 + O(s^5) \end{aligned}$$

Examining these equations, one sees that there is a crucial equation:

$$(3\kappa_\Gamma - 2\kappa)T = \kappa_\Gamma T_\Gamma.$$

If $\kappa \neq \frac{3}{2}\kappa_\Gamma$ then we may solve uniquely for T and all other surface and thread quantities. If $\kappa = \frac{3}{2}\kappa_\Gamma$ then (under our genericness assumptions) we must have $T_\Gamma = 0$ and T can be arbitrary. We may then solve for all other thread and surface quantities. ■

7.2 Helicoidal thread-wire surfaces

Definition 7.2. For β a non-zero real constant, we define the β -*helicoid* \mathcal{H}_β to be the surface parameterized by

$$X(u, v) = (u \cos \beta v, u \sin \beta v, v).$$

Lemma 7.3. The helicoid \mathcal{H}_β is a minimal surface.

Proof. To see this, let \vec{H} be a normal vector field on \mathcal{H}_β so

$$\langle N, \vec{H} \rangle = -\langle \nabla_X N, Y \rangle$$

for unit normal fields N and tangent fields X, Y on \mathcal{H}_β . In other words, \vec{H} encodes the mean curvature as a normal vector field. Rotating space around the x -axis by 180 degrees sends the helicoid to itself, which means \vec{H} must vanish along the x -axis.

There is a rigid motion of space

$$\Xi_t(x, y, z) = (x \cos \beta t + y \sin \beta t, -x \sin \beta t + y \cos \beta t, z + t)$$

which sends the image of X to itself:

$$\Xi_t(X(u, v)) = X(u, v + t).$$

The vector field \vec{H} must be invariant under Ξ so it vanishes everywhere and \mathcal{H}_β is a minimal surface. ■

We calculate derivatives for future use:

$$\begin{aligned}
 X_u &= (\cos \beta v, \sin \beta v, 0) \\
 X_v &= (-\beta u \sin \beta v, \beta u \cos \beta v, 1) \\
 X_{uu} &= (0, 0, 0) \\
 X_{uv} &= (-\beta \sin \beta v, \beta \cos \beta v, 0) \\
 X_{vv} &= (-\beta^2 u \cos \beta v, -\beta^2 u \sin \beta v, 0) \\
 X_{uuv} &= (-\beta^2 \cos \beta v, -\beta^2 \sin \beta v, 0) \\
 X_{vvv} &= (\beta^3 u \sin \beta v, -\beta^2 u \cos \beta v, 0)
 \end{aligned}$$

Note that X is *not* a conformal parameterization of \mathcal{H}_β .

The helicoid is foliated by helices

$$\gamma^c(t) = X(c, t)$$

with

$$\begin{aligned}
 \dot{\gamma}^c(t) &= \frac{1}{\sqrt{1 + c^2 \beta^2}} (-\beta c \sin \beta t, \beta c \cos \beta t, 1) \\
 \ddot{\gamma}^c(t) &= \frac{\beta^2 c}{1 + c^2 \beta^2} (-\cos \beta t, -\sin \beta t, 0) \\
 \dddot{\gamma}^c(t) &= \frac{\beta^3 c}{(1 + c^2 \beta^2)^{3/2}} (\sin \beta t, -\cos \beta t, 0)
 \end{aligned}$$

We see that each helicoid has constant curvature

$$|\ddot{\gamma}^c(t)| = \frac{\beta^2 c}{1 + c^2 \beta^2}$$

and the curvature vector points tangentially to \mathcal{H}_β .

Let M be a domain on \mathcal{H}_β bounded by γ^c for $c > 0$ on one side and by a curve Γ on the other, so that Γ touches γ^c at exactly two points P_1, P_2 making null angles at each. Then M is a stationary thread-wire surface for wire Γ and thread γ given by the arc of γ^c joining P_1 to P_2 .

In this discussion we restrict to the case that γ lies on \mathcal{H}_β in the region $u > c$.

Here are further useful calculations. We construct a normal field

$$N = \frac{X_u \times X_v}{|X_u \times X_v|} = \frac{1}{\sqrt{1 + \beta^2 u^2}} (\sin \beta v, \cos \beta v, \beta u).$$

Orient \mathcal{H}_β so the Gauss image of the $u > c$ part is in the upper (“northern”) hemisphere. Then the Gauss image of $u \geq c$ is a spherical cap missing the north pole. The Gauss image of M lies in this set, with boundary given by an arc of the cap’s bounding circle. This confirms the property that the image of the thread should always turn inward—towards the Gauss images of nearby interior points on the thread-wire surface. (See Section 3.2.)

7.3 Beeson’s skewed chevron

In this thesis, we prove a conjecture (Conj. 1.2) that the local geometry of the wire at a surface corner dominates the global influence of the wire and causes a simply-described C^1 regularity at the surface corner. The reader may be interested to examine another example of strong local control in minimal surface theory. See **Figure 7-2**.

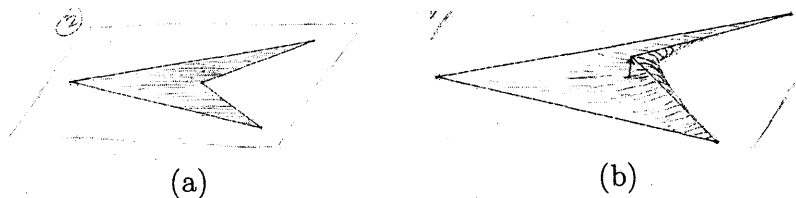


Figure 7-2: Beeson’s skewed chevron. Perturbing the “skewed chevron” in (a) out of the plane *any positive amount* causes the normal field at that point to flip over. (See (b).) This demonstrates dominant influence by the corner of the wire over long-range effects by the rest of the wire.

Chapter 8

Physical experiment

Given a wire loop Γ in three-dimensional space, what area-minimizing or area-critical surfaces span it? One line of inquiry has focused on the total curvature $\int |\kappa_\Gamma| ds$ of the curve. If the total curvature is less than 4π , then exactly one area-minimizing disc spans the wire loop [2]. If the total curvature is less than 6π then finitely many area-critical discs span the wire loop [4].

It seems highly desirable to give a full description of the Morse theory of area-critical surfaces spanning a wire loop, and to do so using greater geometric detail about the wire, beyond the total curvature.

Thinking along these lines, I imagined a *thread-pull* process for creating area-critical surfaces spanning a wire loop, which would respond to the geometry of the wire in an intimate fashion. Here is my thought experiment: Take an arbitrary wire loop Γ (**Figure 8-1a**). Place a bead on the wire at some location. Take a piece of thread and pass it through the bead, lay it along the wire, and pass it back out through the bead. Paint the thread with soap-water so it adheres to the wire. (See **Figure 8-1b**.) Grasp the two ends of the thread dangling from the bead and slowly pull on them, causing the length of thread bounded by the bead to decrease. This should cause soap-water surfaces to form as

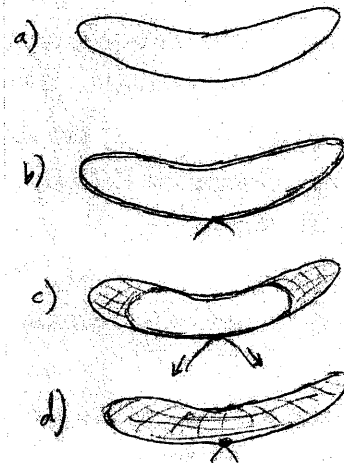


Figure 8-1: Thought experiment.

the thread pulls away from the wire (**Figure 8-1c**). By pulling on the thread slowly, I imagined progressing through a family of surfaces which locally minimize area subject to the thread's length constraint. If I succeed in finding such a surface for length constraints which finally arrive at zero, then I succeed in finding a local area-minimizing surface spanning the wire loop Γ (See **Figure 8-1d**).

I thought this process might be particularly interesting for a curve like the tie-clip curve (**Figure 8-6**). This curve is invariant under a rigid motion. It has two area minimizers, neither of which has this symmetry. (They are in fact interchanged by this symmetry.) When a symmetric system minimizes a natural functional in an asymmetric way, it is known as *symmetry breaking*. How would the thread-pull proceed for the tie-clip curve? More generally, how would it proceed for curves which are spanned by more than one area-minimizing surface?

I investigated the thread-pull experimentally and found that it was remarkably robust. For many wires, it proceeded continuously until the thread pulled tight against the bead and it found a stable soap-water surface spanning the wire loop. On the other hand, I found at least one example where the thread-wire surface suddenly jumped to a new position as I slowly pulled the thread. Actually, this is to be expected. See **Figure 8-3**.

I have not yet shown that the thread-pull gives useful information about the Morse theory of areas of surfaces spanning a contour. It may be that studying the thread-pull is actually harder to understand than the original problem. On the other hand, I did find immediate benefits from studying the thread-pull, because I gained intuition about the static problem.

8.1 Experimental method

These experiments were done using stainless steel wire; copper wire quickly corrodes and stains things blue-green. The thread is cotton; this has the advantage of being a generous reservoir of soap water when wet. Consequently, there is plenty of soap water

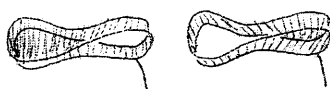


Figure 8-2: The symmetric tie-clip curve supports two area minimizers.

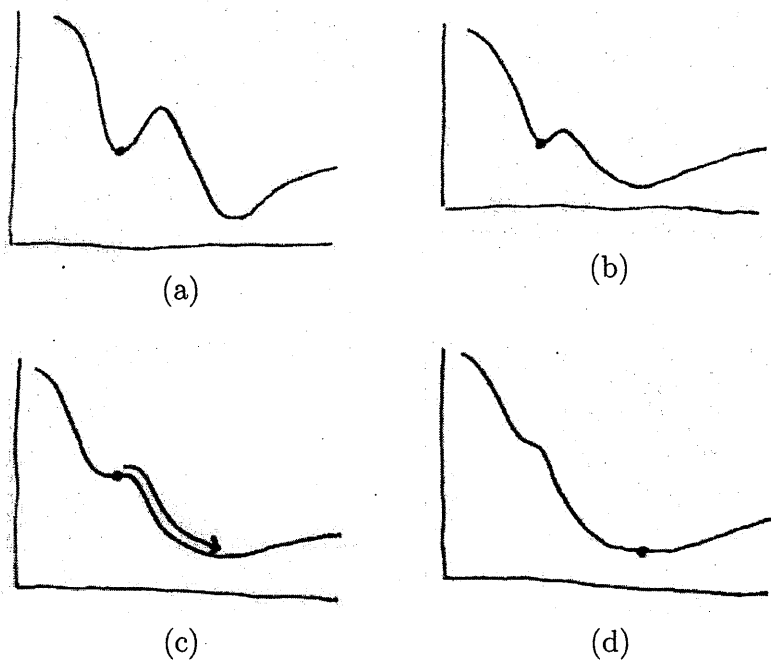


Figure 8-3: Constrained minimization can jump. Think of these functions as representing a cost function for different values of a constraint function. If our system is at a local minimum of cost and we continuously change the constraint value, we are not guaranteed being able to stay continuously at a local min. In this example, once we have reached (c), our local minimum has become unstable and we are dumped into a new local minimum as the constraint moves slightly to (d).

available for the formation of new crescents as the thread pulls away from the wire. The disadvantage of cotton thread is that it has a high coefficient of friction with the wire. I had hoped to reduce friction using silk thread. This does not hold as much soap water; I have not yet had success.

The soap solution contains Ultra Ivory liquid soap, physical experiment!glycerin, and Cambridge tap water. The glycerin increases the lifetime of the surfaces from around 10 seconds to over a minute. I captured video [25] of my experiments using a Unibrain Fire-i webcam. The videos may be viewed at my website, www.bkstephens.net. In the sections below we discuss the videos using stills. Unfortunately the stills do not come out well in black-and-white; visiting the website may be helpful.

8.2 Heart curve

This planar wire loop is in the shape of a heart. It demonstrates the formation of coalitions. See **Figure 8-4**.

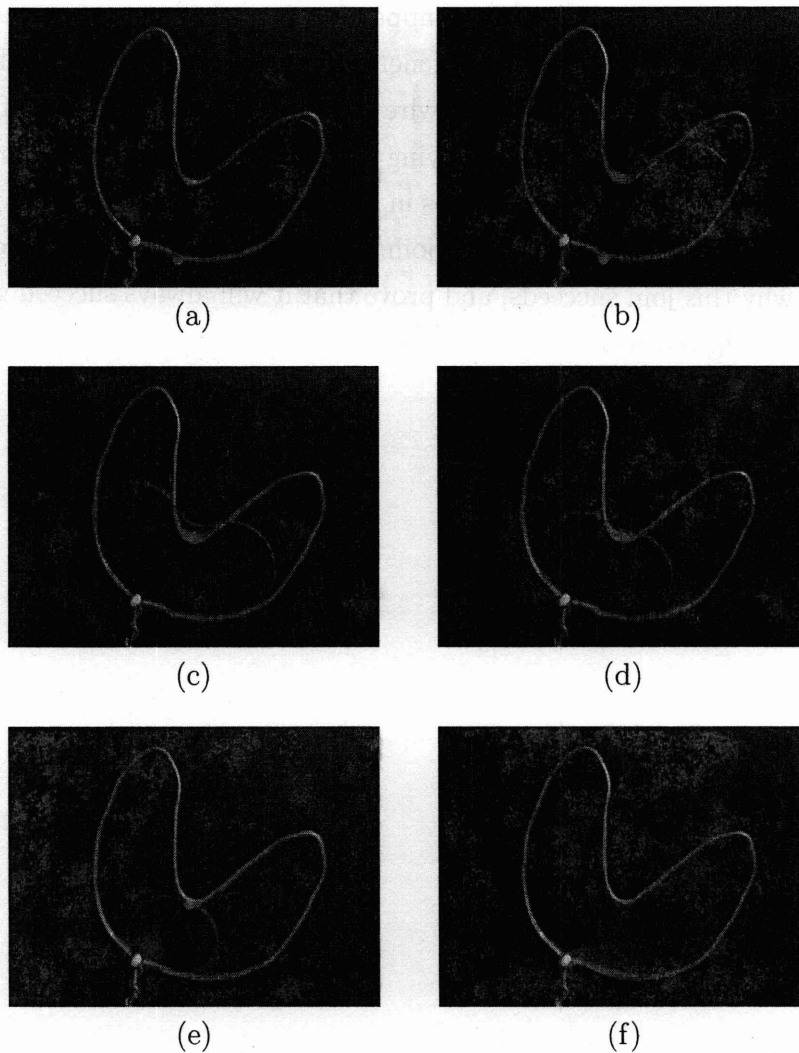


Figure 8-4: Heart thread pull. Pulling the thread in a heart-shaped wire. Initially the thread clings to the wire and there is no soap surface (a). As the thread tightens, the thread pulls away at three local maxima of wire curvature (b). This forms three crescents of soap surface which join to form a coalition (c). The outer two crescents advance at the expense of a shrinking middle crescent (d), which disappears (e). The other crescents join and a circle of thread shrinks down to the bead, forming the planar Plateau solution (f).

8.3 Bent paperclip curve

In general, the thread pull causes crescents to appear at local maxima of curvature and then grow together. When they join, they generally have different tangent planes at the join point. The so-called bent paperclip wire is a fundamental example of this behavior. The wire consists of two circular arcs lying in orthogonal planes which join to form a bent "S." The thread passes through loops in the wire at each end. As one pulls the thread, the crescents grow and successfully join. I am keen to understand from a formal point of view why this join succeeds, and prove that it will always succeed given certain conditions. See **Figure 8-5**.

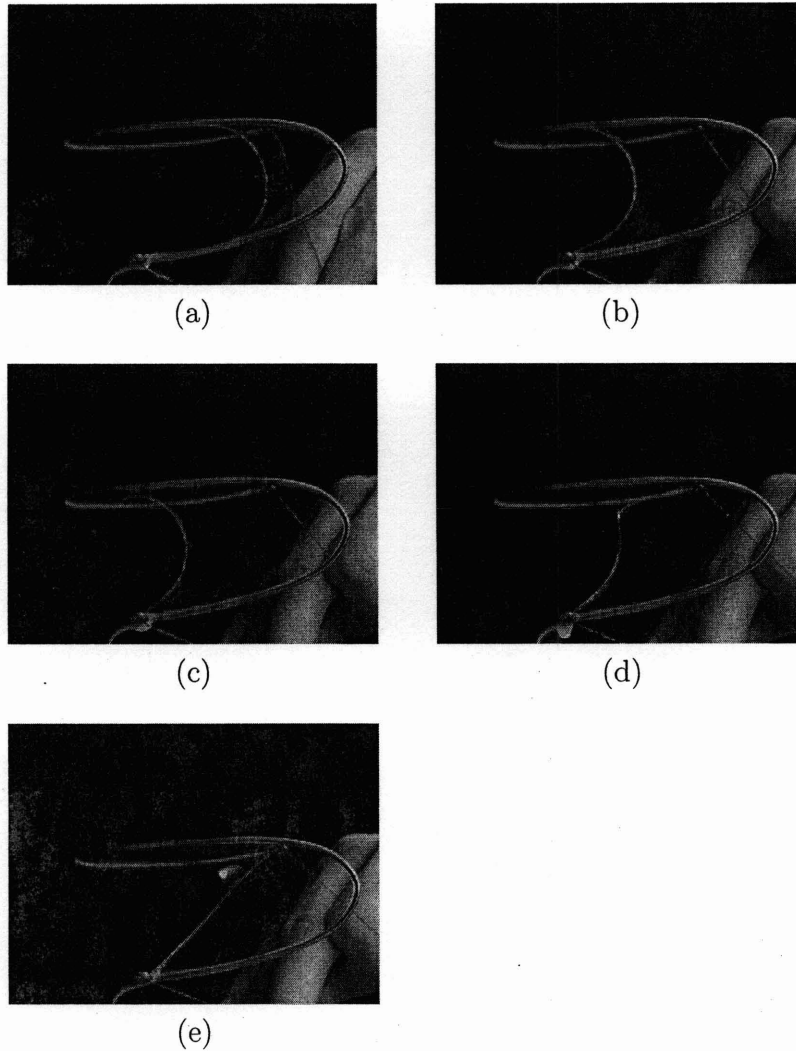


Figure 8-5: “Bent paperclip” thread pull. Pulling the thread on the “bent paperclip.” Initially the thread clings to the wire and there is no soap surface. As the thread tightens, the thread pulls away at the two local maxima of wire curvature (a). These crescents grow and, at a critical moment, they meet (b). At this moment if you trace the curvature vector moving along the thread, you will see it undergo a discontinuous, right-angle jump at the join point. The torsion of the thread at the join point is modelled on a delta function. In the next few moments that delta function mollifies and the two crescents join as the thread pulls away from the wire (c). This process continues (d) and ends (e) when the thread is stretched tautly between the ends of the wire.

8.4 Tie-clip curve: Bifurcation

In **Figure 8-6** we see the wire loop which I call the tie-clip wire. It looks like the edge of a tie-clip. The tie-clip is interesting because it admits two different disc-type minimal surfaces.

But initially, the idealized thread pull process should always do the same thing: four crescents should grow at each of the four tongue-like ends of the tie-clip loop. If the wire were perfectly symmetric, there would be a moment where the four crescents join simultaneously at four points. At this moment there would be a loss of stability and there would be a choice: to make one pair of parallel crescents grow and the other pair recede. This would be the point of “symmetry breaking.”

In **Figure 8-7** and **Figure 8-8**, we show stills from a video of the author pulling the thread on the tie-clip curve. Friction between the thread and wire cause the physical experiment to deviate significantly from the idealization. Friction strongly affects the initial crescent creation and affects which of the two stable thread-wire surface is chosen in the end.

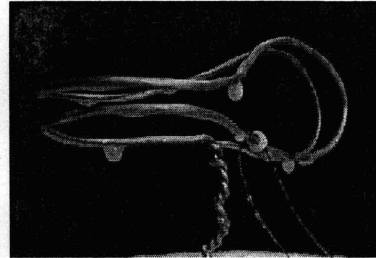


Figure 8-6: Tie-clip curve.

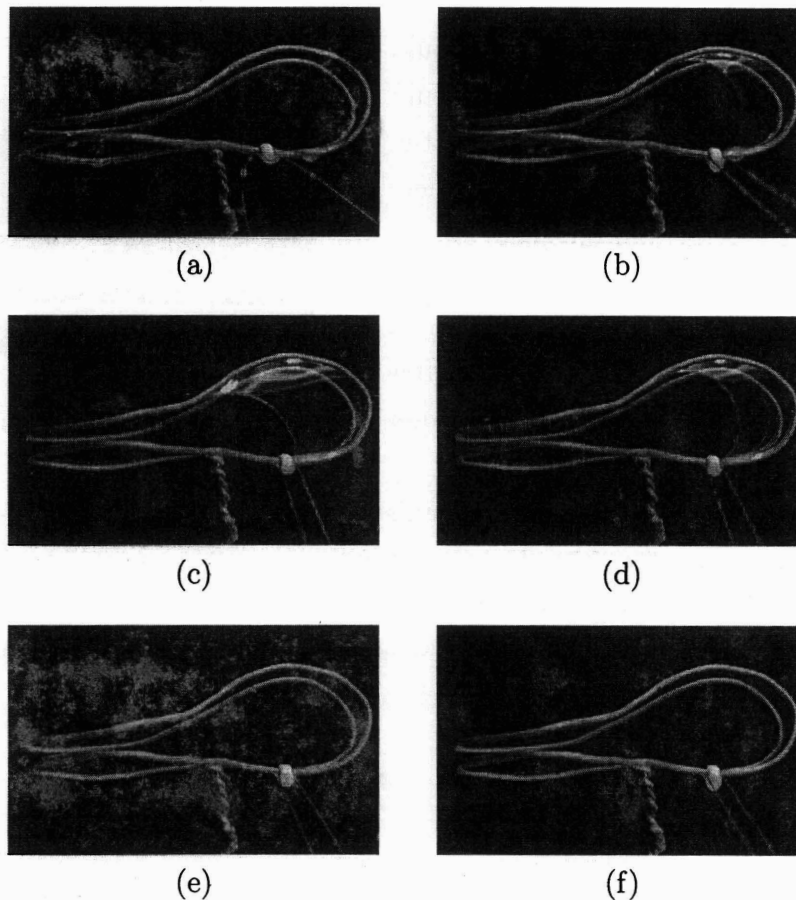


Figure 8-7: Tie-clip horizontal solution. Initially the thread clings to the wire and there is no soap surface (a). As the thread tightens, crescents form on the tongues closest to the bead. But the top left and back right tongues do not form crescents due to friction (b). In (c) we see the thread finally pull away from the top left tongue. The large thread-wire angle to the right of the bead indicates how much force this requires. In (d) the top left tongue has continued to grow and small crescent pulls away from the back right tongue. But this is far too late, the top left crescent grows more and the back right crescent recedes and disappears (e). In the end (f), the thread pulls tight to the bead and creates the mostly horizontal Plateau solution.

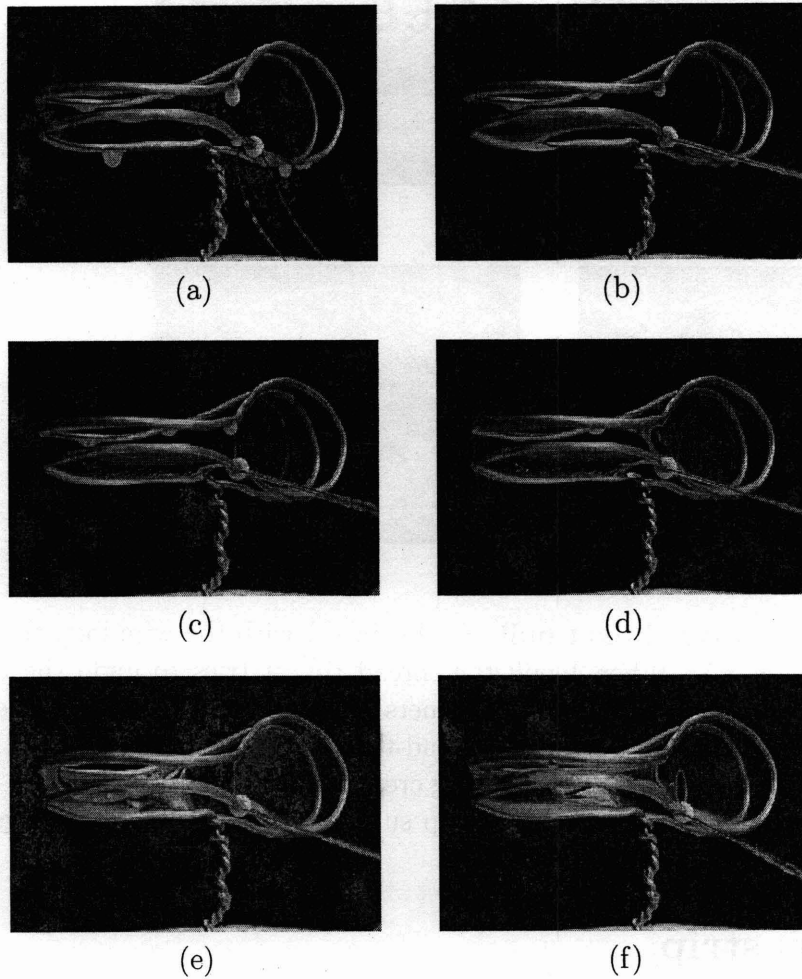


Figure 8-8: Tie-clip vertical solution. We start (a) with the same tie-clip wire as in **Figure 8-7**, seen from a different angle. The bead is in a similar place. The white globs are drips of soap water. As we pull the thread, a crescent forms on each tongue adjoining the bead (b). The back right crescent pulls away (c) and finally the top left one pulls away a little (d). But this crescent is very short-lived and it returns to the wire as the back left crescent barrels through (e) and joins its opposite. In (f) the thread has almost pulled down to the bead. Finally, the thread pulls tight to the bead and creates the mostly vertical Plateau solution.

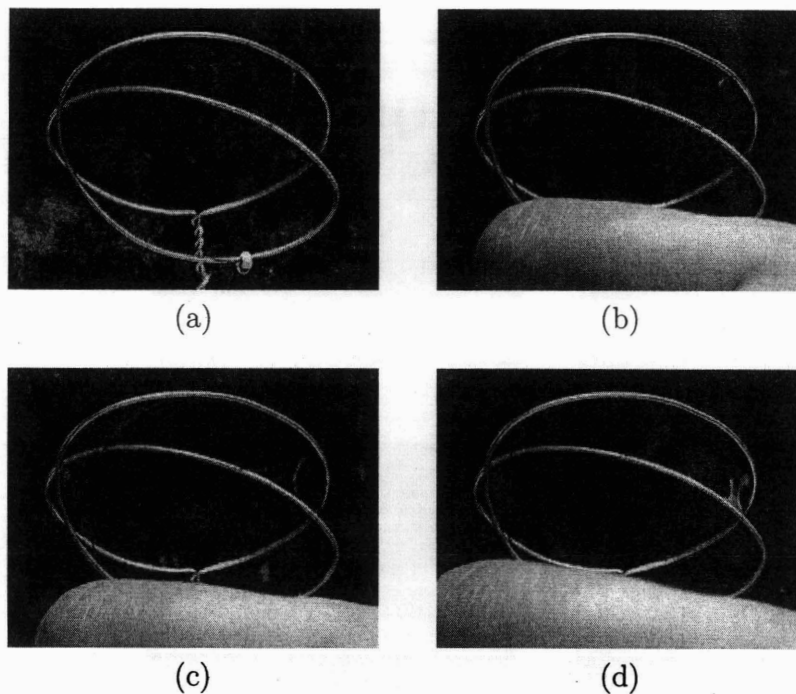


Figure 8-9: Möbius strip thread pull. We begin (a) with the wire loop threaded as described in section 8.5. When I pull the thread (b), it tries to undo the bridge where it connects with the wire (as these corners are the most curved parts of the thread). The friction is very high at this thread-thread interface, and so the thread pulls away where it otherwise would not, in long crescents at top-left and bottom-right. The thread bridge widens into a bridge of soap surface (c). In (d) the bridge grows. (continued in **Figure 8-10**)

8.5 Möbius strip

This paper focuses on disc-type minimal surfaces. But the thread pull is capable of creating surfaces with other topologies as well. In this example we start with a wire loop supporting wet thread in a unique way. Instead of tracing the wire around until it returns to the bead, the thread leaves the wire and makes a bridge to another point of the wire. Then the thread traverses the wire until it returns to the other end of the bridge, whereupon it crosses again, forming a double-stranded bridge. It then returns to the bead location. What happens when you pull the thread? See **Figure 8-9** and **Figure 8-10**.

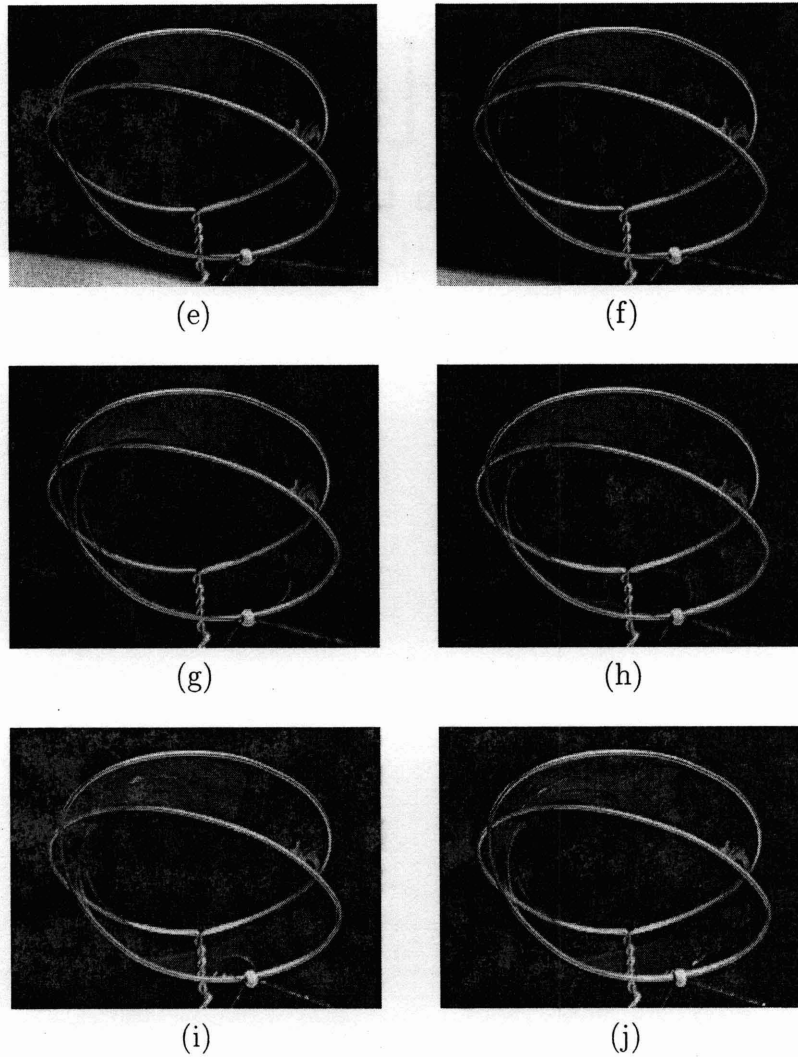


Figure 8-10: Möbius strip thread pull, continued. In (e) the two initial crescents return to the wire. The right side of the bridge turns away from the camera and peeks out below where the wire crosses itself on the right. In (f) and (g) we see the left side of the bridge follow the wire on the left without turning over. Finally, the two sides of the original bridge meet (h) forming a perfect circle of thread. This circle shrinks down to the bead (i), finally forming the Möbius strip solution (j) to this Plateau problem.

Appendix A

Appendix

A.1 Properties of Frenet curves

In this section we prove a lemma about Frenet curves. We also demonstrate useful expansions for curves relative to their Frenet frame at a point.

Lemma A.1. Let $\Psi(s) = (x(s), y(s), z(s))$ be a C^2 Frenet curve, parametrized by arclength. Assume that its binormal $\eta_c(s)$ satisfies

$$|\eta_\Psi(s) - (0, 0, 1)| < \epsilon. \quad (\text{A.1})$$

Then its projection $\psi(s) = (x(s), y(s), 0)$ satisfies

$$|\kappa_\psi(s) - \kappa_\Psi(s)| < C\kappa_\Psi(s)\epsilon.$$

Proof. Given any curve $b(u)$, not necessarily parametrized by arclength we have that its curvature vector is

$$\vec{\kappa}_b(u) = \frac{1}{|b_u|} \left(\frac{b_u}{|b_u|} \right)_u = \frac{b_{uu}}{|b_u|^2} - \frac{\langle b_{uu}, b_u \rangle}{|b_u|^3} = P(b_u/|b_u|, b_{uu}/|b_u|^2)$$

where $P(e, w) = w - \langle e, w, e \rangle$ projects w onto the orthogonal complement of e for unit vector e . So we have

$$\kappa_\Psi = |\Psi_{ss}| = |P(\Psi_s, \Psi_{ss})| \quad (\text{A.2})$$

and

$$\kappa_\psi = |P(\psi_s/|\psi_s|, \psi_{ss}/|\psi_s|^2)|. \quad (\text{A.3})$$

We note that $\psi(s)$ is not parametrized by its arclength. Our goal is to show that (A.2) and (A.3) are close to each other by showing that the inputs to P in the second equation have changed by quantities bounded by $C\epsilon$.

Subclaim A.2. (i) The corresponding vectors of the Frenet frames of Ψ and ψ are within distance $C\epsilon$.

$$(ii) \quad |z_{ss}| < C\kappa_{\Psi}\epsilon.$$

$$(iii) \quad |\Psi_{ss} - \psi_{ss}/|\psi_s|^2| < C\kappa_{\Psi}\epsilon.$$

Proof. Equation (A.1) establishes (i) for the binormals. We then observe that (A.1) and $\langle \Psi_s(s), \eta_{\Psi}(s) \rangle = 0$ imply that

$$|z_s| < C\epsilon. \tag{A.4}$$

We have

$$|\psi_s|^2 = 1 + O(\epsilon^2) \tag{A.5}$$

and

$$\langle \psi_s/|\psi_s|, \Psi_s \rangle = 1 + O(\epsilon).$$

This clinches (i). Then the identity $\Psi_{ss}(s) = \kappa_{\Psi}(s)\nu_{\Psi}(s)$ and (i) clinch (ii). But then $\psi_{ss} = (x_{ss}, y_{ss}, 0)$. Combining our results, we get (iii). ■

Define $\delta_1 = \psi_s/|\psi_s| - \Psi_s$ which has size $C\epsilon$ by (i), and define δ_2 to be the value of the left side of (iii). Then

$$\begin{aligned} \kappa_{\psi} &= |P(\Psi_s + \delta_1, \Psi_{ss} + \delta_2)| \\ &= |P(\Psi_s, \Psi_{ss}) + \delta_1 + \langle \delta_1, \Psi_{ss} \rangle \Psi_s + \langle \Psi_s, \delta_2 \rangle \delta_2 + \langle \Psi_s, \Psi_{ss} \rangle \delta_2 + O(\epsilon^2)| \\ &= \kappa_{\Psi} + C\kappa_{\Psi}\epsilon. \end{aligned}$$

This proves Lemma ??.

Finally, we demonstrate useful expansions for Frenet curves. Here we use the dot symbol to indicate differentiation by arclength. We omit the dependences on arclength

to make the formulas more readable.

$$D_F = \begin{pmatrix} \frac{\partial}{\partial t} & -\kappa & 0 \\ \kappa & \frac{\partial}{\partial t} & T \\ 0 & -T & \frac{\partial}{\partial t} \end{pmatrix}. \quad (\text{A.6})$$

So we have

$$\begin{pmatrix} w_1 \\ w_2 \\ w_3 \end{pmatrix} \rightarrow \begin{pmatrix} \dot{w}_1 - \kappa w_2 \\ \kappa w_1 + \dot{w}_2 + T w_3 \\ -T w_2 + \dot{w}_3 \end{pmatrix} \rightarrow \begin{pmatrix} \ddot{w}_1 - \kappa^2 w_1 - \dot{\kappa} w_2 - 2\kappa \dot{w}_2 - \kappa T w_3 \\ \ddot{w}_2 - (T^2 + \kappa^2) w_2 + 2\kappa \dot{w}_1 + \dot{\kappa} w_1 + \dot{T} w_3 + 2T \dot{w}_3 \\ \ddot{w}_3 - 2T \dot{w}_2 - \dot{T} w_2 - T^2 w_3 - \kappa T w_1 \end{pmatrix}. \quad (\text{A.7})$$

Now we assume we have a smooth curve $\sigma(s)$ parameterized by arclength. Below is its Taylor expansion out to fifth order. This can be calculated by hand using the Frenet differentiation matrix above. Or one can program a software package like Maple to help, which is what the author did. The coefficients such as κ, T refer to geometric quantities evaluated at 0. Dots indicate differentiation by arclength. For example $\dot{\kappa}$ means the first derivative of the curvature of σ , evaluated at zero.

$$\begin{aligned} \sigma(s) - \sigma(0) = & \left(s - \frac{\kappa^2}{6} s^3 - \frac{\kappa \dot{\kappa}}{8} s^4 - \frac{30\dot{\kappa}^2 + 30\kappa \ddot{\kappa} + \kappa(\ddot{\kappa} - \kappa^3 - \kappa T^2)}{120} s^5 + O(s^6), \quad (\text{A.8}) \right. \\ & \frac{\kappa}{2} s^2 + \frac{\dot{\kappa}}{6} s^3 - \frac{\kappa^3 - \ddot{\kappa} + \kappa T^2}{24} s^4 - \frac{60\kappa^2 \dot{\kappa} - \ddot{\kappa} + T(3\dot{\kappa}T + 21\kappa \dot{T})}{120} s^5 + O(s^6), \\ & \left. - \frac{\kappa T}{6} s^3 - \frac{2\dot{\kappa}T + \kappa \dot{T}}{24} s^4 + \frac{T(\kappa^3 - 3\ddot{\kappa} + T^2 \kappa) - 30\dot{\kappa} \dot{T} - \kappa \ddot{T}}{120} s^5 + O(s^6) \right). \end{aligned}$$

It is often helpful to rewrite this expansion in terms of the x coordinate of the curve. Inverting the first component of (A.8) gives

$$s = x + \frac{\kappa^2}{6} x^3 + \frac{\kappa \dot{\kappa}}{8} x^4 + \frac{9\kappa^4 + 3\dot{\kappa}^2 + 8\kappa \ddot{\kappa} - \kappa^2 T^2}{120} x^5 + O(x^6) \quad (\text{A.9})$$

Substituting this into (A.8) gives

$$\sigma(s(x)) - \sigma(0) = \left(x, \right. \tag{A.10}$$

$$\frac{\kappa}{2}x^2 + \frac{\dot{\kappa}}{6}x^3 + \frac{3\kappa^3 + 2\ddot{\kappa} - \kappa T^2}{24}x^4 + \frac{19\kappa^2\dot{\kappa} + 6\ddot{\kappa} - 3\kappa T\dot{T} - 3\dot{\kappa}T^2}{120}x^5 + O(x^6),$$

$$\left. -\frac{\kappa T}{6}x^3 - \frac{2\dot{\kappa}T + \kappa\dot{T}}{24}x^4 - \frac{9\kappa^3T + 6\ddot{\kappa}T + \kappa T^3 - 3\dot{\kappa}T - 2\kappa\dot{T}}{120}x^5 + O(x^6) \right).$$

A.2 Generalized Descartes's rule

The following is a straightforward generalization of Descartes's rule of signs for polynomials.

Lemma A.3. [Generalized Descartes's Rule] Let f be a C^n real-valued function on an interval $[0, b]$. Assume that $f^{(n)}(x)$ has a definite sign on the entire interval. Let m be the number of sign changes in the sequence $\{f^{(k)}(0), k = 0, \dots, n\}$, where elements that are zero have been removed. Then f has at most m zeroes on $[0, b]$.

Proof. We prove this lemma by induction on n . The base case, $n = 0$, is trivial. Now we treat the inductive step.

Assume that the lemma holds with $n = n_0$. Let f be a function satisfying the conditions for $n = n_0 + 1$, and having $m = m_1$ sign changes. Let $f^{(r)}(0)$ be the first non-zero entry in the sequence $\{f^{(k)}(0), k = 1, \dots, n\}$. We know $1 \leq r \leq n$. Let

$$\delta = \begin{cases} 1, & f(0) \neq 0 \text{ and has a different sign from } f^{(r)}(0) \\ 0, & \text{else.} \end{cases}$$

Applying the inductive assumption, we conclude that f' has at most $m_1 - \delta$ zeroes on $[0, b]$. Now consider f on $[0, b)$. For each zero z of f , trace the graph of f to the left until you hit either a critical point of f or $x = 0$. If z itself is a critical point of f , just stay at z . This process defines an injection $\eta: Z \rightarrow T$, where

$$Z = \{x \in [0, b] \mid f(x) = 0\}$$

$$T = \{x \in [0, b] \mid f'(x) = 0\} \cup \{0\}.$$

A property of the process is that for $z \in Z$,

$$f \neq 0 \text{ on } [\eta(z), z]. \quad (\text{A.11})$$

Indeed, if $f(c) = 0$ for an interior point $c \in (\eta(z), z)$, then by Rolle's Theorem there would be a critical point of f in (c, z) . This would be a contradiction.

We can estimate the size of $\text{Im } T$ by

$$\#\text{Im } T \leq \#\{x \in [0, b] \mid f'(x) = 0\} + \omega \leq m_1 - \delta + \omega$$

where

$$\omega = \begin{cases} 1, & 0 \in \text{Im } T \text{ and } f'(0) \neq 0 \\ 0, & \text{else.} \end{cases}$$

If $\omega = 1$, then we know that when we trace left from the first zero, z_1 , of f , we hit $x = 0$. By (A.11), we know $f(0) \neq 0$. Moreover, as we moved left on $[0, z_1]$, the function f must have changed strictly monotonically. Therefore, the first non-zero derivative of f at zero, $f^{(r)}$, must have a sign opposite to that of $f(0)$. We conclude that $\delta = 1$. This shows that $\delta \geq \omega$.

Finally, we estimate the number of zeroes of f by

$$\#Z \leq \#T \leq m_1 - \delta + \omega \leq m_1.$$

This completes the inductive step. ■

A.3 Immersive lifts of a curve

Lemma A.4. [Curve Lift] Let $K \subset \mathbb{R}^2$ be a closed domain which is the image of a planar polygonal region under a C^n diffeomorphism of the plane. Let $\sigma \in C^\infty([0, \ell(\sigma)], \Delta)$ be a simple curve, parametrized by arclength, which ends in $\partial\Delta$. Let $\hat{p} \in K$ be a preimage of the starting point of the curve:

$$W(\hat{p}) = \sigma(0).$$

We demonstrate the existence of **the lift of σ by W from $\sigma(0)$ to \hat{p}** , which is a simple curve $\hat{\sigma} \in C^n([0, s^*], K)$ lying over σ ,

$$W(\hat{\sigma}(s)) = \sigma(s).$$

To do this we require the following:

- (a) **Beginning:** The map W is an immersion at \hat{p} . The lift point \hat{p} either lies in the interior K° , or it lies on the boundary ∂K , not at a corner point. In this case, we require that it satisfy an **entry condition**:
- (a₁) **Transverse entry:** The pair of vectors $W_x(0), \sigma'(0)$ is a basis and has the same orientation as the basis $W_x(0), W_y(0)$.
- (a₂) **Possibly nontransverse entry:** Let W_0 extend W to a diffeomorphism in a neighborhood of 0. For all $s > 0$ in a neighborhood of 0, we require that $W_0^{-1}\sigma(s)$ lies in K° .
- (b) **Continuation:** The map $W \in C^n(K, \Delta^\circ)$ is an immersion on the preimage $W^{-1}(\sigma((0, \ell(\sigma))))$ of the curve minus its starting point.

The lift we define is **maximal** in the sense that it parametrizes the entire connected component of $W^{-1}(\text{Im } \sigma)$ containing \hat{p} . It has **positive length**

$$s^* > 0$$

and terminates at a boundary:

$$\hat{\sigma}(s^*) \in \partial K.$$

The lift satisfies a **uniqueness** property: if $\hat{\sigma}_1 : [0, s_1^*] \rightarrow K$ and $\hat{\sigma}_2 : [0, s_2^*] \rightarrow K$ are both lifts of σ by W from $\sigma(0)$, then $\hat{\sigma}_1(s_1^*) = \hat{\sigma}_2(s_2^*)$ implies that $s_1^* = s_2^*$ and $\hat{\sigma}_1$ and $\hat{\sigma}_2$ are identical maps.

Proof. Now let us consider the set $Z = W^{-1}(\sigma((0, \ell(\sigma)))) \cup \{\hat{p}\}$. We claim that the connected component C of \hat{p} in Z is the same as the connected component C' of \hat{p} in $W^{-1}(\text{Im } \sigma)$. Indeed, by condition (a) we know that W may be restricted to provide a diffeomorphism between an open neighborhood \mathcal{N}_1 of \hat{p} and an open neighborhood \mathcal{N}_2 of $\sigma(0)$. Then let C_2 be $C \setminus \mathcal{N}_1$. We know that W sends C_2 to outside the \mathcal{N}_2 neighborhood of $\sigma(0)$. So by continuity of W , there is an open neighborhood \mathcal{N}_3 of

C_2 in $\text{dom } W$ disjoint from an open neighborhood \mathcal{N}_4 of $W^{-1}(\{\sigma(0)\})$. Then the neighborhood $\mathcal{N}_1 \cup \mathcal{N}_3$ of Z is disjoint from a neighborhood of $W^{-1}(\{\sigma(0)\}) \setminus \{\hat{p}\}$. Together this shows that the connected component C of \hat{p} in Z is the same as the connected component C' of \hat{p} in $W^{-1}(\text{Im } \sigma)$. In particular C is compact.

Since σ is a simple curve, we may extend it to a slightly longer simple curve $\underline{\sigma} : [-\epsilon, \ell(\sigma) + \epsilon] \rightarrow \text{Tub}_\epsilon K$. Then for each point $s \in [0, \ell(\sigma)]$ we may find an \mathbb{R}^2 neighborhood U_s of $\sigma(s)$ so $U_s \cap \text{Im } \underline{\sigma}$ is parametrizable by $\sigma(t)$ for t in some interval $I_s \subset \text{dom } \tau$. Moreover, we can ensure that σ is a graph over the tangent line to σ at $\sigma(s)$. Also, since W is an immersion on the compact set C (conditions (a) and (b)), and because the domain of W is sufficiently smooth, we may extend W to a C^n map \underline{W} from an open neighborhood of $\text{dom } W$ to \mathbb{R}^2 .

Now by standard argument, we can show the small curves $\sigma|_{I_s}$ to be level sets of locally defined C^n functions. Using the compactness of C and the fact that W is an immersion everywhere on C (conditions (a) and (b)), we can lift $\underline{\sigma}$ (possibly on a slightly smaller neighborhood of $\text{dom } \sigma$) to a curve in $\text{dom } \underline{W}$. The final step is to show that this curve actually enters the interior of $\text{dom } W$ for positive s . This is accomplished by condition (a₂) (which is implied by (a₁)). Therefore, we may restrict our lifted curve to a curve $\hat{\sigma} : [0, s^*] \rightarrow \text{dom } W$ with $s^* > 0$. By construction our curve parametrizes the connected component C which we showed above is the connected component of $W^{-1}(\text{Im } \sigma)$ containing \hat{p} . The curve must terminate at a boundary; otherwise it would have been continued under our construction.

Finally, we prove the uniqueness property. Without loss of generality, assume $s_1^* \leq s_2^*$. Consider the subset of $[0, s_1^*]$,

$$A = \{s \mid \hat{\sigma}_1(s_1^* - s) = \hat{\sigma}_2(s_2^* - s)\}.$$

This is a closed set. On the other hand, by our above construction, if the two curves agree at a given parameter value, they agree on an open neighborhood of that parameter value. We conclude that A is all of $[0, s_1^*]$. Then

$$\hat{\sigma}_1(0) = \hat{\sigma}_2(s_2^* - s_1^*).$$

Since we were given $\hat{\sigma}_2(0) = \hat{\sigma}_1(0)$, we have by the simpleness of the curve $\hat{\sigma}_2$ that $s^* + 2 = s_1^*$. Moreover, we have shown that on their identical domains, the two curves $\hat{\sigma}_1$ and $\hat{\sigma}_2$ are identical. ■

A.4 A family of constant-curvature curves

Lemma A.5. Let Ξ map a rectangle $[0, \lambda] \times [0, 1]$ to a Riemannian 2-manifold (M, g) so each horizontal segment maps to a curve of constant curvature κ . Coordinatize the domain of Ξ by $s \in [0, \lambda]$ and $t \in [0, 1]$. Assume that:

- (i) The curve $\Xi|_{\{0\} \times [0, 1]}$ is a geodesic.
- (ii) The constant curvature curves leave this geodesic normally:

$$g(\Xi_s(0, t), \Xi_t(0, t)) = 0.$$

- (iii) The curves are parametrized by arclength:

$$|\Xi_s|_g = 1.$$

- (iv) The metric has bounded non-positive Gauss curvature:

$$-K_M \leq K_g \leq 0$$

where K_M is a constant.

- (v) The length of the curves satisfies

$$\lambda < \kappa^{-1} \pi / 2.$$

Then the map Ξ is an immersion. Moreover, we have

$$|\Xi_t|_g \geq |\Xi_t^0| \tag{A.12}$$

where Ξ^0 is the map in the flat case

$$\Xi(s, t) = (\cos \kappa s, t + \sin \kappa s).$$

Proof. We have $\Xi : [0, s_*] \times [0, 1] \rightarrow \Sigma$ and we may pull back the metric to $\text{dom } \Xi$. In this section, we use angled brackets to denote this:

$$\langle u, v \rangle := \hat{g}(u, v) = g(d\Xi(u), d\Xi(v)).$$

This bilinear form is a metric on some open subset Ω of $\text{dom } \Xi$ including $\{0\} \times [0, 1]$. We use $|\cdot|$ to denote the norm associated to \hat{g} . Our goal is to show that in fact $\Omega = \text{dom } \Xi$ and Ξ is an immersion.

We have commuting vector fields

$$S = \frac{\partial}{\partial s}, \quad T = \frac{\partial}{\partial t}, \quad [S, T] = 0.$$

Moving along a level set of t corresponds to moving along a curve of constant curvature. We have constructed Ξ so these curves are parametrized by arclength; this gives

$$|S| = 1.$$

We introduce a vector field ν on Ω so

$$\nabla_S S = \kappa \nu.$$

Then S, ν is an orthonormal frame on Ω . The volume form is

$$\text{dvol } \hat{g} = \mathcal{V} ds dt$$

where

$$\mathcal{W} = \mathcal{V}^2 = \langle S, S \rangle \langle T, T \rangle - \langle S, T \rangle^2 = \langle T, T \rangle - \langle S, T \rangle^2.$$

Subclaim A.6. At each point on $\text{dom } \Xi$,

$$\frac{\partial^2}{\partial s^2} \mathcal{W} = -K \mathcal{W} + 2(\langle \nabla_S T, \nu \rangle + \langle S, T \rangle)^2.$$

Here K is the Gauss curvature of \hat{g} .

Proof. Consider a point (s_0, t_0) in $\text{dom } \Xi$. To make our calculation easier, introduce $\underline{T} = T + cS$ (here $c = -\langle S, T \rangle$) so

$$\langle \underline{T}, S \rangle = 0.$$

Then S, \underline{T} has the same associated volume form as S, T ,

$$\mathcal{W} = \langle \underline{T}, \underline{T} \rangle - \langle S, \underline{T} \rangle^2,$$

just as unslanting a parallelogram does not change its volume. We may then calculate

$$\frac{\partial}{\partial s} \mathcal{W} = 2 \langle \nabla_S \underline{T}, \underline{T} \rangle - 2 \langle \kappa \nu, \underline{T} \rangle \langle S, \underline{T} \rangle - 2 \langle S, \nabla_S \underline{T} \rangle \langle S, \underline{T} \rangle.$$

We then differentiate again and evaluate at (s_0, t_0) . For a term to contribute, it cannot have an $\langle S, \underline{T} \rangle$ factor. We find:

$$\begin{aligned} \left. \frac{\partial^2}{\partial s \partial s} \right|_{s_0, t_0} \mathcal{W} &= 2 \langle \nabla_S \nabla_S \underline{T}, \underline{T} \rangle + 2 |\nabla_S \underline{T}|^2 \\ &\quad - 2\kappa^2 \langle \nu, T \rangle^2 - 4 \langle S, \nabla_S \underline{T} \rangle \langle \kappa \nu, \underline{T} \rangle - 2 \langle S, \nabla_S \underline{T} \rangle^2 \end{aligned} \quad (\text{A.13})$$

Applying $[S, \underline{T}] = 0$ and rearranging gives:

$$= 2 \langle \nabla_S \nabla_{\underline{T}} S, \underline{T} \rangle - 2\kappa^2 \langle \nu, T \rangle^2 - 4 \langle S, \nabla_{\underline{T}} S \rangle \langle \kappa \nu, \underline{T} \rangle + 2 (|\nabla_S \underline{T}|^2 - \langle S, \nabla_S \underline{T} \rangle^2). \quad (\text{A.14})$$

We may then introduce the curvature tensor, again exploiting $[S, \underline{T}] = 0$. Also, we simplify the parenthetical term in (A.14) using the S, ν orthonormal frame.

$$= 2 \left\langle R_{S\underline{T}}^{\dot{g}} S + \nabla_{\underline{T}} \nabla_S S, \underline{T} \right\rangle - 2\kappa^2 \langle \nu, T \rangle^2 + 2 \langle \nabla_S \underline{T}, \nu \rangle^2 \quad (\text{A.15})$$

Here we use that $|S|$ is constant and (curv. formula) to simplify to:

$$= -K\mathcal{W} - 2\kappa^2 \mathcal{W} + 2 \langle \nabla_S \underline{T}, \nu \rangle^2 \quad (\text{A.16})$$

$$= -(K + 2\kappa^2) \mathcal{W} + 2 \langle \nabla_S T + \kappa \nu, \nu \rangle^2 \quad (\text{A.17})$$

$$= -(K + 2\kappa^2) \mathcal{W} + 2 (\langle \nabla_S T, \nu \rangle - \kappa \langle S, T \rangle)^2 \quad (\text{A.18})$$

■

The first order term in the previous lemma measures how the level sets of t are spreading apart from each other. We formalize this as

$$\text{Sp} = \langle \nabla_S T, \nu \rangle.$$

How does the Sp evolve? We have

$$\begin{aligned}
\frac{\partial}{\partial s} \text{Sp} &= \langle \nabla_S \nabla_S T, \nu \rangle + \langle \nabla_S T, \nabla_S \nu \rangle \\
&= \langle \nabla_S \nabla_T S, \nu \rangle + \langle \nabla_S T, S \rangle \langle S, \nabla_S \nu \rangle \\
&= \langle R_{ST} S + \nabla_T \nabla_S S, \nu \rangle \\
&= \langle R_{ST} S, \nu \rangle + \kappa \langle \nabla_T S, \nu \rangle \\
&= -K \mathcal{V}
\end{aligned}$$

How does $\langle S, T \rangle$ evolve?

$$\begin{aligned}
\frac{\partial}{\partial s} \langle S, T \rangle &= \langle \nabla_S S, T \rangle + \langle S, \nabla_S T \rangle \\
&= \kappa \mathcal{V} + \langle S, \nabla_T S \rangle = \kappa \mathcal{V}
\end{aligned}$$

Now let's consider $f(s) = \mathcal{W}(s, t_0)$. It satisfies the equation

$$u_{ss}(s) = -(K(s, t_0) + 2\kappa^2)u(s) + 2\left(\int_{\sigma=0}^s (K(s, t_0) - \kappa)\sqrt{u(\sigma)}d\sigma\right)^2$$

and $f(s_0) = 1, f'(s_0) = 0$. This is of the form

$$u_{ss}(s) = -(K(s, t_0) + 2\kappa^2)u(s) + \mathcal{J}(u|_{[0,s]}).$$

where \mathcal{J} is an operator that takes as input a function on variable domain $[0, s]$ and returns a real number. It has a monotonicity property:

$$u \geq v \text{ on } [0, s] \text{ implies } \mathcal{J}(u|_{[0,s]}) \geq \mathcal{J}(v|_{[0,s]}).$$

Assume that

$$0 \leq -K \leq K_M.$$

This equation admits an exponential supersolution: Try $u(s) = e^{As}$ for A to be determined. Then

$$u_{ss}(s) = A^2 e^{As}$$

and

$$\mathcal{J}(u|_{[0,s]}) \leq \frac{8}{A^2} (K_M + \kappa)^2 e^{As}.$$

To get a supersolution we need

$$A^2 \geq K_M + \frac{8}{A^2}(K_M + \kappa)^2$$

So we can pick $A = 1$ or pick A to be the soln of

$$\begin{aligned} a^4 &= K_M + 8(K_M + \kappa)^2; \\ A &= \max\left(1, (K_M + 8(K_M + \kappa)^2)^{1/4}\right). \end{aligned}$$

This ensures that

$$u_{ss} \geq -(K(s, t_0) + 2\kappa^2)u(s) + \mathcal{J}(u|_{[0,s]}).$$

On the other hand, the planar solution $u(s) = \cos^2(\kappa s)$ provides a subsolution for $s \in [0, \lambda]$, with $\lambda = \kappa^{-1}\pi/2$.

Let's look at $\mathcal{Q}(s) = |T(s, t_0)|^2$. We have $\mathcal{Q}(0) = 0, \mathcal{Q}'(0) = 0$,

$$\begin{aligned} \left. \frac{\partial^2}{\partial s \partial s} \right|_{s_0, t_0} \langle T, T \rangle &= 2 \langle \nabla_S \nabla_S T, T \rangle + 2 |\nabla_S T|^2 \\ &= 2 \langle \nabla_S \nabla_T S, T \rangle + 2 |\nabla_S T|^2 \\ &= 2 \langle R_{TS} S + \nabla_T \nabla_S S, T \rangle + 2 |\nabla_S T|^2 \\ &= 2 \langle R_{TS} S + \nabla_T \kappa \nu, T \rangle + 2 |\nabla_S T|^2 \\ &= 2 \langle R_{TS} S, T \rangle + 2\kappa \langle \nabla_T \nu, T \rangle + 2 |\nabla_S T|^2 \\ &= 2 \langle R_{TS} S, T \rangle + 2\kappa \langle \nabla_T \nu, S \rangle \langle S, T \rangle + 2 |\nabla_S T|^2 \\ &= 2 \langle R_{TS} S, T \rangle - 2\kappa \langle \nu, \nabla_T S \rangle \langle S, T \rangle + 2 |\nabla_S T|^2 \\ &= 2 \langle R_{TS} S, T \rangle - 2\kappa \text{Sp} \langle S, T \rangle + 2 \langle \nabla_S T, \nu \rangle^2 \\ &= 2 \langle R_{TS} S, T \rangle - 2\kappa \text{Sp} \langle S, T \rangle + 2 \text{Sp}^2 \\ &= -2K\mathcal{W} + 2 \left(\int_0^s -K\sqrt{\mathcal{W}} \right) \left(\int_0^s -(K + \kappa)\sqrt{\mathcal{W}} \right) \end{aligned}$$

Plugging in our supersolution for \mathcal{V} we see

$$|\mathcal{Q}_{ss}| \leq 2K_M e^{As} + 2K_M e^{As/2} (K_M + \kappa) e^{As/2} = 2K_M (1 + K_M + \kappa) e^{As}$$

and

$$\mathcal{Q}(s) \leq 1 + 2K_M^2 (1 + K_M + \kappa)^2 e^{2As}.$$

In this way, under the assumptions of the lemma, we are able to show that Ξ is C^1 and is an immersion on all of $\text{dom } \Xi$. ■

A.5 Deferred proofs

We omitted several proofs in the body of the thesis. In this section we prove them.

A.6 Proof of Wire-Plane Intersection Number Lemma (Lem. 2.17)

Here we prove Wire-Plane Intersection Number Lemma (Lem. 2.17). We begin with a preparatory definition and lemma.

Definition A.7. Let Γ be an embedded wire curve and let R be small enough that the tubular neighborhood of Γ does not self-intersect. Let Π be the projection of $\text{Tub}_R(\Gamma)$ to $\text{Im } \Gamma$ sending each point p to the point in Γ closest to p . We define the **plane-enclosure arclength** $\ell_{\text{Wire-Plane}}$ to be

$$\ell_{\text{Wire-Plane}}(\Gamma, R) = \max_{V, C} |\Pi(C)| \quad (\text{A.19})$$

where the maximum ranges over all planes V in \mathbb{R}^3 , and C is a component of $V \cap \text{Tub}_R \Gamma$.

Lemma A.8. [Wire-Plane Arclength] Let Γ be a wire curve. We have that $\ell_{\text{Wire-Plane}}(\Gamma, R)$ is non-increasing as R goes to 0. If Γ is generic, then it vanishes bounded by $O(R^{1/3})$.

Proof–Lemma A.8. For notational convenience in this proof, we define

$$\zeta = |\Gamma^{(4)}|_{C^0(\text{dom } \Gamma)} / 24.$$

Let C be a component and V be a plane as in (A.19). We represent V as the zero set of

$$f(w) = \langle w, v \rangle - b \quad (\text{A.20})$$

for some v in the unit sphere and $b \in \mathbb{R}$. We write the interval $\Pi(C)$ as $[s_0 - \ell_0, s_0 + \ell_0]$ for some $\ell_0 > 0, s_0 \in \mathbb{R}$. For every $s \in [s_0 - \ell_0, s_0 + \ell_0]$, there is a point $\omega(s)$ on V with

$d(\omega(s), \Gamma(s)) < R$. Then

$$d(\Gamma(s), V) < d(\Gamma(s), \omega(s)) < R.$$

Let us apply this observation to four values of s :

$$s_0, \quad s_1 = s_0 - \ell_0, \quad s_2 = s_0 + \ell_0/2, \quad s_3 = s_0 + \ell_0. \quad (\text{A.21})$$

Then for $i = 0, \dots, 3$,

$$\langle \Gamma(s_i), v \rangle - b \in (-R, R). \quad (\text{A.22})$$

Let $v = (v_1, v_2, v_3)$ in Frenet coordinates. The Taylor expansion

$$\sigma(s) = \left(s - \frac{\kappa_\Gamma(s_0)^2}{6}, \frac{\kappa_\Gamma(s_0)s^2}{2} - \frac{\kappa'_\Gamma(s_0)}{6}s^3, -\frac{\kappa_\Gamma(s_0)T_\Gamma(s_0)}{6}s^3 \right)$$

approximates Γ for any $s_0 \in \text{dom } \Gamma$ and $s \in [s_0 - \ell_0, s_0 + \ell_0]$ as

$$|\Gamma(s) - \sigma(s)| \leq \zeta \ell_0^4.$$

We may then write (A.22) as

$$\begin{aligned} |0 \cdot v_1 + 0 \cdot v_2 + 0 \cdot v_3 - b| &< R \quad (\text{A.23}) \\ \left| \left(-\ell_0 - \frac{\kappa_\Gamma(s_0)^2}{6} \ell_0^3 \right) v_1 + \left(\frac{\kappa_\Gamma(s_0)}{2} \ell_0^2 - \frac{\kappa'_\Gamma(s_0)}{6} \ell_0^3 \right) v_2 - \frac{\kappa_\Gamma(s_0)T_\Gamma(s_0)}{6} \ell_0^3 v_3 - b \right| &< R + \zeta \ell_0^4 \\ \left| \left(\frac{\ell_0}{2} + \frac{\kappa_\Gamma(s_0)^2}{24} \ell_0^3 \right) v_1 + \left(\frac{\kappa_\Gamma(s_0)}{8} \ell_0^2 + \frac{\kappa'_\Gamma(s_0)}{24} \ell_0^3 \right) v_2 - \frac{\kappa_\Gamma(s_0)T_\Gamma(s_0)}{24} \ell_0^3 v_3 - b \right| &< R + \zeta \ell_0^4 \\ \left| \left(\ell_0 + \frac{\kappa_\Gamma(s_0)^2}{6} \ell_0^3 \right) v_1 + \left(\frac{\kappa_\Gamma(s_0)}{2} \ell_0^2 + \frac{\kappa'_\Gamma(s_0)}{6} \ell_0^3 \right) v_2 + \frac{\kappa_\Gamma(s_0)T_\Gamma(s_0)}{6} \ell_0^3 v_3 - b \right| &< R + \zeta \ell_0^4. \end{aligned}$$

The first relation gives $b \in (-R, R)$. We now have three cases, depending on which component(s) of the unit vector v meet or exceed $1/\sqrt{3}$. In each case we get a polynomial relation

$$P(\ell_0) = C_1 \ell_0 + C_2 \ell_0^2 + C_3 \ell_0^3 + C_4 \ell_0^4 < R$$

with coefficients from the geometry of Γ .

- (i) If $v_1 \geq 1/\sqrt{3}$, then by the second relation we get $P(\ell_0) < R$, where $C_1 = |v_1|/2$. We may continuously change ℓ_0 to $c\ell_0$, for $c \in [0, 1]$. We get that $P(c\ell_0) < R$ for

all $c \in [0, 1]$. By making R is small enough relative to the coefficients C_i , we may ensure that $[0, \ell_0]$ lie in a neighborhood of a zero of P . Which zero of P can they be nearby? Only 0. So by choosing R small, we can constrain ℓ_0 to be small. So for R less than a small constant, we may establish

$$\ell_0 < CR.$$

(ii) If $v_2 \geq 1/\sqrt{3}$, then by combining the second and fourth relations we get $P(\ell_0) < R$, where $C_1 = 0$ and C_2 is nonzero. Similar reasoning as before shows that if R is less than a small constant,

$$\ell_0^2 < CR.$$

(iii) If $v_3 \geq 1/\sqrt{3}$, then by doing elimination using the second through fourth relations, we get $P(\ell_0) < R$ where $C_1 = C_2 = 0$ and C_3 is nonzero. Similar reasoning as before shows that if R is less than a small constant,

$$\ell_0^3 < CR.$$

Putting this together, we see that if R is less than a small constant, we may bound

$$\ell_0 < CR^{1/3}.$$

■

We now prove Wire-Plane Intersection Number Lemma (Lem. 2.17).

Proof–Lemma 2.17. Given our Generic Wire Assumption 2.15, at any point $\Gamma(s_0)$ on the wire where the torsion is non-zero, we may perturb the $\Gamma'(s_0)$ - $\nu_\Gamma(s_0)$ plane to get a plane which intersects the wire arbitrarily close to $s = s_0$ and does so at three distinct points. This shows claim (i) of the lemma.

To prove claim (ii) of the lemma we proceed as follows. We have by the Generic Wire Assumption that T_Γ may vanish at finitely many places, and when it does, T'_Γ is non-zero. Because Γ is assumed to be C^4 , we can find $\delta_1, \delta_2 > 0$ so if s is within δ_1 of a zero $T_\Gamma(s)$, then

$$2\kappa'_\Gamma(s) + \kappa_\Gamma(s)T'_\Gamma(s) \geq \delta_2. \quad (\text{A.24})$$

Moreover, the function $T_\Gamma(s)$ has a positive minimum δ_3 on the set of s which is at

least δ_1 away from every zero of $T_\Gamma(s)$.

Definition A.9. Choose ℓ_0 to be the minimum of

- (a) $\frac{1}{\sqrt{3}|\kappa_\Gamma|_{C^0(\text{dom } \Gamma)}}$,
- (b) $\frac{\min_{\text{dom } \Gamma} \kappa_\Gamma}{\sqrt{3}|\Gamma^{(3)}|_{C^0(\text{dom } \Gamma)}}$,
- (c) $\frac{\delta_3 \min_{\text{dom } \Gamma} \kappa_\Gamma}{\sqrt{3}|\Gamma^{(4)}|_{C^0(\text{dom } \Gamma)}}$,
- (d) $\frac{\delta_2}{\sqrt{3}|\Gamma^{(5)}|_{C^0(\text{dom } \Gamma)}}$.

By Wire-Plane Arclength Lemma (Lem. A.8), there is a unique R_0 so $\ell_{\text{Wire-Plane}}(\Gamma, R_0) = \ell_0$. Consider a component C of $\Lambda_{\Gamma, R}^{-1}(V)$ of a plane V for $R < R_0$. We may write $\Pi(C) = [s_0 - \ell, s_0 + \ell]$ with $\ell < \ell_0$.

Consider the function $h(s) = f(\Gamma(s))$ for $s \in [s_0 - \ell, s_0 + \ell]$. (See (A.20).) We now show claim (ii) of the lemma. To prove this claim (and this claim only), we are further allowed to assume that Γ is C^5 . Assume to the contrary of claim (ii) of the lemma that h vanishes at least 5 times on its domain. Then applying Rolle's theorem to consecutive zeroes, we see that

- (a') h' must vanish at least 4 times,
- (b') h'' at least 3 times,
- (c') h''' at least twice, and
- (d') $h^{(4)}$ at least once.

Now the vector v normal to the plane V is a unit vector. So if we write it with respect to the basis $\Gamma'(s_0), \nu_\Gamma(s_0), \eta_\Gamma(s_0)$, one of its components must meet or exceed $1/\sqrt{3}$.

(I) Say it happens that $|\langle v, \Gamma'(s_0) \rangle| \geq 1/\sqrt{3}$. Then by the mean value theorem,

$$\begin{aligned} |h'(t)| &\geq |h'(s_0)| - |h''|_{C^0(\text{dom } \Gamma)} |s - s_0| \\ &\geq 1/\sqrt{3} - |\kappa_\Gamma|_{C^0(\text{dom } \Gamma)} \ell_0 \end{aligned}$$

which is positive on the domain of h by Definition A.9.(a). This contradicts (a').

(II) Or say that $|\langle v, \nu_\Gamma(t_0) \rangle| \geq 1/\sqrt{3}$. Then by the mean value theorem,

$$\begin{aligned} |h''(s)| &\geq |h''(s_0)| - |h'''|_{C^0(\text{dom } \Gamma)} |s - s_0| \\ &\geq \min_{\text{dom } \Gamma} (|\kappa_\Gamma|)/\sqrt{3} - \sqrt{\kappa_\Gamma^4 + (\kappa'_\Gamma(0))^2 + \kappa_\Gamma(0)^2 T_\Gamma^2} |_{C^0(\text{dom } \Gamma)} \ell_0 \end{aligned}$$

which is positive on the domain of h by Definition A.9.(b). This contradicts (b').

(III) What if $|\langle v, \eta_\Gamma(t_0) \rangle| \geq 1/\sqrt{3}$? We have two choices:

(A) Say T_Γ does not vanish on $[s_0 - \delta_1, s_0 + \delta_1]$. Then

$$\begin{aligned} |h'''(s)| &\geq |h'''(s_0)| - |h^{(4)}|_{C^0(\text{dom } \Gamma)} |s - s_0| \\ &\geq |\kappa_\Gamma| \delta_3 / \sqrt{3} - |\Gamma^{(4)}|_{C^0(\text{dom } \Gamma)} \ell_0 \end{aligned}$$

which is positive on the domain of h by Definition A.9.(c). This contradicts (c').

(B) On the other hand, what if T_Γ does vanish on $[s_0 - \delta_1, s_0 + \delta_1]$? Then

$$\begin{aligned} |h^{(4)}(s)| &\geq |h^{(4)}(s_0)| - |h^{(5)}|_{C^0(\text{dom } \Gamma)} |s - s_0| \\ &\geq \delta_2 / \sqrt{3} - |\Gamma^{(5)}|_{C^0(\text{dom } \Gamma)} \ell_0 \end{aligned}$$

which is positive on the domain of h by Definition A.9.(d). This contradicts (d').

We took an arbitrary plane V and component C and showed that the component intersected the wire at most 4 times. This proves claim (ii) of the lemma.

This leaves claim (iii) of the lemma. Given a critical point m of κ_Γ on $\text{dom } \Gamma$, pick a subarc $\hat{\Gamma} = \Gamma|_{[m-\ell, m+\ell]}$ which has $\ell < \ell_0$ and on which T_Γ does not vanish. This is possible because of Generic Wire Assumption 2.15.(v). Pick R_0 so $\ell_{\text{Wire-Plane}}(\Gamma, R_0) = \ell$. Then for $R < R_0$, we claim $n_{\text{Wire-Plane}}(\Gamma, R) \leq 3$. Assume to the contrary that there is a plane V and component C with at least 4 intersections. Then we proceed to define the function h as above; this time we have that h', h'', h''' each vanish at least once on $[m - \ell, m + \ell]$. We then consider cases (I), (II), (III.A) above and see that they cannot occur. We conclude that in fact $n_{\text{Wire-Plane}}(\Gamma, R) \leq 3$; combined with claim (i) of the lemma, this proves claim (iii). \blacksquare

A.7 Smoothing a kink in the thread

In the physical model of the thread problem, we see that the thread does not have kinks in it, except maybe at the wire if there is friction. We expect that the thread of an Alt minimizer is C^1 . (In fact we even expect that a suitably-defined stationary thread-wire surface should have a C^1 thread.) Alt has already shown this at a corner of a crescent abutting a positive length piece of wire-adhering thread. (He assumed the wire was smooth; see [?, alt]. Below we prove a stronger result.

Lemma A.10. Let Γ be a C^1 wire curve. Let $(B, M) \in \mathcal{C}_{\text{Alt}}(\Gamma, L)(\Gamma, L)$ be an Alt competitor with $x_0 \in [-1, 1]$ lying in the boundary of a disc of the domain B . Assume that in a neighborhood of x_0 , the map M has essentially bounded derivative.¹ Then either

¹Actually, the idea that the thread should be C^1 on its interior should apply generally. We show it here, in the near-wire case. But it should be provable generally. The author does not know of such a proof; there are technical difficulties. If two adjacent corners form a kink in the thread, we want to modify the conformal map of each crescent to blunt the kink to first order while adding very little Dirichlet energy (more like second order). There does not appear to be a simple way to do this, given that the conformal parametrization might have large derivative on the boundary. We could modify

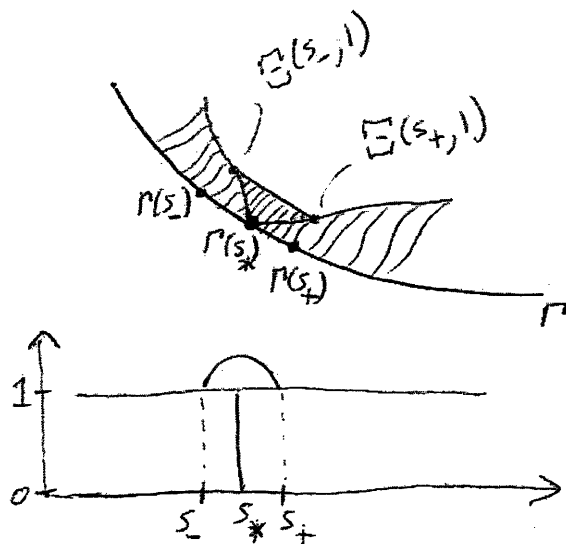


Figure A-1: Joining two crescents to remove a kink in the thread. If there is a kink in the thread where it touches the wire, we may demonstrate an energy-decreasing variation. In this diagram we show two adjacent crescents. The proof also covers the case where a crescent is isolated on one side, but the thread does not meet the wire tangentially.

the thread curve, parametrized by arclength, is C^1 near x_0 , or we may modify (B, M) to find another Alt competitor with less area.

Proof. This proof uses the tools for Alt competitors introduced in Section ??, especially Definition 2.3. Let $s_* = \xi(x_0)$ be the corresponding wire domain point. (See (2.2).) If we are in the case where x_0 is in the boundary of one disc of B , but there is no disc nearby on the other side, we modify B by adding a disc on that side. On this disc, we define $M(x, y) = M(x, 0)$. We may then proceed, with two discs on either side of x_0 . Assume to the contrary that the thread forms a kink at x_0 . We may pull back the map M near the crescent meeting as:

$$\Xi(s, t) = M(s, tp_-^B(s)).$$

We begin our geometric construction. The reader may wish to follow in **Figure A-1**. Pick $s_+ = s_* + \epsilon$, and $s_- = s_* - \epsilon$. Augment the domain of Ξ by a half-disc above $t = 1$ from $s = s_-$ to $s = s_+$. Define an extension Ξ^ϵ of Ξ on this augmented domain so for $s' \in (s_-, s_+)$, the map Ξ^ϵ sends $s = s', t > 1$ linearly to the segment from $\Xi(s', 1)$ to the intersection between the normal disc $D(s')$ and the segment from $\Xi(s_-, 1)$ to $\Xi(s_+, 1)$. As ϵ goes to zero, we have

$$A(\Xi^\epsilon) = A(\Xi) + c_1\epsilon^2 + O(\epsilon^3)$$

and

$$\ell(\gamma^\epsilon) = \ell(\gamma) - (\sin \alpha/2)\epsilon + O(\epsilon^2).$$

We have thus decreased the length of the thread much more than we increased area. We may now act as we did in section 3.1 to transform this into a change which gives us a better Alt competitor and violates the given minimization property of (X, ϕ_-) . Indeed, pick a point q on the interior of the free thread. Near here the surface is a graph over the tangent plane V to the surface at q . Let $\gamma(s)$ parametrize the thread by arclength near $\gamma(0) = q$ and let u, v, w be Frenet coordinates for the thread at q . Let $h(s)$ equal 1 for $|s| \leq \epsilon$ and $h(s) = 0$ for $|s| > 2\epsilon$. Locally retract the surface along itself so the thread point $\gamma(s)$ moves distance $2c_1\epsilon w(s)$ in the negative v direction. Then

the map so its area does not increase very much – but to apply Morrey's lemma and translate this into a small increase in Dirichlet energy we need to at least start with *finite* Dirichlet energy. More needs to be done on this technical point.

this decreases area by $2c_1\epsilon^2 + O(\epsilon^3)$ and increases length by $\kappa 2c_1\epsilon^2 + O(\epsilon^3)$. The final effect is

$$\Delta \text{ Area} = -c_1\epsilon^2 + O(\epsilon^3)$$

and

$$\Delta \text{ Length} = -(\sin \alpha/2)\epsilon + O(\epsilon^2).$$

For sufficiently small ϵ we thus demonstrate a modification of (X, ϕ_-) which decreases area and decreases length. ■

Lemma A.11. Let Γ be an embedded Frenet wire curve. Let (B, M) be an Alt minimizer lying in a tubular neighborhood of Γ . For sufficiently small R , we are guaranteed that $\kappa > 0$.

Proof. Assume to the contrary that we have $\kappa = 0$. First, assume that R is sufficiently small so Slicewise Parametrization Lemma (Lem. 4.4) applies. Our first result is that the thread cannot meet the wire in a kink, forming positive angles with the wire on each side. Indeed, in such a situation, we may apply²[6, p. 175, Thm. 1] to conclude that the conformal parametrization of M near each corner has bounded derivative. We may then apply Lemma A.10 to obtain a contradiction. Thus we see that the thread cannot meet the wire in a kink which makes a positive angle with the wire at the two adjoining crescent corners. This leaves two possibilities. One is that one of the crescent corners has angle zero. But then we may trace the thread in this direction. It must hit the wire again. But for sufficiently small R , given that Γ is a Frenet curve with κ_Γ having a positive lower bound, it will not hit the wire again without leaving the tubular neighborhood. So we have disposed of this case. We are left with the case that the thread meets the wire transversely and is C^1 at each crossing. In other words, the thread curve is a straight line. But again, for sufficiently small R , the tubular neighborhood of a Frenet curve does not contain any straight lines joining the endpoints of the wire. So we have a contradiction. ■

²Note the comment above the theorem in [6, p. 175] as well. This reference presents the work of Dziuk, [9], [10], [11], [12].

Appendix B

Appendix: Series solutions

In this section we study two local problems situated for the thread in thread-wire surface. Essentially, we will be satisfying the conditions for our thread-wire surface to be stationary. We summarize the two problems below. Let (B, M) be an embedded Alt minimizer and let $M(x)$ parametrize a point on the thread.

QUESTION 1: ThIP problem. How does $\text{Im } M$ behave when x corresponds to an interior point of the free thread? Here we have the (constant) curvature of the thread and the coefficients of the torsion $T(s)$ of the thread as inputs. As output we have the coefficients describing the graph of the surface relative to the tangent plane of the surface at $X(x)$. We call this the thread-interior point (ThIP) problem.

QUESTION 2: WOC problem. How does $\text{Im } M$ behave when p marks the corner of a crescent of M ? When the thread and wire form a positive angle, there is a known expansion for this from the Classical case.¹ We focus on the case where the corner angle is zero, so the corner is a wire-osculating corner. We call this the WOC problem.

REMARK. In this thesis we only use our solution to the ThIP problem, and we wouldn't need as detailed a discussion as this one to yield the needed ThIP result. However I have included the full discussion because I think it is interesting and even surprising in places (e.g. the role played by the "critical curvature ratios"). Further work is needed. In particular, we would like to study the convergence of these expansions.

¹See Beeson's work [3] and also the presentation of this work in [6]. See Section 7.3 for a remarkable application of Beeson's corner analysis.

Definition B.1. Given a curve $\sigma(t)$ in \mathbb{R}^3 , we use component notation

$$\sigma(t) = (\sigma_{[x]}(t), \sigma_{[y]}(t), \sigma_{[z]}(t)).$$

We write formal expansions for the coefficients as

$$\sigma_{[x]}(t) = \sum_{p=0}^{\infty} \sigma_{[x,p]} t^p$$

and similarly for the other components. A **multi-index** I is an n -tuple (i_1, i_2, \dots, i_n) for $n \geq 0$. We define

$$\#I = n, \quad |I| = i_1 + i_2 + \dots + i_n.$$

The **zero-tuple** $()$ has $\#() = |()| = 0$. If we have a power series

$$a_0 + a_1 x + a_2 x^2 + \dots,$$

then we define

$$a^I := \prod_{p=1}^n a_{i_p}$$

and, for example,

$$\sigma_{[x]}^I = \prod_{p=1}^n \sigma_{[x,i_p]}.$$

REMARK. Here's a formal example: If $f(y) = \sum_{i=0}^{\infty} f_i y^i$, and $g(x) = \sum_{j=0}^{\infty} g_j x^j$, then

$$f(g(x)) = \sum_{n=0}^{\infty} \left(\sum_{|I|=n} f_{\#I} g^I \right) x^n.$$

Definition B.2. For C^2 functions, we define the **minimal surface operator**

$$MS[f] := (1 + f_y^2) f_{xx} - 2f_x f_y f_{xy} + (1 + f_x^2) f_{yy}.$$

Definition B.3. A **formal degree N series solution to the stationary wire-osculating corner thread-wire surface problem (the WOC problem)** consists of the following:

- A degree $N \geq 2$. We allow N to be $+\infty$.

- A formal expansion

$$f(x, y) = \sum_{n=1}^N \sum_{i=0}^n b_{i, n-i} x^i y^{n-i} \quad (\text{B.1})$$

with $b_{0,0} = b_{0,1} = b_{1,0} = 0$.

- A formal expansion

$$T(s) = \sum_{p=0}^{N-3} T_p s^p. \quad (\text{B.2})$$

- A "thread" curve $\gamma(s)$ parameterized by arclength with $\gamma'(0) = \gamma'(0)$, torsion $T(s)$ and constant curvature κ . The data in the expansion of $T(s)$ determine γ up to order $N + 1$ in the x and y components, and up to N in the z component.

These objects must satisfy the following conditions:

(*MS*) We require that f satisfy the minimal surface equation to appropriate order

$$MS[f] = o(|(x, y)|^{N-2}). \quad (\text{B.3})$$

(*WI*) The wire curve Γ lies in the surface defined by f

$$f(\gamma_{[x]}(s), \gamma_{[y]}(s)) - \gamma_{[z]}(s) = o(s^N). \quad (\text{B.4})$$

(*TH*) The thread curve lies in the surface defined by f :

$$f(\gamma_{[x]}(s), \gamma_{[y]}(s)) - \gamma_{[z]}(s) = o(s^N). \quad (\text{B.5})$$

(*TG*) We require that the curvature vector of the thread curve point tangentially to the graph of f . This may be expressed using the scalar triple product:

$$\begin{vmatrix} 1 & 0 & f_x(\gamma_{[x]}(s), \gamma_{[y]}(s)) \\ 0 & 1 & f_y(\gamma_{[x]}(s), \gamma_{[y]}(s)) \\ \gamma''_{[x]}(s) & \gamma''_{[y]}(s) & \gamma''_{[z]}(s) \end{vmatrix} = o(s^{N-2}). \quad (\text{B.6})$$

It will be convenient to adopt the notation that $MS_{i,j}$ is the coefficient of $x^i y^j$ in the MS equation, WI_i is the coefficient of s^i in the WI equation, and so on for TH and TG .

By **WOC series solution** we mean a formal degree ∞ solution to the WOC problem. A **convergent WOC series solution** is a series solution, along with radii of convergence on which (B.1) and (B.2) converge.

Definition B.4. We define the **ThIP problem** by repeating the previous definition verbatim, but with condition (WI) removed, the $T(s)$ function changed from an unknown to a given, and all "WOC" 's changed to "ThIP" 's.

Relevant to both problems is the following remarkable sequence.

Definition B.5. [Sequence of critical curvature ratios] We define the **sequence of critical curvature ratios** to be the decreasing sequence

$$\begin{aligned}\xi_m &= \frac{m(m+1)}{m(m+1)-2}, \quad m \geq 2 \\ &= \frac{3}{2}, \frac{6}{5}, \frac{10}{9}, \frac{15}{14}, \frac{21}{20}, \frac{28}{27}, \dots\end{aligned}$$

which tends to 1. We say a ratio of two curvatures is **critical** if it belongs to this sequence.

With this sequence in hand, we may state a theorem for each of the two problems. We will prove these at the end of the section, after a general discussion.

Theorem B.6. [Series Solutions to ThIP problem] Let γ parameterize a real-analytic thread with curvature κ and torsion $T(s)$ not identically zero. Then there is a unique expansion solution to the ThIP problem for this thread, and it converges in neighborhood of zero. The zero set $f = 0$ has the structure of a graph near 0, and 0 has valence $2m + 4$ where m is the lead order of $T(s)$ at zero. Of these edges, $m + 1$ emanate into the lower half-plane at non-zero angle relative to $y = 0$. Another $m + 1$ emanate into the upper half-plane at non-zero angle relative to $y = 0$. This leaves two borderline edges which emanate from 0 parallel to the x -axis, deviating at second order like $\frac{\kappa}{2\xi_{m+2}}s^2$. These edges stay on the surface side of the thread, which in this model deviates like $\frac{\kappa}{2}s^2$. But we see that as m gets large, the quadratic separation between border-line edge and thread goes to zero.

Theorem B.7. [Series Solutions to WOC problem] Let $\gamma(s)$ parameterize a wire Γ real-analytically for $|s| < R_\Gamma$. Define

$$\begin{aligned}\kappa_p^\Gamma &= p! \left. \frac{\partial^p}{\partial s^p} \right|_{s=0} \kappa_\Gamma(s) \\ T_p^\Gamma &= p! \left. \frac{\partial^p}{\partial s^p} \right|_{s=0} T_\Gamma(s)\end{aligned}$$

so $\kappa_\Gamma(s) = \sum_{p=0}^{\infty} \kappa_p^\Gamma s^p$ and $T_\Gamma(s) = \sum_{p=0}^{\infty} T_p^\Gamma s^p$. Let κ be any constant other than κ_0^Γ .

- (i) If κ/κ_0^Γ is *not* a critical curvature ratio, then there is a unique series solution to the WOC problem.
- (ii) If $\kappa/\kappa_0^\Gamma = \xi_m$ for some m then there is a unique degree $m - 1$ series solution to the WOC problem. Further behavior is determined by the top wire torsion coefficient at degree m : T_{m-2}^Γ . There is a sequence of universal functions τ_p which depend only on $\kappa_i^\Gamma, i \leq p$, and $T_i^\Gamma, i < p$, which decide this.
 - (a) If $T_{m-2}^\Gamma \neq \tau_{m-2}(\Gamma)$, then there are no series solutions to our WOC problem of degree greater than m .
 - (b) If $T_{m-2}^\Gamma = \tau_{m-2}(\Gamma)$, then we say Γ has **critical $(m - 2)$ -torsion** or **critical torsion at degree m** . In this case the series solutions to the WOC problem form a 1-parameter family parameterized by T_{m-2} , which can take all values of \mathbb{R} .

We give an algorithmic definition of the universal functions τ_p . The first few are:

$$\begin{aligned}\tau_0(\Gamma) &= 0 \\ \tau_1(\Gamma) &= \frac{14T_0^\Gamma \kappa_1^\Gamma}{3\kappa_0^\Gamma}.\end{aligned}\tag{B.7}$$

Given our wire Γ , we define $\xi(\Gamma)$ to be the set of m such that Γ has critical torsion at degree m . Define a domain D in the plane consisting of the x -axis minus the points of the critical curvature ratio sequence, union vertical lines at $x = \xi_p$ for every $p \in \xi(\Gamma)$. Then the set of series solutions to our problem is homeomorphic to D . We define the homeomorphism by mapping the series solutions of (i) to $(\kappa/\kappa_0^\Gamma, 0)$ and the series solutions of (ii.b) to $(\kappa/\kappa_0^\Gamma, T_{p-2})$. Call the inverse of this map \mathcal{W} . We can describe how the torsions of the series solutions vary along D :

- For $p \in \xi(\Gamma)$, we have $T_{p-2} = 0$ everywhere on $\mathcal{W}(D)$ except for solutions $\mathcal{W}((\xi_p, y))$, where $T_{p-2} = y$.
- For p not in $\xi(\Gamma)$, we have that T_{p-2} of $\mathcal{W}((c, 0))$ diverges as c approaches ξ_p .

REMARK. Does every subset of $\mathbb{Z}_{\geq 0}$ appear as $\chi(\Gamma)$ for some wire Γ ?

B.1 The Taylor expansion of a minimal surface

Let $f(x, y)$ be a function which is real-analytic at 0. Then in its disc of convergence, it satisfies the minimal surface equation

$$H[f] := (1 + f_y^2)f_{xx} - 2f_x f_y f_{xy} + (1 + f_x^2)f_{yy} = 0.$$

Let f have expansion (B.1). Let us consider the terms of $H[f]$:

$$\begin{aligned} MS_{i,j} &= (i+1)(i+2)b_{i+2,j} + (j+1)(j+2)b_{i,j+2} & (B.8) \\ &- 2 \cdot \sum_{\substack{u,v,p,q,r,s \\ u+p+r=i \\ v+q+s=j}} (u+1)(q+1)(r+1)(s+1)b_{u+1,v}b_{p,q+1}b_{r+1,s+1} \\ &+ \sum_{\substack{p,q,r,s \\ 2p+r=i \\ 2q+s=j}} (p+1)^2(r+1)(r+2)b_{p+1,q}^2b_{r+2,s} + (q+1)^2(s+1)(s+2)b_{p,q+1}^2b_{r,s+2}. \end{aligned}$$

We see that the first two coefficients have total degree $(i+j)+2$. The latter products of coefficients have total degree $(i+j)+4$. The minimal surface equation can be seen as a perturbation of Laplace's equation.

Let us think about how we can build expansions of solutions to the minimal surface equation. If we have already chosen the values of lower terms, we have exactly two degrees of freedom in choosing terms of degree n . Given any b_{i_0, j_0} of degree n , we may solve for all other coefficients $b_{i,j}$ of degree n with parity of j the same as j_0 . In particular our two degrees of freedom may be represented as choices of $b_{n,0}$ and $b_{n-1,1}$.

Definition B.8. The homogeneous degree of $b_{i,j}$ is $i+j$; the parabolic degree of $b_{i,j}$ is $i+2j$. If j is odd, we say $b_{i,j}$ is a **y -odd degree $(i+j)$ coefficient of f** . In this case its **inductive degree** is $i+j+1$. If j is even, we say $b_{i,j}$ is a **y -even degree $(i+j)$ coefficient of f** . In this case we say its inductive degree is $i+j$. We say

the coefficient T_i has degree i and inductive degree $i - 3$. Expressions not containing $b_{i,j}$ or T_p have inductive degree 0. We denote inductive degree by IndDeg and declare $\text{IndDeg}(A \cdot B) = \max(\text{IndDeg}(A), \text{IndDeg}(B))$.

B.2 WOC Relations

In this section we expand the relations of Definition B.3 as power series. We also think about how we could solve for the unknown coefficients $b_{i,j}$, T_p , given the known values κ , κ_p^Γ , T_p^Γ . It is helpful to note the natural units of each quantity:

- $b_{i,j}$ has units dist^{1-i-j} ,
- κ has units dist^{-1} ,
- $T_p^\Gamma, \kappa_p^\Gamma$ have units dist^{-1-p} .

For each relation, we need to identify the highest degree coefficient appearing from the two families (b , T) of unknown coefficients. To understand the expansions, we need the beginning of the expansions for the thread and wire curves. See Section A.1.

$$\begin{aligned} \gamma(s) &= \left(s - \frac{(\kappa_0^\Gamma)^2}{6} s^3, \frac{\kappa_0^\Gamma}{2} s^2 + \frac{\kappa_1^\Gamma}{6} s^3, -\frac{\kappa_0^\Gamma T_0^\Gamma}{6} s^3 \right) + O(s^4) \\ \gamma(s) &= \left(s - \frac{\kappa}{6} s^3, \frac{\kappa}{2} s^2, -\frac{\kappa T_0}{6} s^3 \right) + O(s^4) \end{aligned}$$

B.2.1 Inductive plan

Here is our plan: For $m \geq 3$, we solve for the coefficients of inductive degree m in terms of coefficients of lesser inductive degree and in terms of the known quantities κ , κ_p^Γ , T_p^Γ . The coefficients of inductive degree m are the triple $(b_{m,0}, b_{m-2,1}, T_{m+3})$, and the related coefficients $b_{m-2r,2r}$, $0 \leq r \leq m/2$, and $b_{m-2-2r,1+2r}$, $0 \leq r \leq (m+2)/2$.

If we succeed, then we will have produced a degree $m - 1$ series solution to the WOC problem. We will also have a piece of data needed for the degree m solution: $b_{m,0}$. It turns out that this “uneven” approach is the right way to solve the problem inductively.

What do we already know? We have $b_{0,0} = b_{0,1} = b_{1,0} = 0$. And

$$\begin{aligned} MS_{1,1} : 0 &= 2b_{2,0} + 2b_{0,2} \\ WI_2 : 0 &= b_{2,0} \\ TH_2 : 0 &= b_{2,0} \end{aligned}$$

give $b_{2,0} = b_{0,2} = 0$. So we know the values of all the predecessors of the unknown coefficients ($T_0, b_{3,0}, b_{1,1}$) to be solved for the $m = 2$ case.

We now demonstrate our inductive step. To define the algorithm, we need only calculate the top inductive order term appearing in each equation. We present more than that: we calculate the top *two* inductive orders appearing. Perhaps this will be helpful in the future.

B.2.2 Wire lies in surface

In this section we expand the (WI) relation (B.4), which encodes the property that the wire lies in the surface. We have

$$WI_n : 0 = -\gamma_{[z,n]} + \sum_{\substack{I,J \\ \#I+\#J \leq n \\ |I|+|J|=n}} b_{\#I,\#J} \gamma_{[x]}^I \gamma_{[y]}^J. \quad (\text{B.9})$$

Because $\gamma_{[x]}$ has lead order 1 and $\gamma_{[y]}$ has lead order 2, we see that every element of I must be at least 1 and every element of J must be at least 2 in order to contribute to the sum. This implies

$$|I| \geq \#I, \quad |J| \geq 2\#J. \quad (\text{B.10})$$

We search for coefficients $b_{i,j}$ appearing in the equation with $i + j \leq n$ as required.

- We find $b_{n,0}$ appears with $I = (1, 1, \dots), \#I = n; J = ()$, contributing a term with inductive degree n :

$$b_{n,0}.$$

Terms $b_{n-r,r}, r \geq 1$ cannot appear because then $|I| + |J| \geq n + r > n$.

- Next we consider $b_{n-1-r,r}$. We see that $r = 0$ fails because then $J = ()$ and each element of I is 1 or is at least 3. However, $r = 1$ succeeds with $I = (1, 1, \dots), \#I =$

$n - 1, J = (2)$ yielding the inductive degree n term

$$\frac{\kappa_0^\Gamma}{2} b_{n-2,1}.$$

Values of $r \geq 2$ fail because then $|I| + |J| \geq n - 1 - r + 2r > n$.

- Next we look among $b_{n-2-r,r}$ for terms with inductive order $n - 1$. We find $r = 1$ works with $I = (1, 1, \dots), \#I = n - 3, J = (3)$, yielding the inductive degree $n - 1$ term

$$\frac{\kappa_1^\Gamma}{6} b_{n-3,1}.$$

Trying $r = 3, 5, 7 \dots$ fails because then $|I| + |J| \geq n - 2 - r + 2r > n$. All other $b_{i,j}$ coefficients appearing have inductive degree less than $n - 1$.

So we have found all terms $b_{i,j}$ with inductive degrees of $n - 1$ and n . The wire terms are all known. Putting this together we have

$$\begin{aligned} WI_n : \quad & b_{n,0} + \frac{\kappa_0^\Gamma}{2} b_{n-2,1} & (\text{IndDeg} = n) \\ & + \frac{\kappa_1^\Gamma}{6} b_{n-3,1} & (\text{IndDeg} = n - 1) \\ & + \dots = 0 & (\text{IndDeg} < n - 1) \end{aligned} \tag{B.11}$$

B.2.3 Thread lies in surface

We investigate the thread-lies-in-surface (TG) equation (B.6) similarly. The additional ingredient we need is to understand how unknown T_p terms appear in $\gamma_{[z,n]}$. This amounts to understanding the most- and second-most- differentiated instances of T in

$$n! \gamma_{[z,n]} = \left(\begin{array}{ccc} \partial_s & -\kappa & 0 \\ \kappa & \partial_s & T(s) \\ 0 & -T(s) & \partial_s \end{array} \right)^{n-1} \left(\begin{array}{c} 1 \\ 0 \\ 0 \end{array} \right) \Bigg|_{s=0} = \left(\begin{array}{ccc} \partial_s & -\kappa & 0 \\ \kappa & \partial_s & T(s) \\ 0 & -T(s) & \partial_s \end{array} \right)^{n-3} \left(\begin{array}{c} -\kappa^2 \\ 0 \\ -\kappa T(s) \end{array} \right) \Bigg|_{s=0}$$

We see that $T(s)$ gets differentiated the most times if the (3,3) element of the matrix hits it every time. So we get $T^{(n-3)}(s)$ appearing as $-\kappa T^{(n-3)}(s)$. What about $T^{(n-4)}(s)$? That only occurs in $\gamma_{[y,n]}$ due to the matrix operator acting with element (3,3) some number of times, then once with element (2,3), and then subsequently always with (2,2). What about $T^{(n-5)}(s)$? This occurs when the matrix operator acts

a_1 times by (3, 3), then once by (2, 3), then a_2 times by (2, 2), then once by (3, 2), then a_3 times by (3, 3). There are $\binom{n-3}{2}$ ways to do this. This yields the term

$$\binom{n-2}{2\kappa T_0^2 T^{(n-5)}(0)}.$$

Evaluating at zero and dividing out by $n!$ gives

$$\begin{aligned} \frac{1}{n!}[-\kappa T^{(n-3)}(0)] &= \frac{1}{n!}[-(n-3)!\kappa T_{n-3}] \\ &= -\frac{\kappa T_{n-3}}{n(n-1)(n-2)} \end{aligned}$$

which is the only term of inductive degree n in $\gamma_{[z,n]}$. Again, there are no inductive degree $n-1$ terms and the next contribution is at $\text{IndDeg} = n-2$.

Putting this together with reasoning similar to that in Section B.2.2 gives

$$\begin{aligned} TH_n : b_{n,0} + \frac{\kappa}{2}b_{n-2,1} + \frac{\kappa T_{n-3}}{n(n-1)(n-2)} & \quad (\text{IndDeg} = n) \\ & + 0 \quad (\text{IndDeg} = n-1) \\ & + \dots = 0. \quad (\text{IndDeg} < n-1) \end{aligned} \quad (\text{B.12})$$

B.2.4 Thread curvature is tangential to surface

In this section we expand the (TG) equation (B.6), which encodes the property that the thread binormal is tangent to the surface.

$$\begin{aligned} TG_n : 0 = & (n+1)(n+2)\gamma_{[z,n+2]} \\ & + \sum_{q=0}^n (q+1)(q+2)\gamma_{[x,q+2]} \left[\sum_{\substack{I,J \\ \#I+\#J \leq n-q \\ |I|+|J|=n-q}} (\#I+1)b_{\#I+1,\#J} \gamma_{[x]}^I \gamma_{[y]}^J \right] \\ & - \sum_{q=0}^n (q+1)(q+2)\gamma_{[y,q+2]} \left[\sum_{\substack{I,J \\ \#I+\#J \leq n-q \\ |I|+|J|=n-q}} (\#J+1)b_{\#I,\#J+1} \gamma_{[x]}^I \gamma_{[y]}^J \right] \end{aligned} \quad (\text{B.13})$$

As in previous sections, we see that the γ term contributes

$$\begin{aligned} -(n+1)(n+2) \frac{1}{n(n+1)(n+2)} \kappa T_{n-1} & \quad (\text{IndDeg} = n+2) \\ + 0 & \quad (\text{IndDeg} = n+1) \\ + \dots & \quad (\text{IndDeg} < n+1) \end{aligned}$$

We see here the appearance of terms of inductive degree $n+2$. This is the highest inductive degree we will see, and so we will only search down to inductive degree $n+1$.

Now let us examine what b coefficients appear. We will use as before the fact that in order to contribute, all entries in I must be at least 1 and all in J must be at least 2. This gives

$$|I| \geq \#I, \quad |J| \geq 2\#J. \quad (\text{B.14})$$

The rules for either sum are

$$\#I + \#J \leq n - q \quad (\text{B.15})$$

and

$$|I| + |J| = n - q. \quad (\text{B.16})$$

We start with the second sum, involving $\gamma_{[y, q+2]}$. We note that if $q = 1$ then this coefficient vanishes. So we must have $q = 0$ or $q \geq 2$. The highest homogeneous degree $b_{i,j}$ which we can find is $i = \#I, j = \#J + 1$ with

$$i + j = \#I + \#J + 1 \leq n - q + 1 \leq n + 1.$$

We see that $i + j = n + 1$ only if $q = 0$.

- Let us start by looking for $b_{i,j}$ with homogeneous degree $n+1$. In this case $q = 0$.

– As $j = \#J + 1$, we start with $b_{n,1}$ and $J = ()$. Then we must have $I = (1, 1, \dots), \#I = n$ to satisfy $|I| + |J| = n$. This gives

$$-1 \cdot 2 \cdot \frac{\kappa}{2} b_{n,1} \cdot 1 \cdot 1 = -\kappa b_{n,1}. \quad (\text{IndDeg} = n+2)$$

– What about $b_{n-r,q+r}$ for $r > 0$? We get

$$|I| + |J| \geq n - r + 2(q + r) \geq n + 1$$

which violates (B.16).

• Now let's look for $b_{i,j}$ with homogeneous degree n . Because we are only searching down to inductive degree $n + 1$, we need only consider the j -odd terms. In this case because of (B.14) and (B.16), we must have $q = 0$.

– First we try $b_{n-1,1}$. This forces $J = ()$. We must satisfy $|I| + |J| = n - q$. The indices in I can be 1 or ≥ 3 . Well, if any index is ≥ 3 , then $|I| \geq \#I + 2 = n + 1$ which is a problem. But then $I = (1, 1, \dots)$, $\#I = n - 1$ which requires $q = 1$. So we do not get anything in this case.

– Next we try $b_{n-r,r}$ for r odd and at least 3. We get,

$$|I| + |J| \geq n - r + 2r \geq n + 3$$

which violates (B.16).

Now we look at the first sum, involving $\gamma_{[x,q+2]}$. We see that we must have $q \geq 1$ because $\gamma_{[x,2]} = 0$. Then the highest homogeneous degree $b_{i,j}$ we can find is

$$i + j = \#I + \#J + 1 \leq n - q + 1 \leq n.$$

Now we are only searching for terms with inductive degrees of $n + 1$ or $n + 2$. So the only contribution we could hope for from this sum is $b_{n-r,r}$ for r odd. However, in these cases we get

$$|I| + |J| \geq n - r + 2r \geq n + 1$$

which violates (B.16). So the first sum does not contribute inductive degree terms higher than degree n .

Putting this together gives

$$\begin{aligned} TG_n : & -\frac{\kappa T_{n-1}}{n} - \kappa b_{n,1} & (\text{IndDeg} = n + 2) \\ & + 0 & (\text{IndDeg} = n + 1) \\ & + \dots = 0. & (\text{IndDeg} < n + 1) \end{aligned} \tag{B.17}$$

B.2.5 Solving the WOC problem: Proof of Theorem B.7

Let us solve for inductive degree m unknowns $(b_{m,0}, b_{m-2,1}, T_{m-3})$ in terms of known quantities of lower inductive degree.

Fortunately we have three equations and three unknowns. Subtracting the TH_m equation (B.12) from the WI_m equation (B.11) and substituting the solution of $b_{m-2,1}$ from the TG_{m-2} equation (B.17) gives:

$$\begin{aligned} \left(\frac{\kappa_0^\Gamma}{2} - \frac{\kappa}{2}\right) \left(\frac{-T_{m-3}}{m-2}\right) - \frac{\kappa T_{m-3}}{(m-2)(m-1)m} & \quad (\text{IndDeg} = m) \\ + \frac{\kappa_1^\Gamma}{6} b_{m-3,1} & \quad (\text{IndDeg} = m-1) \\ + \dots & \quad (\text{IndDeg} < m-1) \end{aligned}$$

We may rewrite the IndDeg = m part as:

$$\begin{aligned} \frac{-\kappa}{2(m-2)} \left(\frac{2}{(m-1)m} + \kappa^\Gamma/\kappa - 1 \right) T_{m-3} &= \frac{-\kappa}{2(m-2)} \left(\frac{\kappa_0^\Gamma}{\kappa} - \frac{(m-1)m-2}{(m-1)m} \right) \\ &= \frac{-\kappa}{2(m-2)} \left(\frac{\kappa_0^\Gamma}{\kappa} - \xi_{m-1}^{-1} \right). \end{aligned}$$

So the coefficient of T_{m-3} vanishes if and only if κ/κ_0^Γ is the critical curvature ratio ξ_{m-1} .

If we set the expression on the right side of the equation to zero, substitute $\kappa = \xi_{m-1} \kappa_0^\Gamma$, and solve for T_{m-3}^Γ , then we get the expression $\tau_{m-3}(\Gamma)$ which appears in the statement of the theorem.

We may then back-solve. From the TG_{m-2} equation (B.17), we get

$$b_{m-2,1} = -\frac{T_{m-3}}{m-2} + \text{lower}().$$

From the WI_{p+1} equation (B.11), we get

$$b_{m,0} = -\frac{\kappa_0^\Gamma}{2} b_{m-2,1} + \text{lower}().$$

B.3 Solving the ThIP problem: Proof of Theorem B.6

The ThIP problem is the same as the WOC problem except that there is no wire condition WI and the torsion data $T(s)$ is a given, not an unknown. We solve the ThIP problem along the same lines as the WOC problem. Our algorithm is inductive; for $p \geq 2$, we solve for the pair $(b_{p+1,0}, b_{p-1,1})$. As before, we use $MS_{1,1}, TH_2$ to show all coefficients of b preceding the $p = 2$ case to be zero. To perform the inductive step, we use the TG_{p-1} equation (B.17) to solve for $b_{p-1,1}$ in terms of the known quantity T_{p-2} and lower (inductively known) quantities:

$$b_{p-1,1} = -\frac{T_{p-2}}{p-1} + \text{lower}().$$

Substituting this into the TH_{p+1} equation (B.12) allows us to solve for $b_{p+1,0}$:

$$b_{p+1,0} = -\kappa \left(\frac{1}{2} - \frac{1}{p(p+1)} \right) b_{p-1,1} + \text{lower}(). \quad (\text{B.18})$$

This is a complete inductive algorithm.

Proof-Theorem B.6. We note that all coefficients $(b_{p+1,0}, b_{p-1,1})$ will be zero if T_{p-2} and all earlier T coefficients are zero. Let m be the lead order of $T(s)$. Then the algorithm will calculate non-zero values for $(b_{m+3,0}, b_{m+1,1})$. The convergence of this is known. (It is just Björling's formula; see Section 7.1.) The zero set of f in the full neighborhood will consist of $2(m+2)$ edges emanating from zero at evenly-spaced angles. What is the quadratic separation of the edges which emanate in the direction of the x -axis? We evaluate our surface function f along the curve $(t, ct^2/2)$:

$$b_{m+3,0}t^{m+3} + b_{m+1,1}t^{m+1}ct^2/2 + \text{lower}() = 0.$$

We see from (B.18) that

$$c = \kappa \left(1 - \frac{2}{(m+2)(m+3)} \right) = \kappa \xi_{m+2}^{-1}.$$

■

List of Figures

0-1	Arcs of the unit circle	10
Introduction		11
1-1	Thought experiment	11
1-2	Non-generic wire with infinite-component Alt minimizer	12
1-3	Crescent as a graph in Frenet coordinates	15
1-4	Gauss image control	17
Background and preliminaries		19
2-1	Thread-wire surface not realizable as integral current	20
2-2	Frenet frame	21
2-3	Alt competitor (B, M)	21
2-4	Alt minimizer (B, M)	24
2-5	Alt crescent (X, ϕ_-)	25
2-6	Arcs of the unit circle	26
Alt minimizers		31
3-1	An Alt competitor with $\kappa < 0$ may be improved	31
3-2	Thread-Bearing-Wire Curvature Bound variation.	34
3-3	Gauss image of thread	35
3-4	Alt crescent lies in convex hull of supporting wire	39
3-5	The adjoint of an Alt crescent, satisfying the adjoint convex hull property	40
3-6	An adjoint surface of an Alt crescent, which does not lie in the convex hull of its supporting wire	41
3-7	Conditions for Intersection Graph Lemma (Lem. 3.6)	43

3-8	Arcs of the unit circle	44
Near-wire Crescent Theorem		51
4-1	Crescent as a graph in Frenet coordinates	52
4-2	Near-wire Alt minimizers could be quite wild, a priori	54
4-3	Slicewise Parametrization Lemma (Lem. 4.4) tames the potential behavior of an Alt minimizer.	55
4-4	Slope bound in Γ' direction	58
4-5	Slope bound in Γ' direction, part II.	59
4-6	Diamond region for ν_Γ slope limitation	61
4-7	Setup for ν_Γ -slope limitation lemma	62
4-8	Definition of planes V_1, V_2	63
4-9	Top view for Bound on ν_Γ -Slope Lemma (Lem. 4.8)	63
4-10	Side view for Bound on ν_Γ -Slope Lemma (Lem. 4.8)	64
4-11	Filling in the diamond	66
4-12	Diamond and annulus on sphere	68
4-13	Control on ρ'	71
4-14	Closeness of Frenet frames of thread and wire	72
4-15	Free thread curvature must be near maximum wire curvature	78
4-16	Slope improvement from quadratic trumpet enclosure I.	80
4-17	Slope improvement from quadratic trumpet enclosure II.	80
4-18	Slope improvement from quadratic trumpet enclosure III.	81
C^1 Corner Theorem		83
5-2	Doubly-cusped domain	86
5-3	Doubly-cusped domain	88
5-1	Gauss image control	94
5-4	Gauss image constrained by quadrants	94
5-5	Lifted curves cross	97
5-6	Gauss wire curve cannot cross supporting ruling segment: I	100
5-7	Gauss wire curve cannot cross supporting ruling segment: II	101
5-8	Gauss wire curve cannot intersect Gauss thread curve	103
5-9	The Gauss thread curve bounds the Gauss image to one side.	105
5-10	Gauss thread curve bounds y -slopes	108

	181
Sufficient $C^{1,1}$ corner regularity implies crescent finiteness	113
6-1 A crescent foliated by constant curvature curves	115
6-2 Crescent geometry: setup	116
6-3 A bijection between the wire and the thread	117
6-4 Uniqueness of length minimizer τ^s	118
6-5 A simple length competitor	118
6-6 Maximum length geodesic	119
Examples	123
7-1 Extensible thread-wire surfaces	124
7-2 Beeson's skewed chevron	130
Physical experiment	131
8-1 Thought experiment	131
8-2 Tie-clip curve supporting two area minimizers	132
8-3 Constrained minimization can jump	133
8-4 Heart thread pull	135
8-5 "Bent paperclip" thread pull	137
8-6 Tie-clip curve.	139
8-7 Tie-clip horizontal solution	140
8-8 Tie-clip vertical solution	141
8-9 Möbius strip thread pull	142
8-10 Möbius strip thread pull, continued	143
Appendix	145
A-1 Joining two crescents to remove a kink in the thread	162

Bibliography

- [1] Alt, H.W. Die Existenz einer Minimalfläche mit freiem Rand vorgeschriebener Länge. Arch. Ration. Mech. Anal. **51**, 304-320 (1973).
- [2] Barbosa, J.L.; do Carmo, M. On the size of a stable minimal surface in \mathbb{R}^3 . Am. J. Math. **98**, no 2., 515-528 (1976).
- [3] Beeson, M. The behavior of a minimal surface in a corner. Arch. Ration. Mech. Anal. **65**, no. 4, 379-393 (1977).
- [4] Beeson, M. The 6π theorem about minimal surfaces. Pac. J. Math. **117**, no. 1, 17-25 (1995).
- [5] Dierkes, U., S. Hildebrandt, A. Küster, O. Wohlrab. Minimal Surfaces I: Boundary value problems. Grundlehren der mathematischen Wissenschaften 295. Springer-Verlag: Berlin, 1992.
- [6] Dierkes, U., S. Hildebrandt, A. Küster, O. Wohlrab. Minimal Surfaces II: Boundary regularity. Grundlehren der mathematischen Wissenschaften 295. Springer-Verlag: Berlin, 1992.
- [7] Dierkes, U., Hildebrandt, S., Lewy, H. On the analyticity of minimal surfaces at movable boundaries of prescribed length. J. Reine Angew. Math. **379**, 100-114 (1987).
- [8] Douglas, J. Solution of the problem of Plateau. Trans. Am. Math. Soc. **36**, 363-321 (1931).
- [9] Dziuk, G. Das Verhalten von Lösungen semilinear elliptischer Systeme an Ecken eines Gebietes. Math. Z. **159**, 89-100 (1978).

- [10] Dziuk, G. Das Verhalten von Flächen beschränkter mittlerer Krümmung an C^1 -Randkurven. *Nachr. Akad. Wiss. Gött., II. Math.-Phys. Kl.*, 21–28 (1979).
- [11] Dziuk, G. On the boundary behavior of partially free minimal surfaces. *Manuscr. Math.* **35**, 105–123 (1981).
- [12] Dziuk, G. Über quasilineare elliptische Systeme mit isothermen Parametern an Ecken der Randkurve. *Analysis* **1**, 63–81 (1981).
- [13] Ecker, K. Area-minimizing integral currents with movable boundary parts of prescribed mass. *Analyse non linéaire. Ann. Inst. H. Poincaré* **6**, 261–293 (1989).
- [14] Evans, L.C. *Partial Differential Equations. Graduate Studies in Mathematics 19.* American Mathematical Society: Providence, RI, 1998.
- [15] Gillbarg, D., Trudinger, N. S. *Elliptic Partial Differential Equations of Second Order.* Springer: Berlin, 1998.
- [16] Gulliver, R., Lesley, F.D. On boundary branch points of minimizing surfaces. *Arch. Ration. Mech. Anal.* **52**, 20–25 (1973).
- [17] Gulliver, R., Osserman, R., Royden. A theory of branched immersions of surfaces. *Am. J. Math.* **95**, 750–812 (1973).
- [18] van der Mensbrugghe, G. Sur la tension des lames liquides. *Bull. Acad. Roy. Sci. Bruxelles (2)* **22**, 270–276, 308–328 (1866).
- [19] Morrey, C.B. On the solutions of quasi-linear elliptic partial differential equations. *Trans. Am. Math. Soc.* **43**, 126–166 (1938).
- [20] Morrey, C.B. The problem of Plateau on a Riemannian manifold. *Ann. Math. (2)* **49**, 807–851 (1948).
- [21] Nitsche, J.C.C. Minimal surfaces with movable boundaries. *Bull. Am. Math. Soc.* **77**, 746–751 (1971).
- [22] Nitsche, J.C.C. The regularity of minimal surfaces on the movable parts of their boundaries. *Indiana Univ. Math. J.* **21**, 505–513 (1971).

- [23] Nitsche, J.C.C. On the boundary regularity of surfaces of least area in Euclidean space. *Continuum Mechanics and Related Problems in Analysis*, Moscow, 375-377 (1972).
- [24] Radó, T. Contributions to the theory of minimal surfaces. *Acta Sci. math. Univ. Szeged* **6**, 1-20 (1932).
- [25] Stephens, Benjamin K. QuickTime movies. November 16, 2002: `bball1.mov`, `bball2.mov`, `bdisc1-bigjump.mov`, `bpclip1.mov`, `bpclip2.mov`. November 19: `sd1.mov`. November 22: `sd2-upper-lower.mov`, `heart3.mov`. February 24, 2003: `möbius.mov`. Most are viewable on <http://www.bkstephens.net>.

Index

- (B, M) pairs: Alt competitors, 22
 $A(X)$: area of an H^1 map X , 28
 $\mathcal{C}_{\text{Alt}}(\Gamma, L)$: the set of Alt competitors for thread problem $\mathcal{P}(\Gamma, L)$, 22
 $C(\Gamma)$: positive constant depending only on the geometry of wire curve Γ ; may have different values in different equations, 10
 $D(B, M)$: Dirichlet energy of Alt competitor (B, M) , 23
 $D(s)$, normal disc to wire Γ at $\Gamma(s)$, 53
 Δ : unit disc, 10
 Γ : wire curve, 20
 $H^1(B^\circ)$: Space of functions which have L^2 derivatives on the interior of a domain B , 23
 IndDeg (inductive degree), 170
 $\mathcal{P}(\Gamma, L)$: thread problem: to find the least area surface spanning wire boundary Γ with thread no longer than L , 11, 23
 $R(\Gamma)$: positive length constant depending only on the geometry of wire curve Γ ; may have different values in different equations, 10
 T_Γ : torsion, 20
 (X, ϕ_-) pair (Alt crescent), 23
 dom : domain (of a function), 10
 η_Γ : Frenet binormal vector, 20
 γ : thread curve, 36
 Im : image (of a function), 10
 κ , (constant) free thread curvature, 27
 $\ell(\Gamma)$: length of curve Γ , 23
 ν : (outer) side-normal to a surface at a boundary, 27
 ν_Γ : Frenet normal vector, a normalization of curve's curvature vector, 20
 $\#$: cardinality of a set, or of a multi-index, 166
 $()$, zero-tuple or empty multi-index, 166
 ϕ_- (gluing map of Alt crescent (X, ϕ_-)), 23
 $||$: absolute value, or the sum of a multi-index, 166
 \hat{s} : slicewise extended arclength function, 53
 $\text{Tub}_r U$: tubular neighborhood of a set U , 10
 ν_Γ : function describing the Gauss wire image relative to the η_Γ ruling, 92
 adjoint surface of Alt minimizer, 39
 Alt competitors, 22
 Alt crescent, 26
 Alt crescents, near wire

- Gauss image, 87
- Alt minimizer, 23, 24
 - adjoint surface of, 39
 - branch points, 27
 - regularity at wire boundary, 28
- Alt minimizer, near wire
 - branch points prohibited, 53
- base corner, 88
- Beeson, M., 130
- bifurcation, 139
- Björling's formula, 123, 178
- Bound on Γ' -Slope Lemma, 57, 58, 67, 69–71
- Bound on ν_T -Slope Lemma, 60, 62, 65, 67, 69, 180
- C^1 Corner Regularity Theorem, 8, 16, 83, 84, 112
- convex hull enclosure result
 - for adjoint surface of Alt minimizer, 39
 - for Alt minimizer, 38
 - for minimal disc with fixed boundary, 38
- Corner Slope Improvement Lemma, 79–81, 84, 93, 95, 96, 106, 107, 109
- Corner Slope Inequality Lemma, 86, 109
- Corner Thread Monotonicity Lemma, 84, 85, 91, 107
- Corner Thread Normal Limit Lemma, 85
- crescents, 11, 23
- Crescents Near Maxima Lemma, 72, 76, 77
- critical curvatre ratio, sequence of, 124
- critical curvature ratios, sequence of, 168
- Curve Lift Lemma, 95, 96, 98, 102, 104, 106, 107, 149
- cuspidal corners, 11
- degree
 - inductive, 170
 - y-even, 170
 - y-odd, 170
- Descartes's rule, generalized, 148
- Dirichlet energy, D , 23
- Douglas, J., 19
- Ecker, K., 20
- eigenvalue of Laplacian on Gauss image
 - with Dirichlet and Neumann boundary conditions, 109
- entry condition, 150
 - nontransverse, 150
 - transverse, 150
- experiment, *see* physical experiment or thought experiment
- extensible thread-wire surfaces, 111
- free thread, 22
 - $C^{1,1}$ regularity, 27
 - C^2 regularity, 27
 - curvature, 27
 - real-analytic on interior, 27
- Frenet frame, 20
 - Frenet binormal vector, 20
 - Frenet normal vector, 20
 - Taylor expansion of curve in, 145
- Frenet frames

- distance between two Frenet frames, 67
- Gauss map, 34, 89
 - image of Alt crescent, 34
- Gauss sphere, 10, 34, 89
- Gauss sphere (unit sphere), 10
- Gauss thread curve, 89
- Gauss wire curve, 89
- Generalized Descartes's Rule Lemma, 90, 148
- generic wire properties, 29
- geometric measure theory, 20
- gluing map (ϕ_-) of Alt crescent (X, ϕ_-) , 23
- graph
 - planar, 44
 - tree, 44
 - valence, 44
- Harmonic Level Set Lemma, 44–46, 48, 49
- intersection
 - of tubular neighborhood with itself, 53
- Intersection Graph Lemma, 42, 43, 50, 54, 56, 70, 90, 179
- intersections
 - of planes and a generic wire near a critical point of curvature, 89
 - of planes and crescents, 42
 - of planes and tubular neighborhoods of generic wires, 29
- kink in thread between crescents, smoothing out a, 71, 162
- length
 - Alt minimizer attains maximum allowed, 23
- lift of curve by immersion
 - maximal, 150
 - positive continuation, 150
 - uniqueness, 150
- Lipschitz control of Alt minimizer in Frenet coordinates, 67, 80
- mathematical model of thread-wire surface experiment, 19
- Maximum Principle, 44, 45
- minimal surface operator, 166
- Möbius strip thread-wire surface, 142
- monotonicity
 - of thread binormal (approximately), 84
 - weak, 24
- Morrey's ϵ -Conformal Lemma, 28
- multi-index, 166
- Near-wire Crescent Theorem, 7, 14, 51, 80, 86–89, 91, 113, 114, 120
- Normal Avoidance Lemma, 56, 57, 60, 65, 79
- normal disc $D(s)$, 53
- notation, 10
- open-and-closed set, (simultaneously open and closed), 50
- physical experiment

- cotton vs. silk thread, 132
- friction, 139
- glycerin, 133
- physical question, 19
- plane-enclosure arclength, 157
- Plateau problem, 19
- positive corner, 88, 89
- Quadratic Trumpet for Thread Lemma, 77
- Quadratic Trumpet Lemma, 79
- Radó's Lemma, 43
- Radó, T., 19, 43
- regular curve, 10
- self-intersecting tubular neighborhood, 53
- Series Solutions to ThIP problem Theorem, 49, 84, 91, 168
- Series Solutions to WOC problem Theorem, 169
- shadow curve
 - thread, 88
 - wire, 88
- side-normal ν to a surface at a boundary, 27
- Slicewise Parametrization Lemma, 35, 55, 69, 164, 180
- stationary thread-wire surface, 123
- supporting wire, 26
- symmetry breaking, 132, 139
- Taylor expansion
 - of curve in Frenet frame, 145
- thought experiment, 131
- thread
 - free, 22
 - wire-adhering, 22
- Thread Interior Point (ThIP) Problem, 168
- thread problem, 11, 19, 23
- thread shadow curve, 15, 52, 86, 88
- thread torsion/wire torsion ratio, 112, 124
- thread-bearing wire, 26
- Thread-Bearing Wire Curvature Bound Theorem, 32
- thread-pull, 11, 131
 - experiment, 131
 - jumps in, 132
- thread-wire surfaces, 11
- tie-clip curve, 132
- torsion, 20
 - critical, of wire at wire-osculating corner, 169
- tubular neighborhood
 - non self-intersecting, 52
 - \hat{s} , slicewise extended arclength function, 53
- twisting slide map, 113
- TWS Adjoint Convex Hull Theorem, 39, 41
- TWS Convex Hull Theorem, 38, 49, 53, 57, 60, 67, 69, 114
- Varying Frenet Frame Graph Lemma, 67, 71, 74, 77, 79, 81, 85
- wire, 20
 - bent paperclip, 136

- crescent-supporting, 26
- Frenet, 20
- generic, 29
- heart curve, 134
- immersed v. embedded, 53
- supporting Möbius strip, 142
- thread-bearing, 26
- tie-clip, 139
- wire loop
 - embedded, 21
- Wire Osculating Corner (WOC) problem, 166
- wire shadow curve, 15, 52, 86, 88
- wire-adhering thread, 22
- Wire-Plane Arclength Lemma, 157, 160
- wire-plane intersection number, 29
- Wire-Plane Intersection Number Lemma,
 - 8, 30, 157, 159
- WOC relations
 - surface is minimal (MS), 167, 170
 - thread curvature vector is tangent to surface (TG), 167, 174
 - thread lies in surface (TH), 167, 173
 - wire lies in surface (WI), 167, 172
- WOC series solution, 168
- zero-tuple, 166